

AD704606

Interim Technical Report 7

RESPONSE OF WINDOWS TO SONIC BOOMS

Prepared for:

NATIONAL SONIC BOOM EVALUATION OFFICE
DEPARTMENT OF THE AIR FORCE
THE PENTAGON
WASHINGTON, D.C.

CONTRACT AF49(638)-1696

STANFORD RESEARCH INSTITUTE

MENLO PARK, CALIFORNIA



Reproduced by the
CLEARINGHOUSE
for Federal Scientific & Technical
Information Springfield Va. 22151



June 1967

Interim Technical Report 7

RESPONSE OF WINDOWS TO SONIC BOOMS

Prepared for:

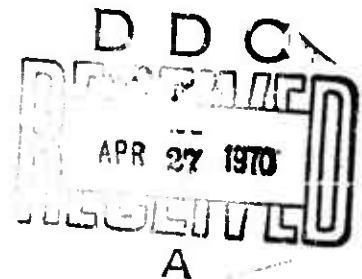
NATIONAL SONIC BOOM EVALUATION OFFICE
DEPARTMENT OF THE AIR FORCE
THE PENTAGON
WASHINGTON, D.C.

CONTRACT AF49(638)-1696

By: L. SEAMAN
MECHANICS DEPARTMENT

SRI Project ETU-5897

Approved: DONALD R. GRINE
MANAGER, SONICS DEPARTMENT



Copy No. 73

This document is for public distribution.

ABSTRACT

A method for calculating the response of simply supported windows to sonic booms has been developed. The procedure is based on a linear one-degree-of-freedom analysis plus estimates of the importance of nonlinear and multimodal effects. Effects of stress raisers and of movement followed by impact of loose windows are not considered.

Significant contributions to the maximum stress in windows subjected to 2 psf sonic booms are made by large deflections (nonlinearities), modes above the fundamental, and the internal pressure built up in the building by the boom.

An attempt to estimate statistically the occurrence of window failure under 2 psf booms was frustrated by the lack of precise knowledge of the statistical distribution of glass strength.

PREFACE

This report is one of a series of technical reports dealing with various effects of sonic booms. The research was sponsored by the National Sonic Boom Evaluation Office of the Air Force.

CONTENTS

	<u>Page</u>
ABSTRACT	111
I INTRODUCTION	1
II GENERAL PROPERTIES OF WINDOWS AND WINDOW GLASS	3
III DEFLECTION AND STRESS OF WINDOWS UNDER SONIC BOOMS	7
A Problem Statement	7
B Window Deflection and Stress Based on Linear Analyses.	9
C Deflection Under Internal Pressures Based on Linear Analyses	12
D Nonlinear Deflections and Stresses Under Booms	18
E Determination of the Amplitude of Internal Pressure	28
F Summary of Window Behavior Under Boom Loading	32
IV STATISTICAL PREDICTION OF FAILURE	35
V SUMMARY	37
VI FURTHER STUDY	39
 APPENDICES	
A Dynamic Amplification Factor: Linear	41
B Response to Internal Pressure	59
C Nonlinear Load-Deflection Relations	63
D Experimental Data on Window Response	75
E Dynamic Amplification Factor: Nonlinear	95
 BIBLIOGRAPHY	 107

ILLUSTRATIONS

<u>Figure</u>		<u>Page</u>
1	Natural Frequencies of Glass Panes	6
2	Pressures On and Within a Building	8
3	Plate Deflection Under Sonic Boom Loading	10
4	Dynamic Amplification Factor for a Square Plate: Linear, First Mode Deflection Under Booms	11
5	Linear, Multimodal Dynamic Amplification Factor for Central Deflection of a Square Plate	13
6	Linear, Multimodal Dynamic Amplification Factor for Stress in the Center of a Square Plate	14
7	Dynamic Amplification Factor for First Mode Deflection of a Square Plate to Internal Pressure Only	15
8	Dynamic Amplification Factor for First Mode Deflection of a Square Plate to Boom and Internal Pressure: $q_2 = 0.25$	16
9	Dynamic Amplification Factor for First Mode Deflection of a Square Plate to Boom and Internal Pressure: $q_2 = 0.50$	17
10	Deflection and Stress in the Center of a Square Plate as a Function of Static Pressure	19
11	Nonlinear Relation Between Central Deflection and Stress	20
12	Nonlinear First Mode Deflection of a Square Plate to a Boom Loading with Amplitude such that $\xi_s = 1.0$. .	22
13	Nonlinear First Mode Deflection of a Square Plate to a Boom Loading with Amplitude such that $\xi_s = 2.0$. .	23
14	Nonlinear First Mode Deflection of a Square Plate to a Boom Loading with Amplitude such that $\xi_s = 3.0$. .	24
15	Summary of Nonlinear First Mode Deflection of a Square Plate to a Boom Loading	25
16	Variation of Apparent Natural Frequency with Central Deflection	26

ILLUSTRATIONS (continued)

<u>Figure</u>		<u>Page</u>
17	Pressures Considered in Calculating the Internal Pressure of a Building.	29
A.1	Flow Chart for Multiplate Program to Compute Multimodal Dynamic Amplification Factors	49
A.2	Flow Charts for Portions of the Main Multiplate Program for Computation of Deflections (Portions for Calculating Moments are Similar)	50
A.3	Subroutines Used in Multiplate Program	51
C.1	Graph for Determination of D_1	73
C.2	Graph for Determination of B_1	74
D.1	Relation Between Applied Pressure and Deflection at Rupture	78
D.2	Experimental and Theoretical Load-Deflection Curves	80
D.3	Deflection at Rupture as a Function of Thickness Ratio, a/h	82
D.4	Deflection at Rupture as a Function of Thickness	83
D.5	Failure Pressure on Plates as a Function of the Thickness Ratio, a/h	84
D.6	Effect of Loading Rate on Ultimate Strength	85
D.7	Bending Stress as a Function of Central Deflection	87
D.8	Membrane Stress as a Function of Central Deflection	88
D.9	Relation Between Central Bending Stress and Applied Pressure	90
D.10	Relation Between Central Membrane Stress and Applied Pressure	91

TABLES

<u>Tsbls</u>		<u>Page</u>
1	Properties of Window Glass	4
2	Nominal Sizes of Square Panes	5
3	Deflection and Stress of Square Windows Under a 2 psf Boom	28
C.1	Coefficients for Large Deflection of Square Plates . . .	71
D.1	Ultimate Deflection and Bursting Pressures	76
D.2	Ultimate Deflection and Bursting Pressures	77
D.3	Stress Data	79
D.4	Statistical Data on Failure	93
D.5	Statistical Data on Breking Stress	93
E.1	Amplitude Reduction for Higher Modes	99
E.2	Frequency Increase for Higher Modes	101

RESPONSE OF WINDOWS TO SONIC BOOMS

SECTION I

INTRODUCTION

The response of windows to sonic boom loadings presents an important problem in the evaluation of sonic boom effects on structures. Experimental studies which have been undertaken to ascertain the effects of booms on windows of various sizes are those of Maglieri, Huckel and Perrott (1961), Blume and Asociatca (1965), and Freynik (1963). These test programs have shown that nearly all windows are broken by boom pressures of 100 psf and that a few will break at pressures of 10 or 20 psf. No lower limit has been established on the pressure required to break a window. These three studies and the static tests of Bowles and Sugarman (1952) and Orr (1957) have shown that windows have a nonlinear behavior even at low pressures.

Nonlinearities become important when the central deflection exceeds one-half the plate thickness, and, for usual window dimensions, a static pressure of 1 psf to 10 psf will cause such a deflection. The consequence of the nonlinearities is that stress and deflection are not proportional to pressure or to each other. Hence, there has been considerable difficulty in interpreting experimental results and in extrapolating the findings. In most cases the data were not correlated with theory. In the dynamic tests the pressures acting on the window were not measured, only the nominal pressure in the vicinity was measured. In cases where window deflection was measured, only maximum excursion was obtained.

Knowledge of window behavior requires careful procuring of the right data and data reduction based on a theoretical analysis of the window motion. This present study is intended to bring together available theoretical knowledge on the subject to

1. indicate the experimental parameters which should be measured,
2. provide a basis for data reduction,
3. provide a basis for prediction of window stresses and deflections in response to booms,

4. indicate those areas where further experimental or theoretical work is most needed.

The study is primarily concerned with boom loadings with peak pressures of about 2 psf.

Nat loading on a window is a function of the stiffness and volume of the structure in which the window occurs. Response of a window to loading is highly nonlinear and depends on the participation of several deflection modes. Because of this complexity the problem has not been solved analytically but has been approximated by considering (1) general properties of windows, (2) the linear response of windows in the fundamental mode, (3) linear response in all modes, (4) effect of internal pressure on the response, and (5) nonlinear response in the first mode. By comparing the results of (2), (3), (4), and (5), we have estimated the nonlinear, multimodal response. Finally, using the calculated response, the statistical probability of window damage was estimated.

SECTION II

GENERAL NATURE OF WINDOWS

To calculate window response, we need to know the normal mounting conditions of windows, strength and modulus of glass, common sizes of windows, and the natural frequencies of windows.

Window glass is mounted either with glazing nails and putty or in a rubber seal. It may be assumed that the edge conditions can be approximated by a simple support with a moveable edge. This assumption has been studied by Freynik (1963). Freynik used square windows mounted with glazing nails and putty. He compared empirical natural frequencies with those from vibration theory for simple supported plates, and compared measured stresses with theoretical values. Both comparisons showed that the experimental results could be explained on the basis of a simple support condition. The results of Bowles and Sugrman (1952) in static testing of windows confirms the existence of the simple, moveable boundary condition.

An unknown, but probably large, fraction of existing windows are loose in their mountings and/or have stress raisers present in poor mountings. The results of this report cannot be applied to such defective windows since the above assumption of simple support edge conditions does not apply. Our results should apply well to calculation of the response of new, well-mounted windows such as those usually encountered in laboratory tests or field test structures.

Strength of window glass has been reported by R. W. McKinley (1964); values for strength and other parameters of glass windows are listed in Table 1. Strengths were determined by the standard ASTM (1965) beam test procedure. Flexural strength was evaluated as failure in tension: glass fails without any significant amount of plastic deformation so that the yield value equals the ultimate strength. There is considerable scatter in results from strength tests. McKinley (1964) states that the strengths are normally distributed and suggests using a coefficient of variation of 25% (that is, the standard deviation is one-fourth the mean strength).

TABLE I
 PROPERTIES OF WINDOW GLASS
 (from McKinley)

Property	Value
Flexurel Strength	
Short duration: sonic booms, blasts	6600 psi
One minute loading: wind	4400 psi
Elastic modulus	10^7 psi
Density	0.09 lb/in ³
Poisson's ratio	0.23

On the other hand, Shand (1958) states that the distribution is not normal, but skewed so that the mean is larger than median and mode; possibly a lognormal or Poisson distribution would fit the data.

Normal sizes for glase panes are dictated by building code requirements which in turn are based on wind loadings and nominal factors of safety. The allowed thicknesses for panes of various areas as specified in the Uniform Building Code (1964) are shown in the first two columns of Table 2. The values are for a wind loading of 20 psf. Dimension of the window may be combined to form the dimensionless parameter, a/h , where a is the length of one side of a square pane and h is the thickness. For a rectangular pane, e is taken as the square root of the area. In a square pane the a/h ratio and the pressure govern the magnitude of stress in the pane under uniform loading. From the building code requirements, the maximum allowable ratio (a/h) was determined and listed in column 3 of Table 2. If it is presumed that a builder will always use the minimum thickness permitted, then we can also obtain a minimum ratio as in column 4 of Table 2. This minimum value of a/h was computed for each thickness using the value of e associated with the next smaller thickness. The minimum values are listed opposite the thickness values used in each computation.

TABLE 2
Nominal Sizes of Square Panes*

Area a^2 (ft ²)	Thickness t , (in.)	Maximum Allowed a/h (dimensionless)	Minimum Probable e/h (dimensionless)
5.8	0.085	340	141**
10.85	0.115	343	251
12	1/8	332	316
27	3/16	332	222
48	7/32, 1/4	380, 333	285, 242
75	5/16	333	268
108	3/8	333	277
190	1/2	331	250

* Data in Column (1) and (2) are from the Uniform Building Code (1964).
** Based on a 12 x 12-inch window.

The listings in Table 2 show that the range of a/h values is not very large. Since most of the values are between 220 and 340, this range was used in the analyses of this report.

The natural frequencies of windows are important for studies of dynamic loadings. For this analysis the windows are treated as simply supported plates undergoing small deflections. This approach appears to be adequate for deflections which are less than the pane thickness. Figure 1 is a graph of natural frequency as a function of the area-to-thickness ratio, calculated from the equation shown on the figure. Square and rectangular panes with several aspect ratios are included and the first three frequencies are considered. These three frequencies correspond to modes in which there are one maximum point of deflection, three maxima, and nine maxima. The range of area-to-thickness ratios for various glass thicknesses is also shown to indicate the probable frequencies which are encountered.

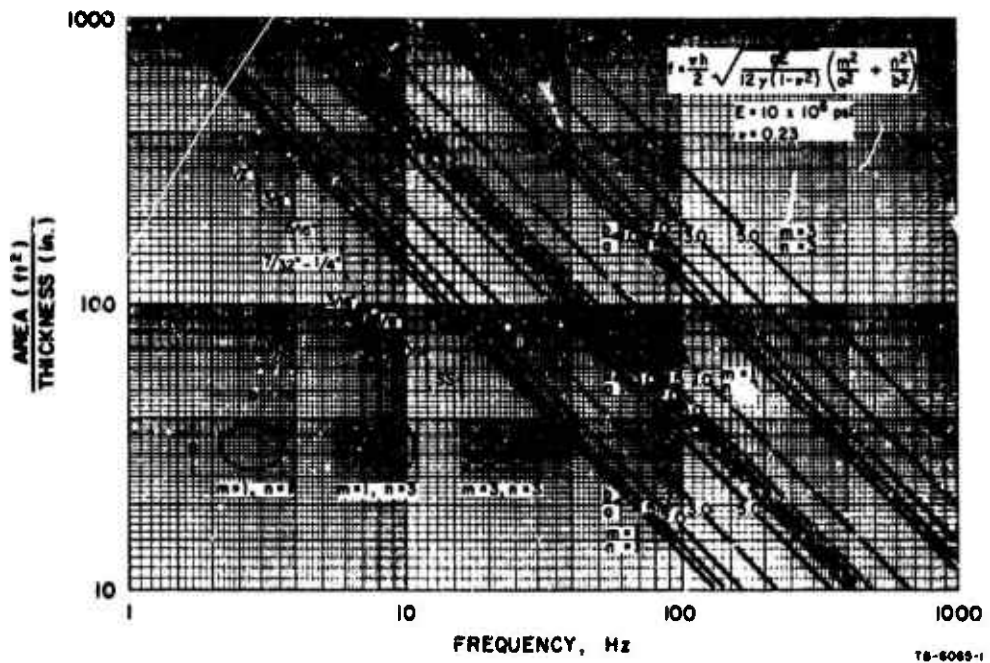


FIG. 1 NATURAL FREQUENCIES OF GLASS PANES

SECTION III

DEFLECTION AND STRESS OF WINDOWS UNDER SONIC BOOMS

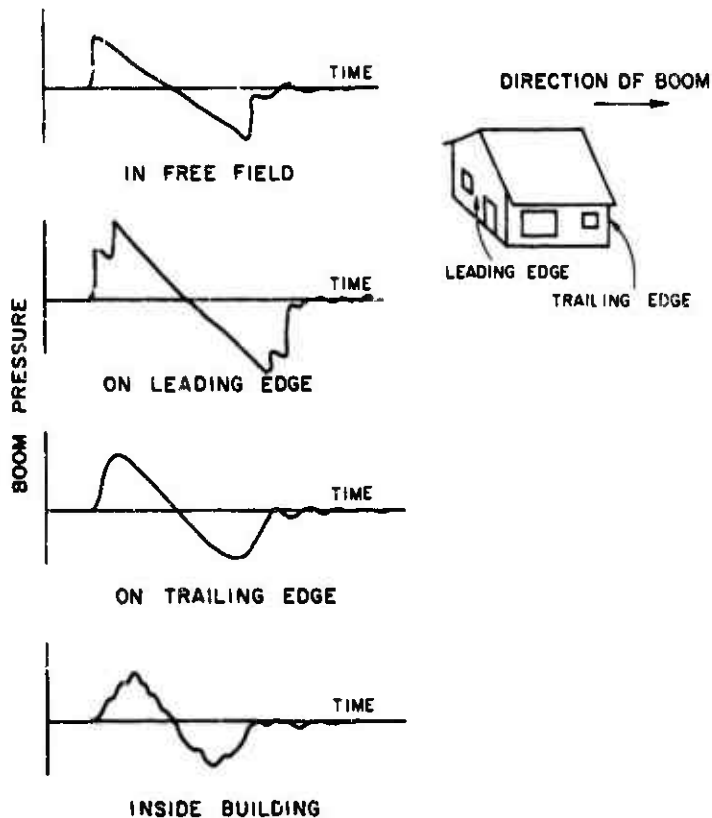
A. Problem Statement

To determine the deflection and stress of windows under booms let us examine qualitatively pressures on the buildings and reaction of the building. Characteristic boom pressures related to structure reaction are shown in Fig. 2. In the free field the pressure rises sharply. At the front wall of the building the pressure shows a sharp rise and evidence of reflections from the ground and wall. The boom pressure at the rear shows a more gradual rise and follows that on the front face by a few milliseconds. The pressure at each point on the roof has a sharp rise, but the average roof pressure has a longer rise time, corresponding to the travel time of the wave across the roof.

The effects of these loadings on the building are of two types:

- (1) general compression of the building followed by a rarefaction,
- (2) racking of the building first in the direction of travel of the boom and then in the reverse direction. The overall compression of the building causes an increase in the pressure inside the building. This internal pressure is usually one-fourth to one-half the peak boom pressure and significantly adds to the structural stiffness in compression.

Window deflections during a sonic boom are a function of the external pressure, structure motion, and internal pressure built up through compression of the building. The external pressure shows evidence of reflections from ground and buildings and passage around buildings and so may not correspond closely to the free-field boom pressure. To calculate the internal pressures and building motion it will be necessary to know (1) motion of the walls and roof caused by a boom pressure, and (2) motion of the walls, ceiling, and roof caused by internal pressure. If internal and external pressure are known, window motion can be calculated as the motion of a nonlinear, multimodal system under the action of known forces. Such an analysis would be a major effort. Instead, a one-degree-of-freedom analysis was made and the contribution of nonlinearities and higher modes computed as perturbations of the single mode solution.



TS-6085-28

FIG. 2 PRESSURES ON AND WITHIN A BUILDING

To make the problem tractable the following assumptions were introduced:

1. The outside boom is an ideal symmetric N-wave. This assumption eliminates the rise time and minor irregularities in the wave form. If the period of the structure is much longer than the rise time or durations of irregularities, then this assumption is justified.
2. The inside pressure has the form of a full sine wave with the same duration as the boom signature. This pressure history is a simplification of observed internal pressure histories.

3. The variation in arrival times around the building can be neglected.

The several analyses required are

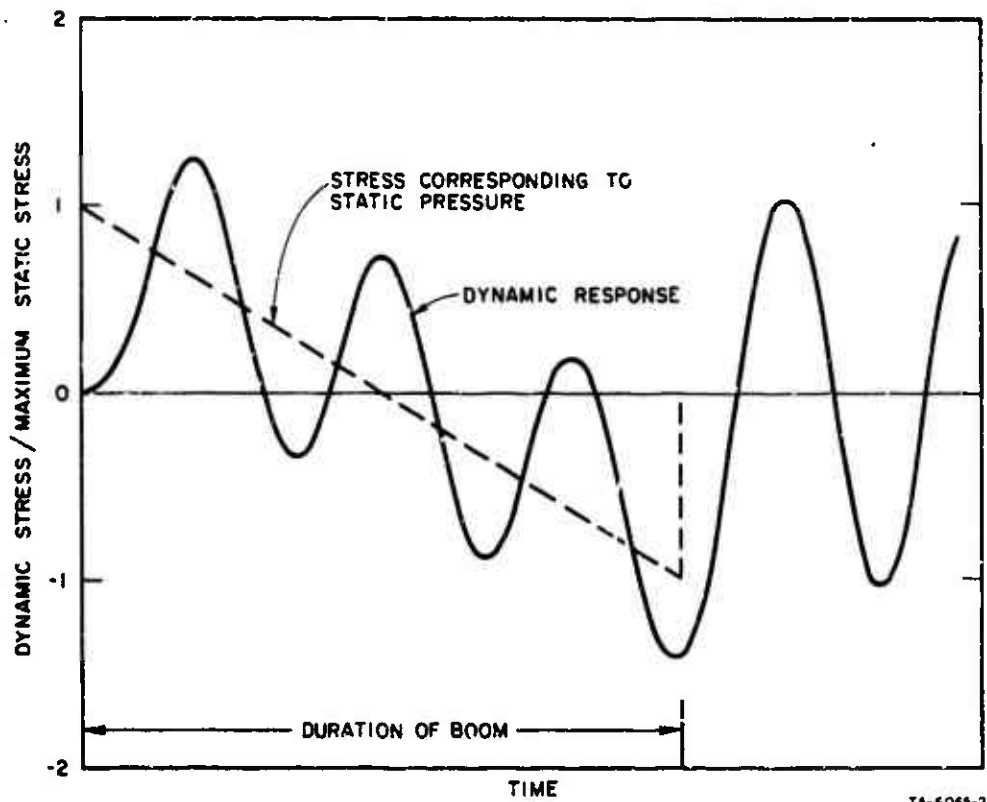
- Linear analysis of first mode motion under an N-wave
- Linear analysis of first mode motion under internal pressure
- Linear analysis of first mode motion under an N-wave and internal pressure
- Linear analysis of multimode motion under an N-wave
- Large deflection analysis of first mode motion under an N-wave
- Calculation of the amplitude of internal pressure

The results of these analyses are presented next. Following them, the results are collected to produce an analysis of the window motion and stress.

B. Window Deflection and Stresses Based on Linear Analyses

Figure 3 is an illustration of the probable history of central deflection of a window (fundamental mode only) to an N-shaped pressure wave. The applied pressure is shown as the dotted line with an amplitude corresponding to the stress which would occur if the pressure were applied statically. The dynamic deflection curve shows oscillation at the fundamental frequency of the plate. The plate is oscillating about the static deflection curve so that the dynamic deflection appears as a superposition of static deflection and free vibrations. In this figure the maximum negative deflection is approximately equal to the maximum positive. The two maxima are 26% and 40% higher than the static stress corresponding to the maximum applied pressure. The ratio of maximum dynamic stress or deflection to the static value is referred to as the dynamic amplification factor.

The dynamic amplification factor for the fundamental mode of a square plate (applicable to both stress and deflection) is shown in Fig. 4. The loading was a symmetric N-shaped pressure wave. In this figure there are separate curves for the maximum positive and negative deflection during the boom and the magnitude of the free oscillation following the boom. These curves were derived from the analysis in Appendix A for linear



TA-6065-2

FIG. 3 PLATE DEFLECTION UNDER SONIC BOOM LOADING

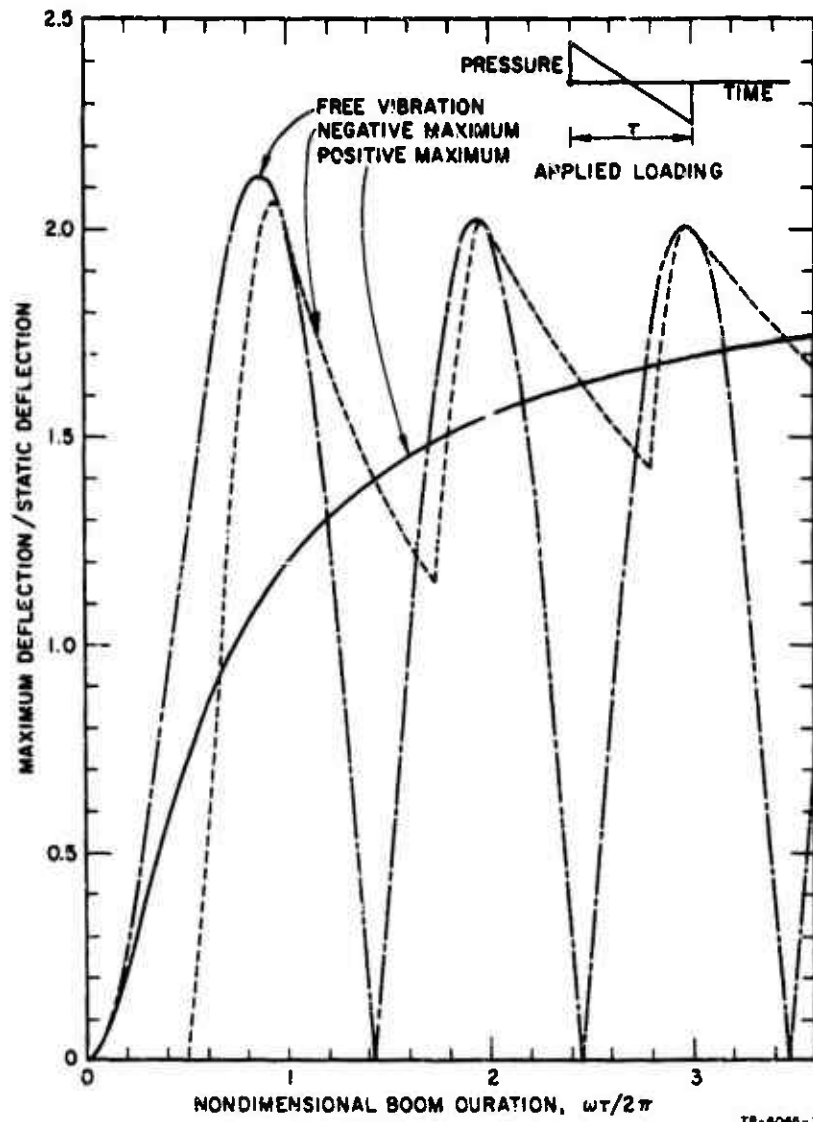


FIG. 4 DYNAMIC AMPLIFICATION FACTOR FOR A SQUARE PLATE: LINEAR, FIRST MODE DEFLECTION UNDER BOOMS

amplification factors. The abscissa is $\omega\tau/2\pi$, a nondimensional relation between ω , the fundamental circular frequency of the window, and τ , the duration of the N-wave.

Higher modes also contribute to the deflection and stress in the window. Dynamic amplification factors for the deflection and stress under a symmetric N-shaped pressure wave for the first eleven modes are shown in Figs. 5 and 6. The first eleven modes were calculated but the main contributors were the first (1,1) and second symmetric (1,3) modes. For comparison the two figures include the positive and free vibration maxima for the fundamental mode. We note that, while the amplification factor was the same for stress and deflection in the fundamental mode, it differs for the multimodal case. The factor for deflection is modified only very slightly by the contributions of higher modes: the first peak is about 4% higher and other curves are modified less. The amplification factor for stress is increased 0.60 in some regions of the abscissa and the peaks of the curve are broadened. In addition the second symmetric mode is sufficiently important to provide well-defined humps on some of the curves. On the average the stress increase during free vibration is 0.28 and for the positive maximum the increase is 0.26.

C. Deflection Under Internal Pressure Based on Linear Analyses

The response of a one-degree-of-freedom system to a pressure in the form of a full sine wave is shown in Fig. 7. This is the expected form of internal pressure. Again the positive maximum, negative maximum, and free vibration maximum are shown as a function of fundamental frequency. The amplification factor is larger than 2.0 only near coincidence of the forcing frequency and the natural frequency. The analysis on which these curves are based is detailed in Appendix B.

In Appendix B an analysis is also made of the response of a one-degree-of-freedom system to a combination of the N-wave and internal pressure. Some results are shown in Figs. 8 and 9 for deflection (stress curves are identical). The main effect of increasing the internal pressure is to greatly decrease the amplification factors in the vicinity of $\omega\tau/2\pi = 1.0$.

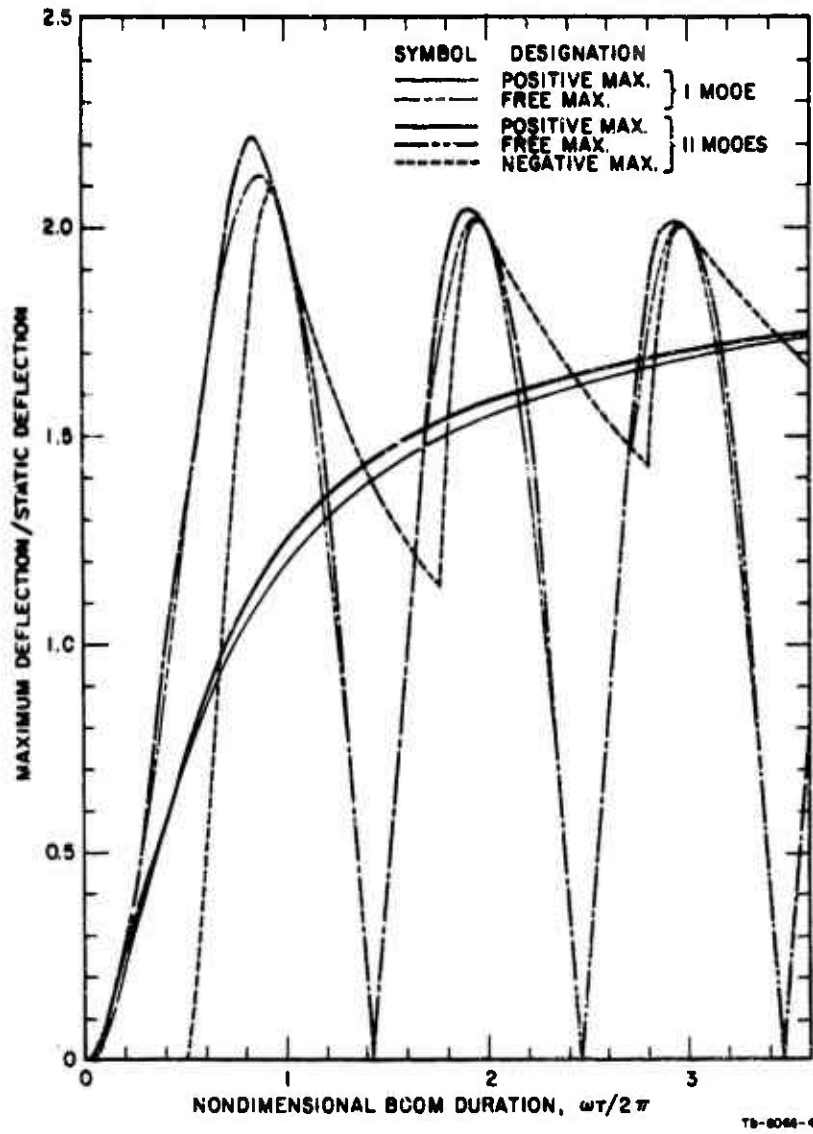


FIG. 5 LINEAR, MULTIMODAL DYNAMIC AMPLIFICATION FACTOR FOR CENTRAL DEFLECTION OF A SQUARE PLATE

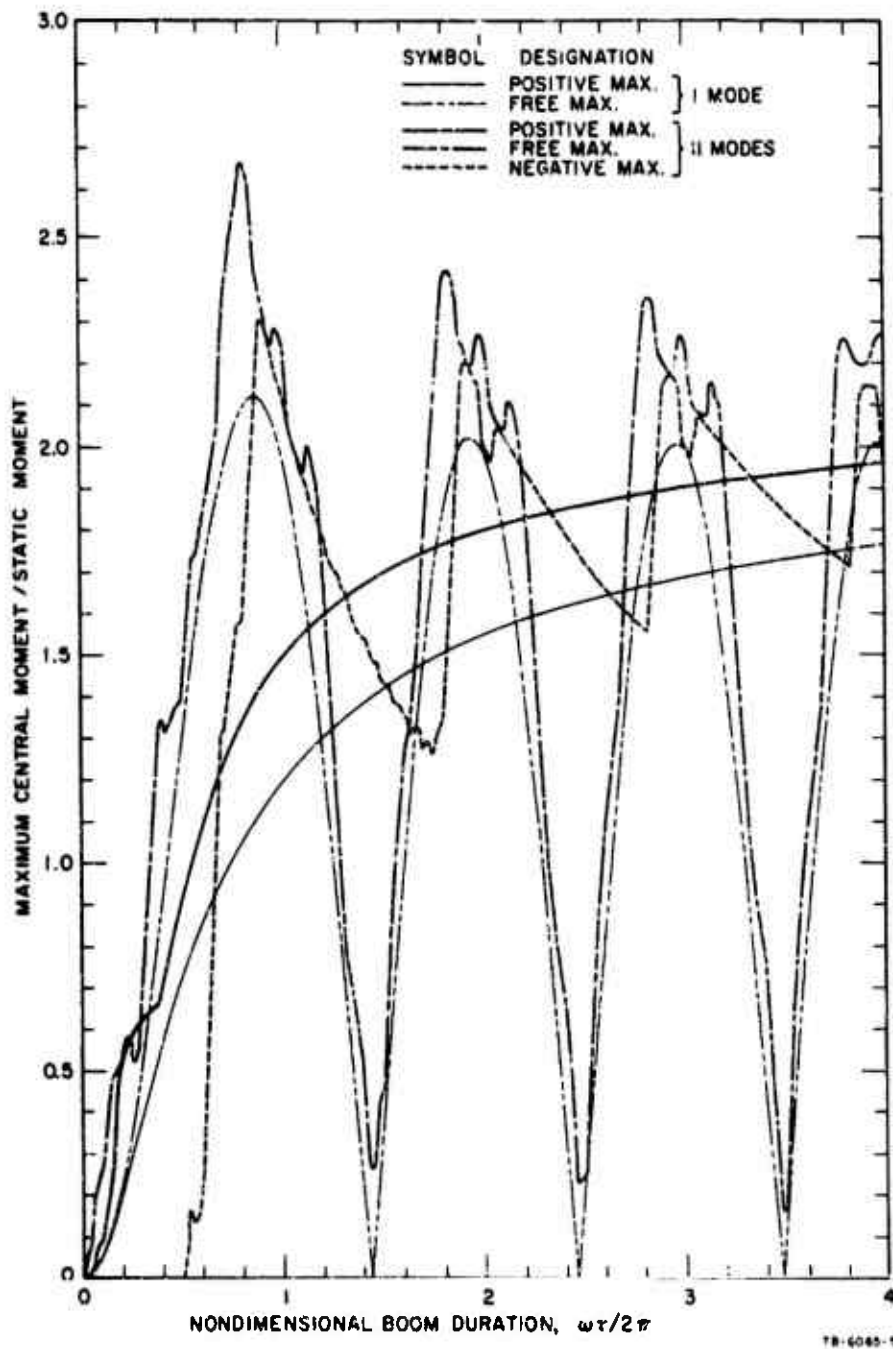


FIG. 6 LINEAR, MULTIMODAL DYNAMIC AMPLIFICATION FACTOR FOR STRESS IN THE CENTER OF A SQUARE PLATE

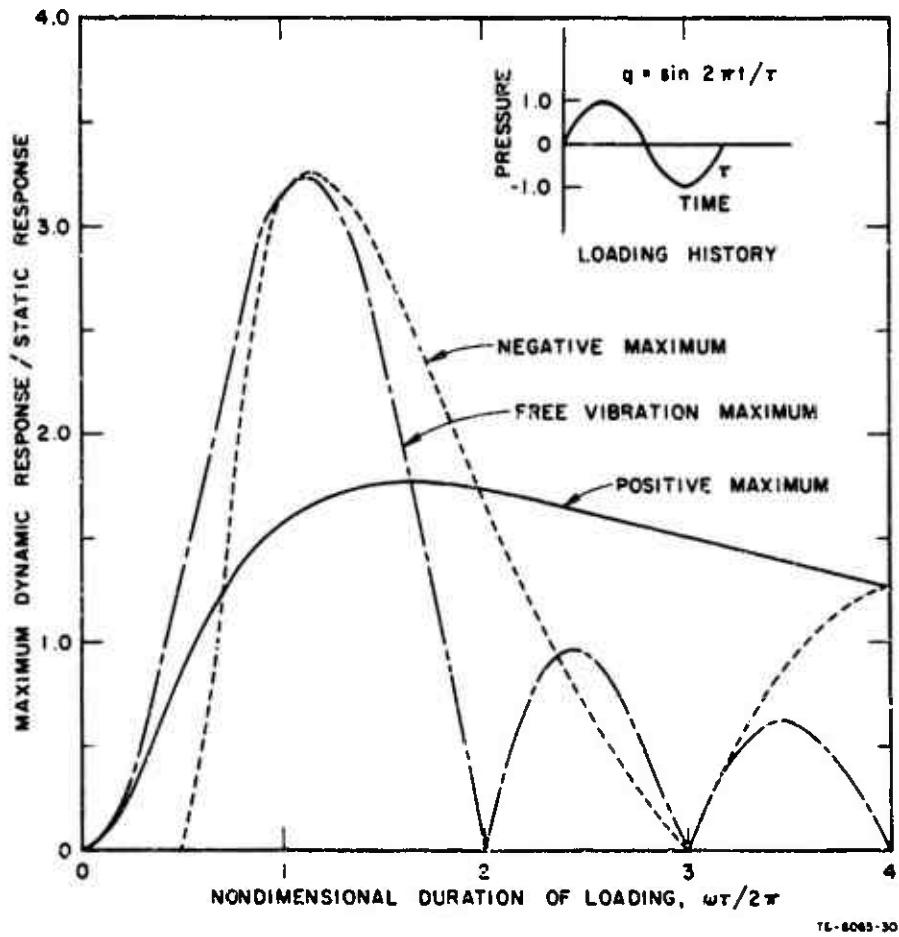


FIG. 7 DYNAMIC AMPLIFICATION FACTOR FOR FIRST MODE DEFLECTION OF A SQUARE PLATE TO INTERNAL PRESSURE ONLY

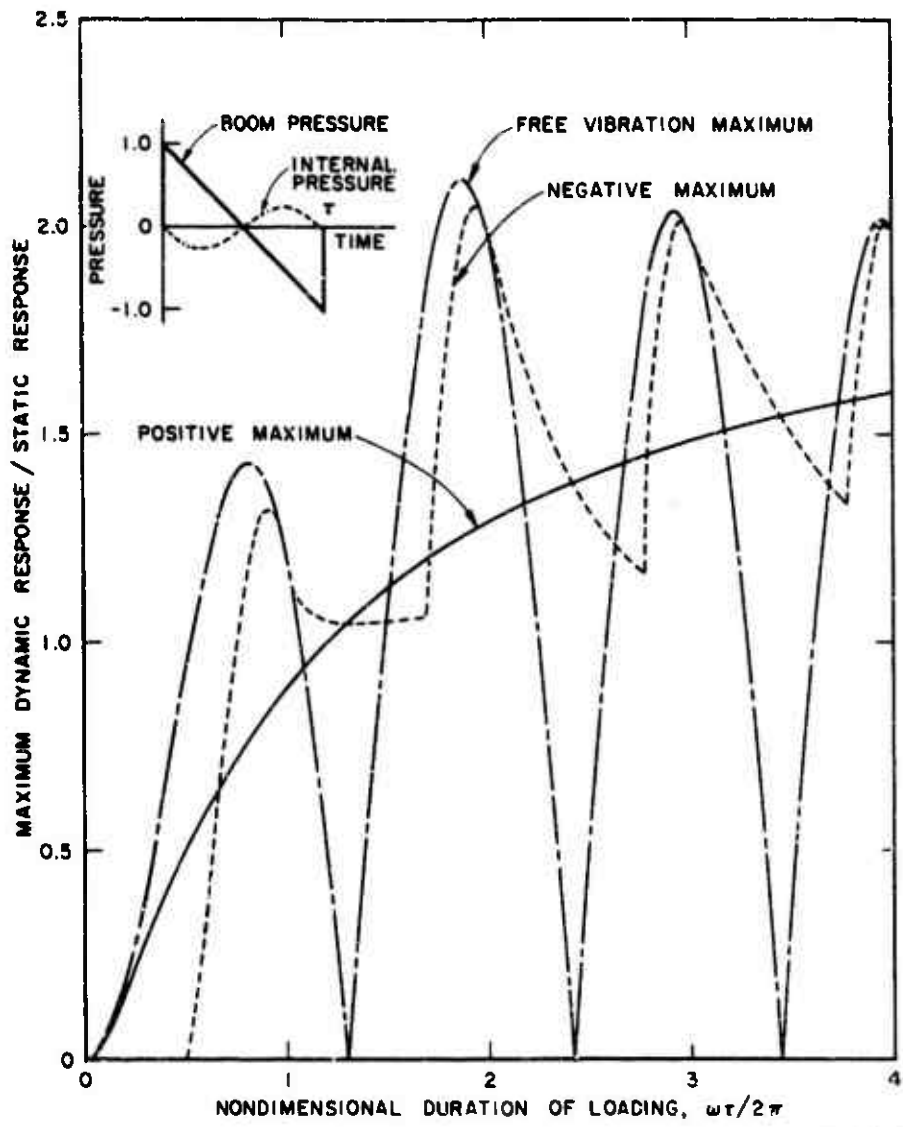


FIG. 8 DYNAMIC AMPLIFICATION FACTOR FOR FIRST MODE DEFLECTION OF A SQUARE PLATE TO BOOM AND INTERNAL PRESSURE: $q_2 = 0.25$

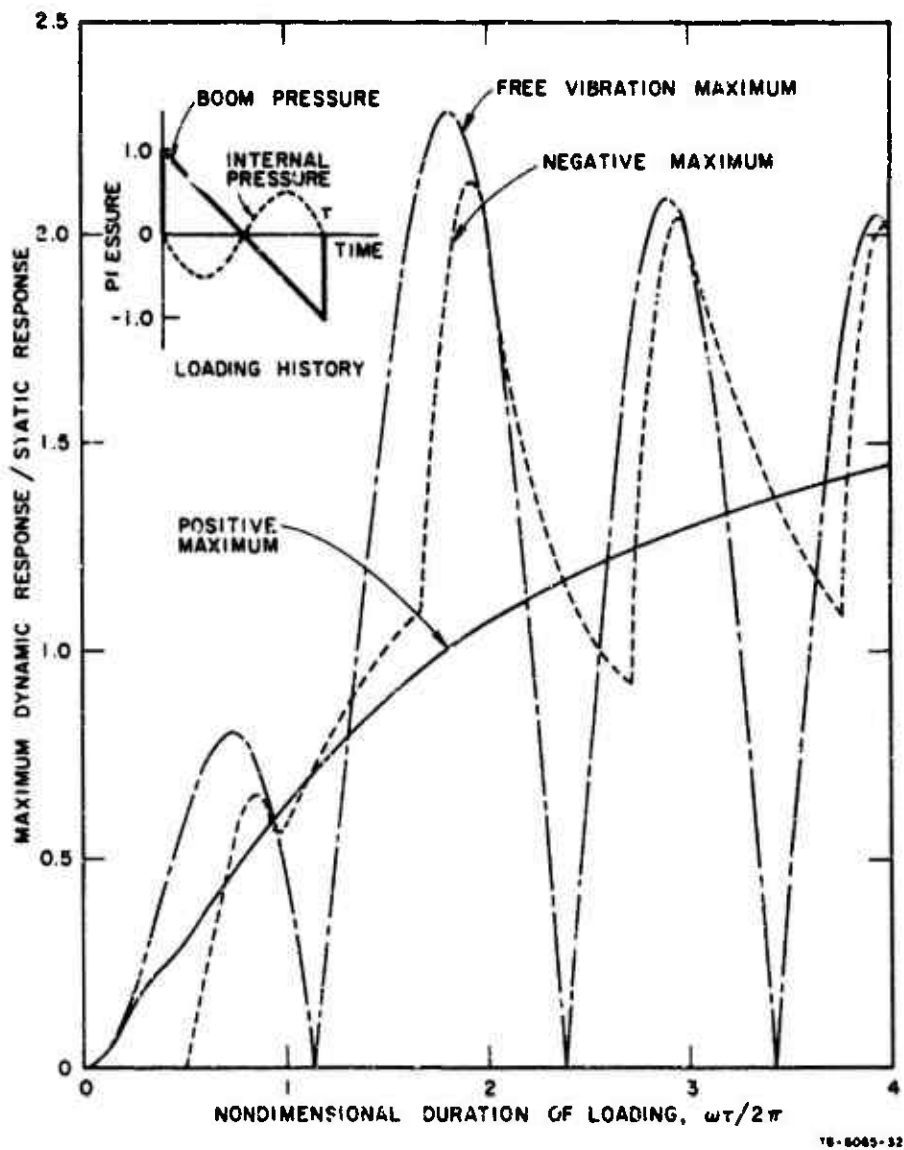


FIG. 9 DYNAMIC AMPLIFICATION FACTOR FOR FIRST MODE DEFLECTION OF A SQUARE PLATE TO BOOM AND INTERNAL PRESSURE: $q_2 = 0.50$

D. Nonlinear Deflections and Stresses Under Booms

In response to normal wind pressure loadings, window deflection is a markedly nonlinear function of the pressure. This nonlinear behavior occurs because the plate resists part of the load as a membrane after the deflection becomes large. According to the discussion of Freynik (1963) this nonlinearity causes the motion to differ considerably from that shown in Fig. 3. Instead of the smooth sinusoidal vibrations, the motion shows abrupt changes in direction. The natural frequencies of a window undergoing large deflections are a function of the deflection amplitude and are almost a continuous band of frequencies above the fundamental. With such a mixture of frequencies in the motion, the natural frequencies cannot be readily determined from the records. The nonlinearities have an important effect on

- stress and deflections,
- natural frequency,
- dynamic amplification factor.

We will consider each of these effects and then provide some numerical values to guide in assessing the seriousness of the nonlinearity.

The variation of stress and deflection with applied static pressure is shown in Fig. 10 based on the calculations in Appendices C and D. In Appendix C the forms of the equations are derived theoretically. The coefficients of the equations are evaluated in Appendix D from experimental data of other investigations. Figure 10 shows the nondimensional quantities w_0/h (deflection, ξ), $\sigma a^2/Eh^2$ (stress, S), and qa^4/Eh^4 (pressure, Q), where

- w_0 = central deflection of the square plate
- σ = stress (bending, membrane, or both)
- q = uniform pressure on the plate
- a = side of plate
- h = thickness of plate
- E = elastic modulus of plate material

The nonlinearities become important for a deflection greater than 0.5 times the plate thickness. A 2 psf boom will cause deflections up to 1.9 times the thickness in some windows - that is, well into the nonlinear range.

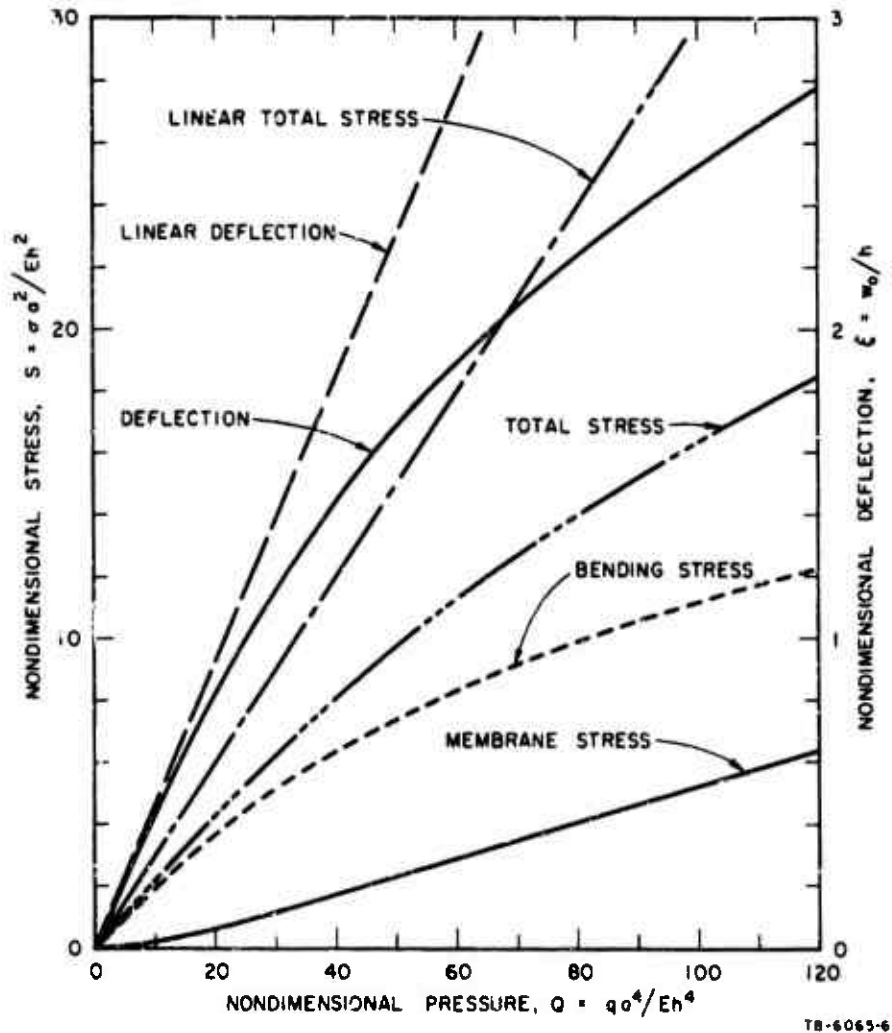


FIG. 10 DEFLECTION AND STRESS IN THE CENTER OF A SQUARE PLATE AS A FUNCTION OF STATIC PRESSURE

In Fig. 11 it is apparent that the relation between deflection and central stress is not altered much by the nonlinearities. The fact that the linear and nonlinear curves do not coincide at the origin suggests that there may be some uncertainties about the experimental values from Appendix D on which the curves are based.

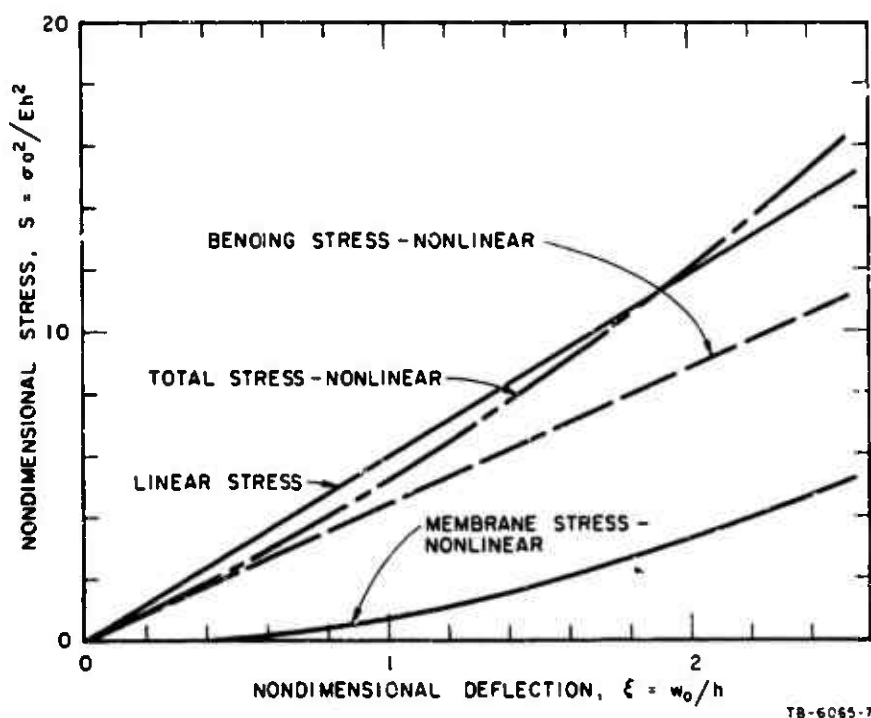


FIG. 11 NONLINEAR RELATION BETWEEN CENTRAL DEFLECTION AND STRESS

Next we consider the large deflection of a window under boom pressures. Dynamic calculations of plates undergoing large deflections normally begin with von Karman's equations. (See Timoshenko (1936) for a derivation of the equations.) However, the results from von Karman's equations did not agree well with experimental data on window deflections (see Appendix D). Therefore we took the pressure-deflection relation derived from the static experiments, restricting attention to motion in the fundamental mode only.

Nonlinear deflection of a window under an N-wave is shown in Figs. 12, 13, and 14 (based on calculations in Appendix E). These three figures correspond to peak pressure amplitudes required to cause static deflections of h , $2h$, and $3h$. (ξ_s is the nondimensional static deflection w_s/h under the peak pressure.) The peaks of these figures and Fig. 4 are summarized in Fig. 15. In the summary figure we see that large deflections tend to reduce the period of the plate so that the maxima occur at smaller values of $\omega\tau/2\pi$ than occur from small deflections. Also, the amplification factor for free vibration is reduced for large deflections but is unaffected for the positive maximum during forcing. The change in the apparent natural frequency with deflection is summarized in Fig. 16.

An estimate of the multimodal nonlinear behavior is made in Appendix E for both stress and deflection. The peak deflections are modified very slightly by the participation of modes above the fundamental. Therefore, it is recommended that the nonlinear response in the fundamental mode be used to calculate deflections with no changes to account for higher modes.

The estimate for peak stress is more complicated, and the accuracy of the estimate may be considerably less than that for deflection. The estimation procedure to be outlined appears logical but has not been verified in any way. The procedure includes two elements:

- Conversion of the nonlinear deflection amplification factor to stress amplification factor
- Addition of an increment to correspond with the contribution of higher modes.

To convert from deflection to stress, Eq. D.8 can be used to relate the stress in the first mode, S_1 , to the total central deflection, ξ ,

$$S_1 = 4.9 F_{\xi} (1 + 0.167 \xi)$$

But the deflection ξ is $F_{\xi} \xi_s$ where

- F_{ξ} is the amplification factor for deflection and
- ξ_s is the static deflection.

Therefore

$$S_1 = 4.9 F_{\xi} \xi_s (1 + 0.167 F_{\xi} \xi_s)$$

The next step is to add a factor corresponding to the contribution of

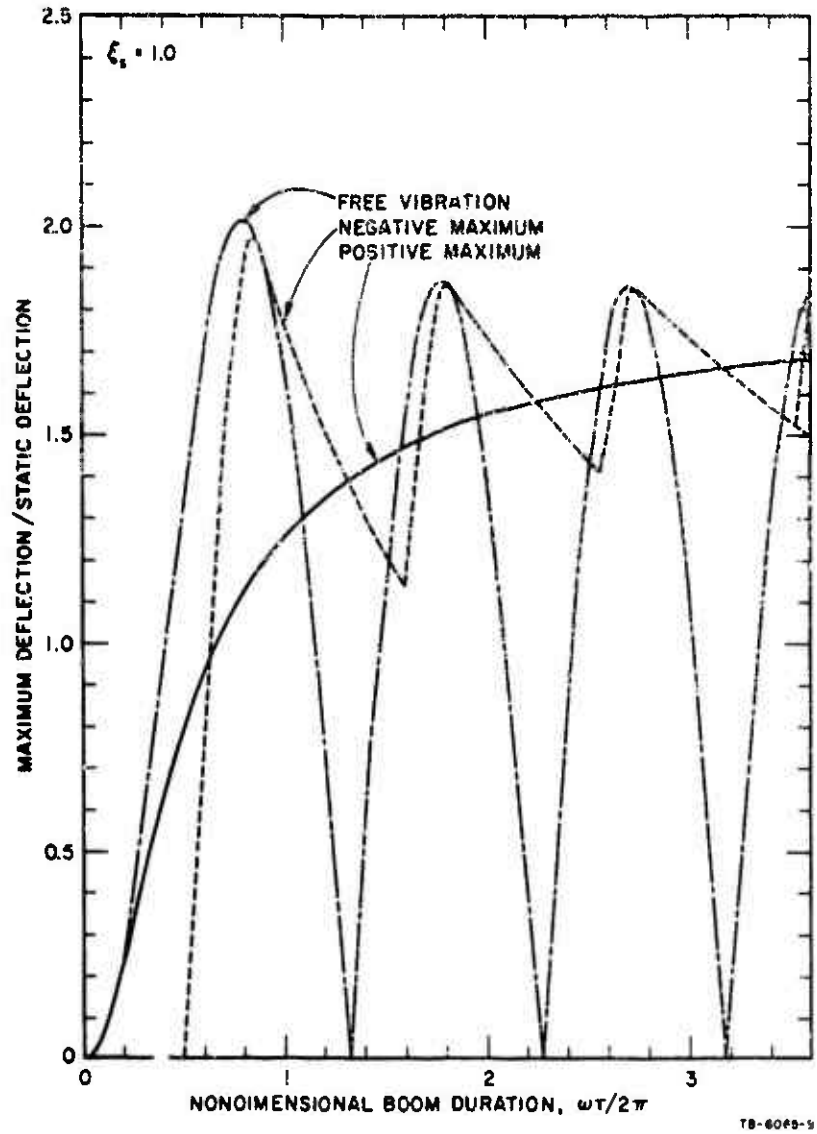


FIG. 12 NONLINEAR FIRST MODE DEFLECTION OF A SQUARE PLATE TO A BOOM LOADING WITH AMPLITUDE SUCH THAT $\xi_s = 1.0$

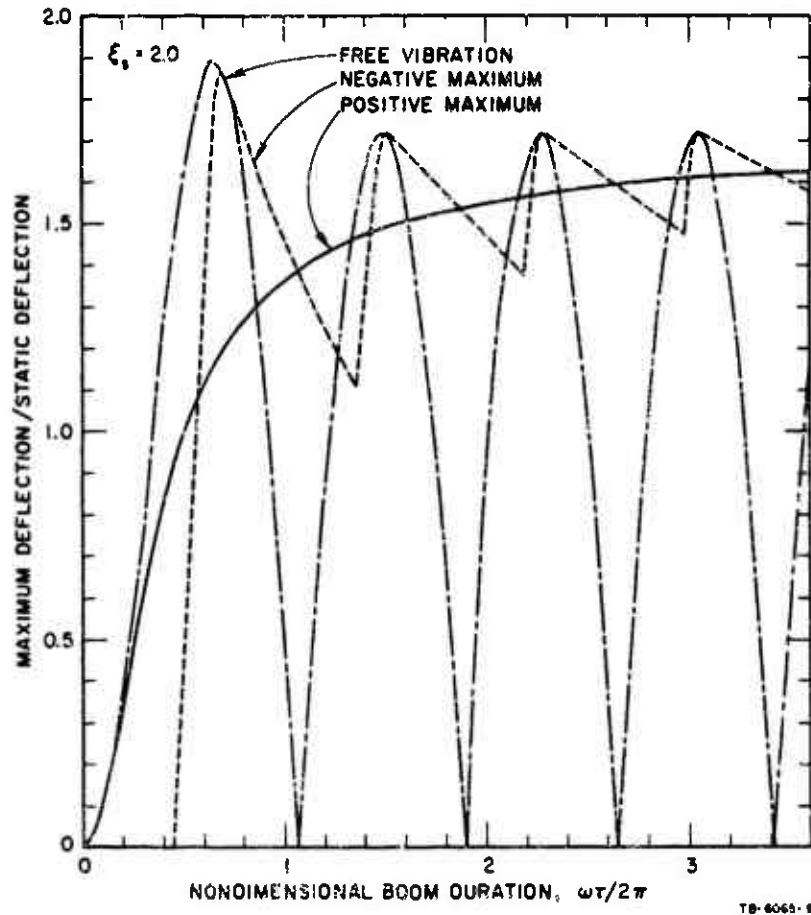


FIG. 13 NONLINEAR FIRST MODE DEFLECTION OF A SQUARE PLATE TO A BOOM LOADING WITH AMPLITUDE SUCH THAT $\xi_s = 2.0$

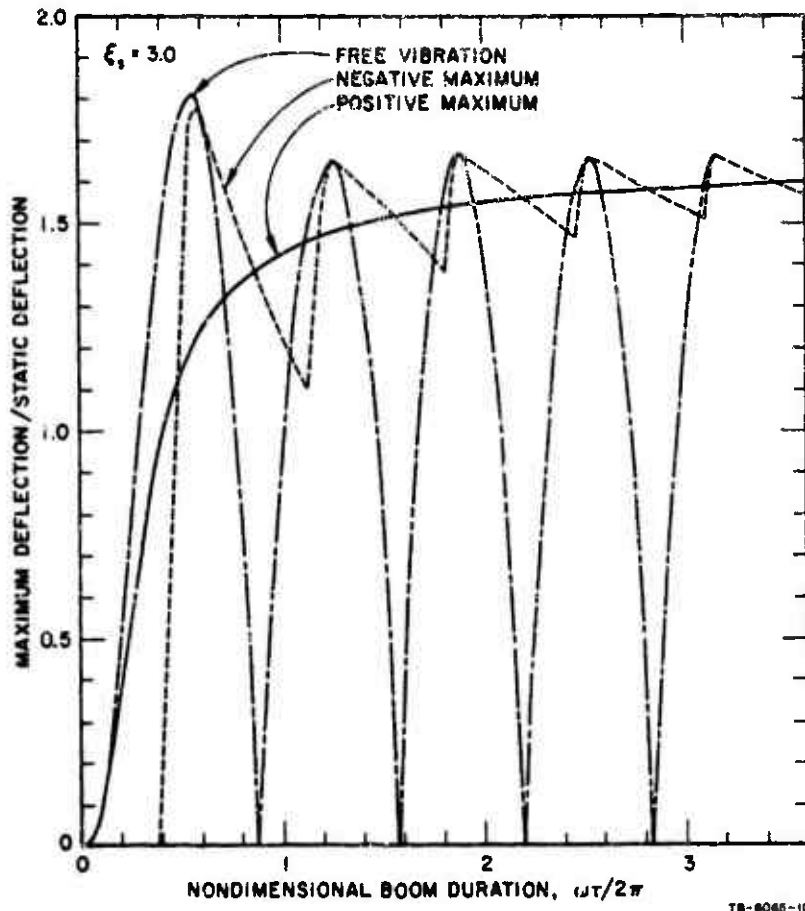


FIG. 14 NONLINEAR FIRST MODE DEFLECTION OF A SQUARE PLATE TO A BOOM LOADING WITH AMPLITUDE SUCH THAT $\xi_s = 3.0$

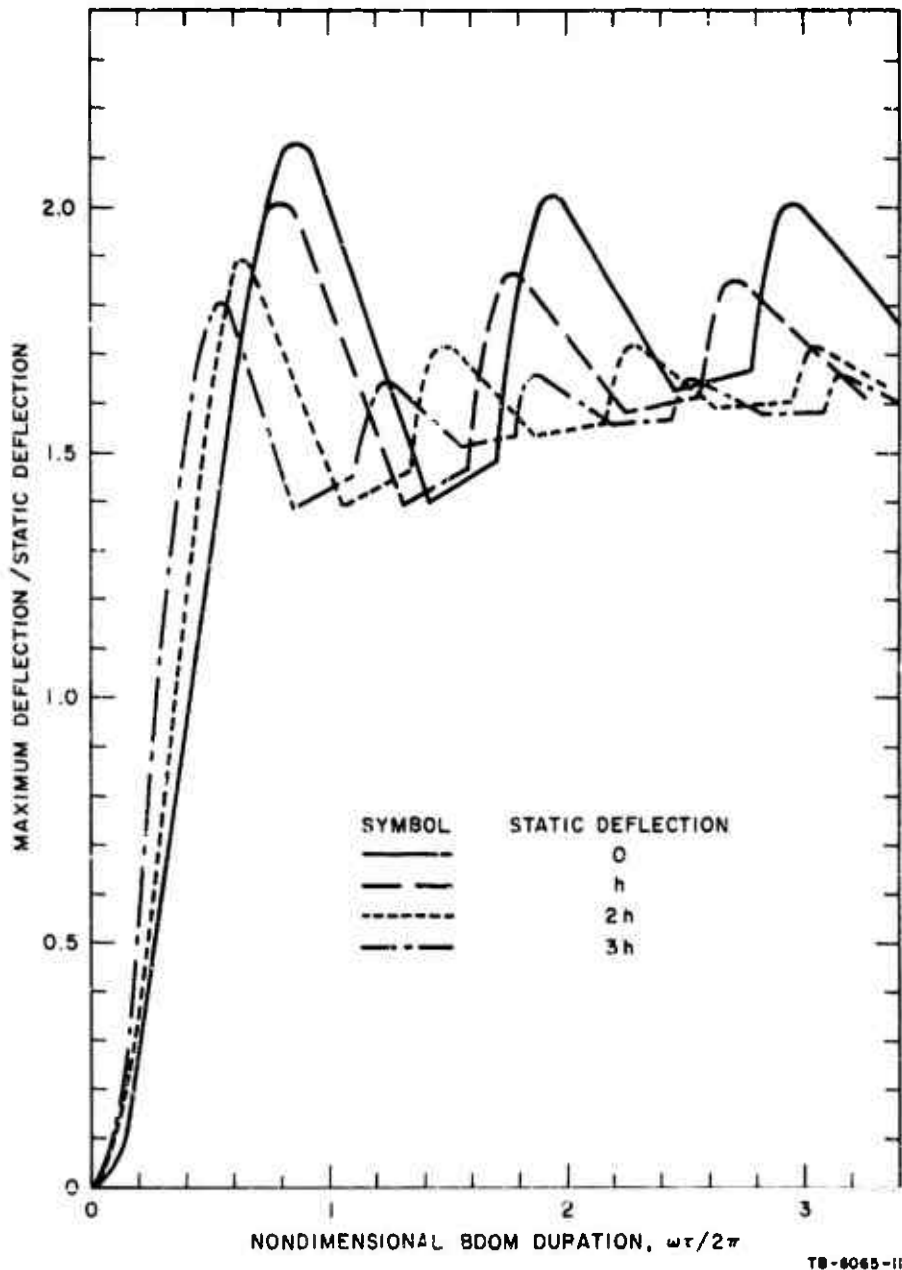


FIG. 15 SUMMARY OF NONLINEAR FIRST MODE DEFLECTION OF A SQUARE PLATE TO A BOOM LOADING

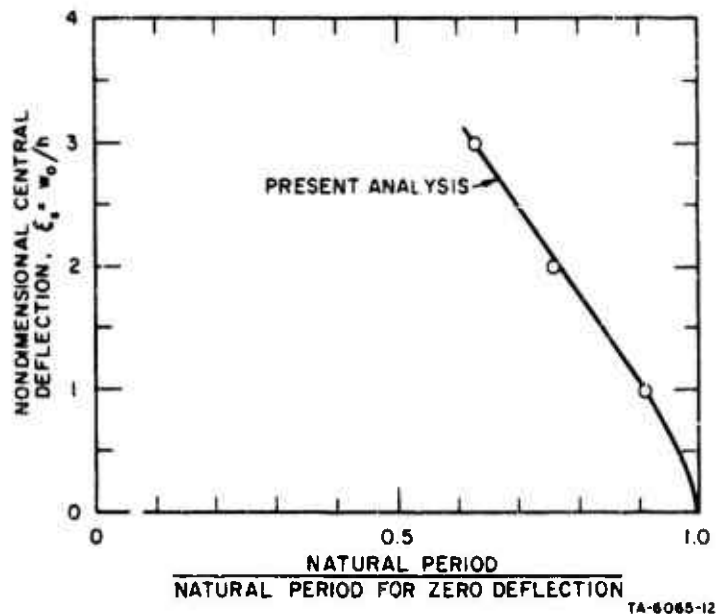


FIG. 16 VARIATION OF APPARENT NATURAL FREQUENCY WITH CENTRAL DEFLECTION

the higher modes. According to the analysis of Appendix E, the stress associated with these modes is primarily bending (not membrane) stress and hence equal to that obtained for the linear case. Therefore add 0.28 times the total linear static stress if the peak occurs during free vibration, or 0.26 if the peak occurs during forcing. That is, for free vibration the dynamic stress is

$$S = 4.9 F_{\xi} \xi_s (1 + 0.167 F_{\xi} \xi_s) + 0.28 (4.4) \xi_s$$

The stress amplification factor, F_{ξ} , is found by dividing S by S_s where

$$S_s = 4.4 \xi_s (1 + 0.186 \xi_s)$$

As an example consider a square window and a boom with the following characteristics

Window area = 45 square feet

Thickness = 1/4 inch

Natural frequency = 7.4 Hz

Boom duration = 0.1 seconds

Peak pressure = 8.85 psf

Nondimensional pressure = 66

According to Fig. 10, the static deflection under the peak pressure is 2h. F_{ξ_1} is 1.80 according to Fig. 15, using an abscissa of 0.1 (7.4) = 0.74. Then for moment we compute

$$F_{\sigma} = \frac{4.9 (1.80) (1 + 0.167 \times 2.0 \times 1.80) + 0.28 (4.4)}{4.4 (1 + 0.186 \times 2.0)}$$
$$= 2.54 \text{ (nondimensional)}$$

a value which appears quite reasonable.

Now let us take three examples of windows and determine the deflections, stresses, and frequencies in response to a 2 psf boom, disregarding internal pressure. The maximum and minimum slenderness ratios (340 and 220) and an intermediate value will be used for the comparison. The calculated values are given in Table 3. Included in the table are values from the linear analysis of the same problem. The window with the largest a/h value gives the most markedly nonlinear behavior. For this window the large deflection theory gives a deflection just 84% of that from the linear theory, and stresses 75% of those from the linear theory. The windows with smaller a/h ratios give deflections about equal to the linear values although the stresses are considerably lower.

TABLE 3

DEFLECTION AND STRESS OF SQUARE WINDOWS UNDER A 2 PSF BOOM

a/h	Static Loading		Dynamic Loading		Linearized Analysis, Dynamic Loading	
	w ₀ /h Deflection -	σ Stress (psi)	w ₀ /h Deflection -	σ Stress (psi)	w ₀ /h Deflection -	σ Stress (psi)
220	0.15	160	0.30	370	0.30	440
280	0.39	240	0.75	560	0.78	730
340	0.78	350	1.43	810	1.70	1080

NOTE: The boom duration and fundamental frequency of the window were presumed to be such that $\omega T/2\pi = 1.0$.

E. Determination of the Amplitude of Internal Pressure

The pressure in a building which is struck by a boom may be caused by

1. flow of the pressure wave through openings in the building (open doors, windows, ventilation ports),
2. overall compression of the building,
3. transmission through flexible areas such as windows.

The third is essentially a different way of stating the second with the added presumption that the only elements which will deflect appreciably are windows. The third cause was assumed by Blume (1965) to be the most important. In this section a calculation is presented determining the pressure rise as a function of overall building compression. The calculation shows that building compression may be the prime cause of internal pressure.

For the calculation we will assume that the history of the internal pressure is sinusoidal with period equal to the boom duration. Internal pressure is calculated from the equilibrium condition between the boom pressure, wall deflection and internal pressure. The necessary equations are derived using the variables illustrated in Fig. 17. The maximum deflection of the roof is

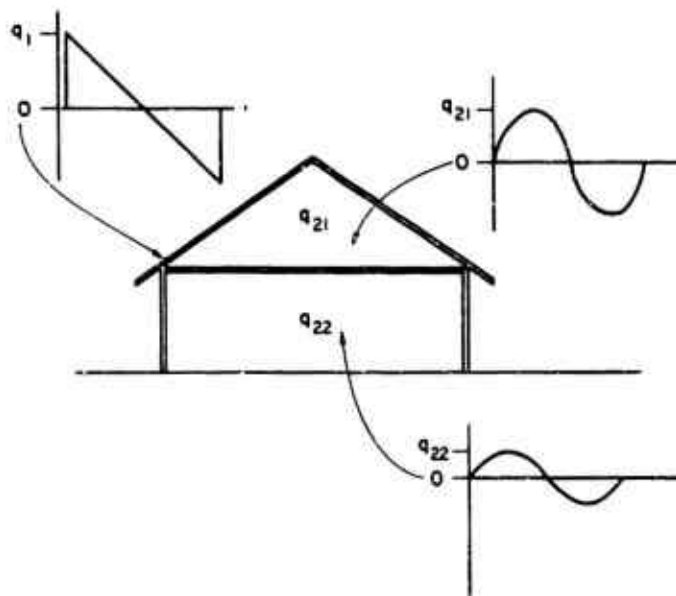
$$w_R = F_{BR} w_{SR} q_1 - (F_{BR} - F_{BIR}) w_{SR} q_{21} \quad (1)$$

where F_{BR} is a dynamic amplification factor for the roof under boom loading.

F_{BIR} is a dynamic amplification factor for the roof under boom and internal pressure (as shown in Figs. 6 and 9).

w_{SR} is average static deflection under unit pressure.

q_1, q_{21} are outdoor boom and attic peak pressures.



TA-6085-29

FIG. 17 PRESSURES CONSIDERED IN CALCULATING THE INTERNAL PRESSURE OF A BUILDING

Comparable equations can be written for the wall and window deflections. Similarly, the ceiling deflection is

$$w_C = F_{IC} w_{SC} (q_{21} - q_{22}) \quad (2)$$

where

F_{IC} is the dynamic amplification factor for the ceiling under internal pressure

w_{SC} is the average static ceiling deflection under unit pressure

q_{22} is the pressure in the first floor rooms.

The internal pressure is caused by deflection of the structural surfaces so that

$$q_{22} = w_C G_C + w_W G_W + w_B G_B \quad (3)$$

$$q_{21} = w_R G_R - w_C G_{RC} \quad (4)$$

where

w_W = window deflection

w_B = wall deflection

G_C , G_W , G_B , G_R , and G_{RC} are factors relating the average deflection to the change in pressure.

The main contribution to internal pressure is from large panel elements such as the roof, large doors, or windows.

To validate the method, a calculation was made of the peak internal pressure in a simple rectangular one-story structure designated PF-6 in the White Sands sonic boom test report of John A. Blume and Associates (1965).

The experimental results obtained during the sonic boom tests indicate a nonlinear relation between internal and external pressure. For low pressures the ratio is about 40% for booms from an F-104. At 5 psf the ratio is 30%. For our calculation the 2 x 4's in the walls and roof

were assumed to provide all the stiffness to those elements and to be fixed at both ends. The positive maximum amplification factor was used from Figs. 4, 7-9. The boom duration was assumed to be 0.10 seconds, a nominal value for the F-104. Calculated frequencies of the structural elements were

Windows 18 Hz

Walls 25 Hz

Roof, Ceiling 8 Hz

Equations 1 through 4 were solved for a 1 psf boom to give

$q_{21} = 0.64$ psf (peak attic pressure)

$q_{22} = 0.36$ psf (peak pressure in first floor rooms)

The value of 0.36 for q_{22} should be compared to the internal pressure of 30 to 40% measured by Blume and Associates.

The correspondence between the calculated and experimental values is very good considering the uncertain basis for some of the assumptions. The present calculations also show the relative importance of the contribution of each element to the pressure rise in the structure. For PF-6, the pressure caused by motion of the roof and ceiling was 32% of the internal pressure, q_{22} . The walls contributed 8%, windows 10%. While the calculations are not verified sufficiently to use for predictions, the results led us to believe that compression is the main cause of the rise in internal pressure.

The preceding procedure is dependent on the validity of certain assumptions concerning the end fixity of wall and roof members, and on windows and doors being closed. Instead of conducting this procedure, which is unverified, it is reasonable to depend on an estimate of the internal pressure based on the experimental results of Blume (1965). For a flexible structure the internal pressure might be estimated at 50% of the boom pressure. If the roof or ceiling or upper floor is a stiff element and the walls are not abnormally flexible, an educated guess indicates that the internal pressure is 25% or less of the boom pressure. Following the reduction of the Edwards Air Force Base test data it is expected that a more reliable basis for these pressure estimates will be available.

F. Summary of Window Behavior Under Boom Loading

Determination of the response of windows to booms requires the computation of a host of factors. Now that each of the factors has been introduced, a summary of the calculation is presented:

1. Estimate window deflection using some guess at internal pressure; use Figs. 4, 8, and 9. This estimate is required for Step 2.
2. Compute the internal pressure acting on the inside of the window as outlined in Section E.
3. Determine the amplification factor for the window as a one-degree-of-freedom system to boom pressure and internal pressure; use Figs. 4, 8, and 9.
4. Modify the computed factor for nonlinear effects: Find the dynamic amplification factors for appropriate static deflection and for zero deflection; multiply the amplification factor from Step 3 by the ratio of these factors to obtain F_{ξ_1} .
5. Modify the values for the multimodal effect: For deflection, let $F_{\xi} = F_{\xi_1}$. For moment or stress, compute F_{σ} , the dynamic amplification factor from the relation

$$F_{\sigma} = \frac{1.115 F_{\xi} (1 + 0.167 F_{\xi} \xi_s) + 0.28}{1 + 0.186 \xi_s}$$

The values of stress and deflection can then be found from the equations

$$\xi = F_{\xi} \xi_s$$

and

$$S = F_{\sigma} S_{\sigma} = 4.4 \xi_s (1 + 0.186 \xi_s) F_{\sigma}$$

It is expected that the dominant displacement response of square windows to a 2 psf far-field sonic boom will be resonance in the fundamental frequency of the window. For longer rectangular windows there will be oscillation in the first and second symmetric modes. The noar-

field boom exhibits oscillations which may excite other window frequencies.

Nonlinear effects are expected for windows with large slenderness ratios (length to thickness over 300) when subjected to 2 psf booms. Instead of a resonance in the fundamental mode at the fundamental frequency, the resonance will occur at a range of frequencies near the fundamental. Freynik (1963) has shown that the Fourier spectrum of response has a continuous band of frequencies with the frequencies from linear theory dominant. The linear frequencies become less dominant as the deflections increase. The magnitude of the peak deflection and stress will be reduced by the nonlinearities. The dynamic amplification factor for deflection and stress will be 1.4 to 2.7.

Maximum stress and maximum deflection are not closely related, even in the static case. Maximum deflection under a uniform static pressure is essentially a function of the first mode response whereas maximum stress receives a contribution of about 10% from the higher modes. In the case of dynamic and particularly nonlinear dynamic response, there is even less correlation between the stress and deflection. Hence, if stress is desired from experimental data, stress should be determined from strain gage measurements, and if deflection is desired, deflection should be measured. One should not depend on calculating one quantity from a measurement of the other at a given point.

SECTION IV

STATISTICAL PREDICTION OF FAILURE

The most important information which should be obtained from a study of window response to sonic booms is an answer to the question: What is the probability of failure of windows under sonic boom pressures? To answer this question we need statistical data of three types:

- Variability of measured maximum pressures for a planned pressure of the sonic boom. These variations are dependent on weather conditions, position, velocity, and acceleration of aircraft, and terrain. With our present state of knowledge about booms, these variations must be handled statistically rather than deterministically.
- Distribution of window sizes in buildings.
- Distribution of window strengths in normal kinds of ceilings.

We have made two computations, assuming first that window glass strengths are distributed normally, and second that they are distributed lognormally. (Available data do not distinguish between these distributions.) We take the coefficient of variation of the strength as 25% as recommended by McKinley (1964) of Pittsburgh Plate Glass. The mean boom strength is taken as 2 psf with a coefficient of variation of 25%. The 25% is characteristic of fairly calm days. The peak stresses used will be those from Table 3, for $a/h = 340$ (most critical case) and for a glass strength of 6600 psi.

The probability of failure is treated from the viewpoint of multiple-valued random phenomena as described by Parzen (1960) (Chap. 7, Sec. 3):

$$P = \int_{-\infty}^{\infty} \varphi_1(x_1) \int_{-\infty}^{x_1} \varphi_2(x_2) dx_2 dx_1 \quad (5)$$

where φ 's are mutually independent probability density functions. For a normal distribution, φ is given by

$$\varphi(x) = \frac{1}{\sqrt{2\pi\sigma}} \exp \left[-1/2 \left(\frac{x-m}{\sigma} \right)^2 \right]$$

PRECEDING PAGE BLANK

and for the lognormal, ϕ is (see Aitchison and Brown (1957))

$$\phi(x) = \frac{1}{\sqrt{2\pi x \sigma}} \exp \left[-1/2 \left(\frac{\log x - m}{\sigma} \right)^2 \right]$$

While an exact analytical solution of Eq. 5 is not possible, the integration can be easily performed numerically. These computations were made for the most critical case of Table 3, that is, for $a/h = 340$. The results are

<u>Distribution</u>	<u>Probability</u>
Normal	.0002
Lognormal	10^{-9}

Evidently then the failure probability is critically dependent on the distribution assumed. It is often said that the normal distribution is impossible because it predicts a finite possibility of negative values of strength and boom pressure. However, if we truncate the normal distribution at zero for the above calculation, we make no noticeable change in the calculated probability. Hence there appears to be neither logical nor experimental bases for determining the correct distribution.

From claim data it appears that the probability of damage for window per 2 psf boom is of the order of 10^{-8} . This indicates that the correct distribution for window strengths may be intermediate between the normal and lognormal. Because of the very low probability value of 10^{-8} , it is not to be expected that laboratory tests can provide the distribution with sufficient accuracy for damage calculations.

SECTION V

SUMMARY

The results of this report apply only to windows which may be considered simply supported. An unknown portion of reel windows are loose or have stress raisers in their mountings. Most windows without such defects will fail under boom pressures of 100 psf or less while at least a few will fail at 10 or 20 psf. Defective windows may fail at even lower levels. At static pressures of 1 to 10 psf the response of simply supported windows becomes nonlinear. The nonlinearity radically effects the relations among deflection, stress, and pressure.

The dominant motion of a window under a 2 psf boom is oscillation in the fundamental frequency. For windows with a length to thickness ratio over 300, nonlinear effects are expected to increase the response in the higher modes. Also the motion in the fundamental mode will occur at a range of frequencies near the fundamental frequency.

A procedure was developed for predicting the deflection and stress of windows under low-pressure booms. The present analysis is adequate although approximate. The procedure is based on a one-degree-of-freedom analysis plus estimates of the multimodal and nonlinear effects and of the interaction with the building motion.

The calculation procedure provides predictions of

- Peak internal pressure caused by incidence of a boom on a building
- Response of a one-degree-of-freedom system to a combined boom and internal pressure loading
- Contribution of higher modes to the stress and deflection of windows
- Modification of window response caused by large-deflection (nonlinear) effects.

The possibility of window failure caused by 2 psf booms is considered from a statistical standpoint. But no reasonable estimate of the statistics of failure can be made because statistical distribution of the strength of glass is not known precisely.

In experimental studies of window motion it is necessary to measure (a) central deflection of the window, (b) strains at several points on both sides of the pane, (c) pressure on both sides of the window, (d) edge fixity of the window. In dynamic studies the history of each of the measurements a, b, and c must be taken. Auxiliary measurements must be made of Young's modulus and Poisson's ratio and the exact dimensions of the glass pane.

A basis for reduction of experimental data on window response is provided. Stress, deflection, and pressure should be nondimensionalized and graphed against each other to show the trends. Dynamic results will require a dynamic analysis similar to those herein to provide an adequate evaluation of the data.

There is need for empirical relations among stress, deflection, and pressure for windows in the usual mountings. Such relations should provide a basis for multimodal response calculations. The next step is a dynamic multimodal calculation. With static relations and dynamic calculations, an adequate base is laid for reducing data from sonic boom tests on windows.

SECTION VI

FURTHER STUDY

To more clearly define the response of windows to sonic booms, four further studies may be considered. The first three should be undertaken in the order listed.

1. An experimental determination of the static and dynamic load-deflection relations for windows. Measurements must be sufficiently complete to provide information on the behavior in several modes.
2. A calculation of the dynamic multimodal response of windows undergoing large deflections.
3. A detailed analysis of the response of windows in test houses at White Sands or Edwards Air Force Base. The required instrumentation consists of an accelerometer, strain gages or displacement gages on the window, and pressure gages on the inside and outside of the window. In addition, a motion gage on the window frame would be useful to show the amount of support movement.
4. A study of the magnitude of internal pressures in buildings subjected to booms. The internal pressure should be measured and calculated from the motion of structural elements. A by-product of such a study would be an accurate method to calculate the frequencies and deflections of building elements in residential construction.

While each of the above studies has scientific and engineering merit, none appears to be justified by the needs of the sonic boom program.

APPENDIX A

DYNAMIC AMPLIFICATION FACTOR: LINEAR

The dynamic amplification factors for the stress and deflection at the center of a simply supported square plate were calculated for a pressure pulse in the form of an N-wave. The static moment and deflection are given by Timoshenko¹⁶ (1959) in the following series form:

$$M_x = \frac{16q_0 a^2}{\pi^4} \sum_{m=1}^{\infty} \sum_{n=1}^{\infty} \frac{m^2 + \nu n^2}{mn(m^2 + n^2)^2} \sin(m\pi x/a) \sin(n\pi y/a) \quad (A.1)$$

$$w = \frac{16q_0 a^4}{\pi^6 D} \sum_{m=1}^{\infty} \sum_{n=1}^{\infty} \frac{1}{mn(m^2 + n^2)^2} \sin(m\pi x/a) \sin(n\pi y/a) \quad (A.2)$$

where M_x is the moment in the x-direction in the plate

w is the deflection

q_0 is the pressure

a is the length of one side of the plate

D is the flexural rigidity of the plate

x, y are coordinates of the plate

ν is Poisson's ratio

m, n are indices denoting the number of modes in the x and y directions respectively.

For purposes of the computer program required to evaluate the equations, nondimensionalized static deflection and moment, Z_0 and M_0 , were defined by

$$w_0 = \frac{16q_0 a^4}{\pi^6 D} Z_0$$

and

$$M_0 = \frac{16q_0 a^2 (1+\nu)}{\pi^4} M_0$$

where w_0 and M_0 are the central deflection and moment under a uniform static pressure. Therefore

$$Z_0 = \sum_{\substack{m=1 \\ \text{odd only}}}^{\infty} \sum_{\substack{n=1 \\ \text{odd only}}}^{\infty} \frac{(-1)^{\frac{m-n}{2}}}{mn(m^2+n^2)^2} = \sum_{\substack{m=1 \\ \text{odd only}}}^{\infty} \sum_{\substack{n=1 \\ \text{odd only}}}^{\infty} R_1(m,n)$$

But for $m = n$

$$R_1(m,m) = \frac{1}{4m^6}$$

and for $m \neq n$

$$R_1(m,n) = R_1(n,m)$$

Now define

$$R(m,m) = \frac{1}{4m^6}$$

and

$$R(m,n) = \frac{2(-1)^{\frac{m-n}{2}}}{mn(m^2+n^2)^2} \text{ for } m \neq n$$

Then the nondimensional static deflection is

$$Z_0 = \sum_{\substack{m=1 \\ \text{odd only}}}^{\infty} \sum_{\substack{n=m \\ \text{odd only}}}^{\infty} R(m,n)$$

The nondimensional static moment is

$$M_0 = \frac{1}{1+\nu} \sum_{\substack{m=1 \\ \text{odd only}}}^{\infty} \sum_{\substack{n=1 \\ \text{odd only}}}^{\infty} (-1)^{m-n} \frac{m^2+\nu n^2}{mn(m^2+n^2)^2} = \frac{1}{1+\nu} \sum_{\substack{m=1 \\ \text{odd only}}}^{\infty} \sum_{\substack{n=1 \\ \text{odd only}}}^{\infty} S_1(m,n)$$

But for $m = n$

$$S_1(m,m) = \frac{1+\nu}{4m^4}$$

and for $m \neq n$

$$S_1(m,n) + S_1(n,m) = \frac{1+\nu}{mn(m^2+n^2)} (-1)^{\frac{m-n}{2}}$$

Therefore, let

$$S(m, n) = \frac{1}{4m^4}$$

and

$$S(m, n) = \frac{(-1)^{\frac{m-n}{2}}}{mn(m^2+n^2)} \quad \text{for } m = n$$

Then

$$MO = \sum_{\substack{m=1 \\ \text{odd only}}}^{\infty} \sum_{\substack{n=m \\ \text{odd only}}}^{\infty} S(m, n)$$

The dynamic deflection is obtained using the mode superposition approach which can be found in many texts (see, for example Norris, et al (1959)). In this method, the deflection is represented as a series of products of three elements:

$$w(t) = \sum_m \sum_n F_{mn}(t) \psi_{mn} \varphi_{mn}(x, y) \quad (A.3)$$

where

- $F_{mn}(t)$ is the dynamic amplification factor
- ψ_{mn} is a participation factor for each mode
- φ_{mn} is the mode shape.

For the square plate

$$\varphi_{mn}(x, y) = \sin(m\pi x/a) \sin(n\pi y/a) \quad (A.4)$$

$$\psi_{mn} = \frac{Q_0 g \int_0^a \int_0^a \varphi_{mn}(x, y) dx dy}{\omega_{mn}^2 \gamma \int_0^a \int_0^a \varphi_{mn}^2(x, y) dx dy} \quad (A.5)$$

$$\omega_{mn}^2 = \frac{\pi^4 Dg}{a^4 \gamma} (m^2 + n^2)^2 \quad (\text{A.6})$$

where

- g is the acceleration of gravity
- γ is the weight per unit area
- ω_{mn} is the natural circular frequency of the mn mode
- q_0 is the maximum of the applied pressure

In the subsequent analyses, we will develop two solutions: one applicable during forcing and the other applicable in the free vibration following forcing. Let the loading be given by the expression $q_0 f(t)$. Then the dynamic amplification factor is

$$F_{mn}(t) = \omega_{mn} \int_0^t f(t') \sin[\omega_{mn}(t-t')] dt' \quad (\text{A.7})$$

For an N-wave the loading is

$$q_0(1-2t/\tau) \text{ for } 0 \leq t \leq \tau$$

where τ is the duration of the N-wave. Then the solution during the time of forcing is given by

$$F_{mn}(t) = 1 - \cos(\omega_{mn} t) - \frac{2t}{\tau} + \frac{2}{\omega_{mn} \tau} \sin(\omega_{mn} t) \quad (0 \leq t \leq \tau) \quad (\text{A.8})$$

$$\psi_{mn} = \frac{16q_0 a^4}{\pi^6 D m n (m^2 + n^2)^2} \quad \text{for } m \text{ and } n \text{ odd} \quad (\text{A.9})$$

$$w(t) = \frac{16q_0 a^4}{\pi^6 D} \sum_{\substack{m=1 \\ \text{odd only}}}^{\infty} \sum_{\substack{n=1 \\ \text{odd only}}}^{\infty} \sin(m\pi x/a) \sin(n\pi y/a) F_{mn}(t) \quad (\text{A.10})$$

Corresponding to this deflection is the moment

$$M_x = \frac{16q_0 a^2}{\pi^4} \sum_{\substack{m=1 \\ \text{odd only}}}^{\infty} \sum_{\substack{n=1 \\ \text{odd only}}}^{\infty} \frac{m^2 + n^2}{m n (m^2 + n^2)^2} \sin(m\pi x/a) \sin(n\pi y/a) F_{mn}(t) \quad (\text{A.11})$$

for $(0 \leq t \leq \tau)$

These values of $w(t)$ and M_x are valid only during the loading, that is, up to $t = \tau$.

Using the quantities R and S , and introducing nondimensionalized central deflection Z and moment M , Eqs. A.10 and A.11 take the following form.

$$Z = \sum_{m=1}^{\infty} \sum_{\substack{n=m \\ \text{odd only}}}^{\infty} R(m,n) \left[1 - \cos(\omega_{mn} t) - \frac{2t}{\tau} + \frac{2}{\omega_{mn} \tau} \sin(\omega_{mn} t) \right] \quad (\text{A.12})$$

$$M = \sum_{m=1}^{\infty} \sum_{\substack{n=m \\ \text{odd only}}}^{\infty} S(m,n) \left[-\cos(\omega_{mn} t) - \frac{2t}{\tau} + \frac{2}{\omega_{mn} \tau} \sin(\omega_{mn} t) \right] \quad (\text{A.13})$$

Figure 3 shows the history of the stress or deflection in the fundamental mode during forcing and during free vibration. Both for deflection and moment in the plate, the major contribution is given by the first mode ($m = n = 1$). Using this fact we can approximately locate the maxima of the deflection and moment by finding the maxima of the first mode. The maxima occur at a time when the derivative of the temporal term is zero, i.e. when

$$\frac{\omega \tau}{2} \sin \omega t = 1 - \cos(\omega t) \quad (\text{A.14})$$

This relation is satisfied in two ways. The positive maxima (defining inward deflection) are given by

$$\omega_{11} t_{\max} = 2 \arctan(\omega_{11} \tau / 2) + 2 i \pi \quad (\text{A.15})$$

where i is zero or a positive integer. The case $i = 0$ is of interest here because it defines the largest of the positive maxima. The negative maxima (defining outward deflection) occur for $\omega_{11} t_{\max} = 2i\pi$ where i is a positive integer. To obtain the largest negative value, i is chosen so that

$$2 i \pi < \omega \tau < 2(i+1) \pi \quad (\text{A.16})$$

The maximum values obtained from Eqa. A.12 and A.13 represent the peak of the first inward motion of the window. To reduce these values to the dynamic amplification factors we divide them by the corresponding static values from Eqa. A1. and A.2. That is

$$F_{\xi} = \frac{Z}{Z_0} = A \text{ or } C$$

and

$$F_m = \frac{M}{M_0} = B \text{ or } E$$

where F_{ξ} and F_m stand for dynamic amplification factors for deflection and moment. A, B, C, E, are names for these factors in the computer program developed to evaluate the equations. A and B are for positive maxima, C and E for negative maxima.

In addition to finding the amplification factor for the multimodal case, it is of interest to find the factor for the first mode. This calculation is easily made because the Eqa. A.15 and A.16 exactly locate the maxima. The amplification factors for deflection and moment in the first mode only are designated A1 and C1. Curves showing the amplification factors for deflection and moment are shown in Figs. 4, 5, and 6.

Following the application of the load the plate undergoes free vibrations which are also associated with deflections larger than the static ones. The deflections during a period of free vibrations have the form

$$w = w_0 \cos [\omega(t-t_0)] + \frac{\dot{w}_0}{\omega} \sin [\omega(t-t_0)]$$

where w_0 and \dot{w}_0 are initial deflection and velocity at the time t_0 . Therefore, the first step in calculating these free motions is to determine the displacement and velocity at the termination of forcing and beginning of free vibration, that is, at $t = \tau$. The displacement and velocity at the center of the plate are

$$w(\tau) = \sum_{\substack{m=1 \\ \text{odd only}}}^{\infty} \sum_{n=1}^{\infty} w_{mn}(\tau) \quad (\text{A.17})$$

and

$$\dot{w}(\tau) = \sum_{m=1}^{\infty} \sum_{n=1}^{\infty} \dot{w}_{mn}(\tau) \quad (\text{A.18})$$

where

$$w_{mn}(\tau) = \frac{16q_0ca^4}{\pi^6 Dmn} \frac{\sin(m\pi x/e) \sin(n\pi y/a)}{(m^2+n^2)^2} \left(-1 - \cos \omega_{mn} \tau + \frac{2}{\omega_{mn} \tau} \sin \omega_{mn} \tau \right) \quad (\text{A.19})$$

$$\dot{w}_{mn}(\tau) = \frac{16q_0e^4}{\pi^6 Dmn} \frac{\omega_{mn} \sin(m\pi x/e) \sin(n\pi y/e)}{(m^2+n^2)^2} \left(\sin \omega_{mn} \tau - \frac{2}{\omega_{mn} \tau} + \frac{2}{\omega_{mn} \tau} \cos \omega_{mn} \tau \right) \quad (\text{A.20})$$

Then for $t \geq \tau$ the deflection is

$$w(t) = \sum_{\substack{m=1 \\ \text{odd only}}}^{\infty} \sum_{n=1}^{\infty} w_{mn}(\tau) \cos \omega_{mn}(t-\tau) + \frac{\dot{w}_{mn}(\tau)}{\omega_{mn}} \sin \omega_{mn}(t-\tau) \quad (\text{A.21})$$

end the nondimensional deflection is

$$Z = \sum_{\substack{m=1 \\ \text{odd only}}}^{\infty} \sum_{n=m}^{\infty} R(m,n) \left\{ \left[(-1 - \cos(\omega_{mn} \tau) + \frac{2}{\omega_{mn} \tau} \sin(\omega_{mn} \tau)) \cos [\omega_{mn}(t-\tau)] \right. \right. \\ \left. \left. + \left[\sin(\omega_{mn} \tau) - \frac{2}{\omega_{mn} \tau} + \frac{2}{\omega_{mn} \tau} \cos(\omega_{mn} \tau) \right] \sin [\omega_{mn}(t-\tau)] \right\}$$

The equations for moment after the loading can be determined by the same procedure. The maxima in the first mode are given by

$$\tan [\omega_{11}(t-\tau)] = \frac{\dot{w}_{11}}{w_{11}\omega_{11}} \quad (\text{A.22})$$

which reduces to

$$\omega_{11}t = \frac{\omega_{11}\tau}{2} + i(\tau) \quad (\text{A.23})$$

where i is zero or a positive integer. i must be large enough so that $t \geq \tau$.

The dynamic amplification factor for the first mode is designated A_2 and is obtained using the time given by Eq. A.23. The multimodal amplification factors are designated AFR and MOMFR, where

$$AFR = \frac{Z}{Z_0} \quad \text{and} \quad MOMFR = \frac{M}{M_0}$$

Z and M are the maximum values of nondimensional deflection and moment which occur during free vibration.

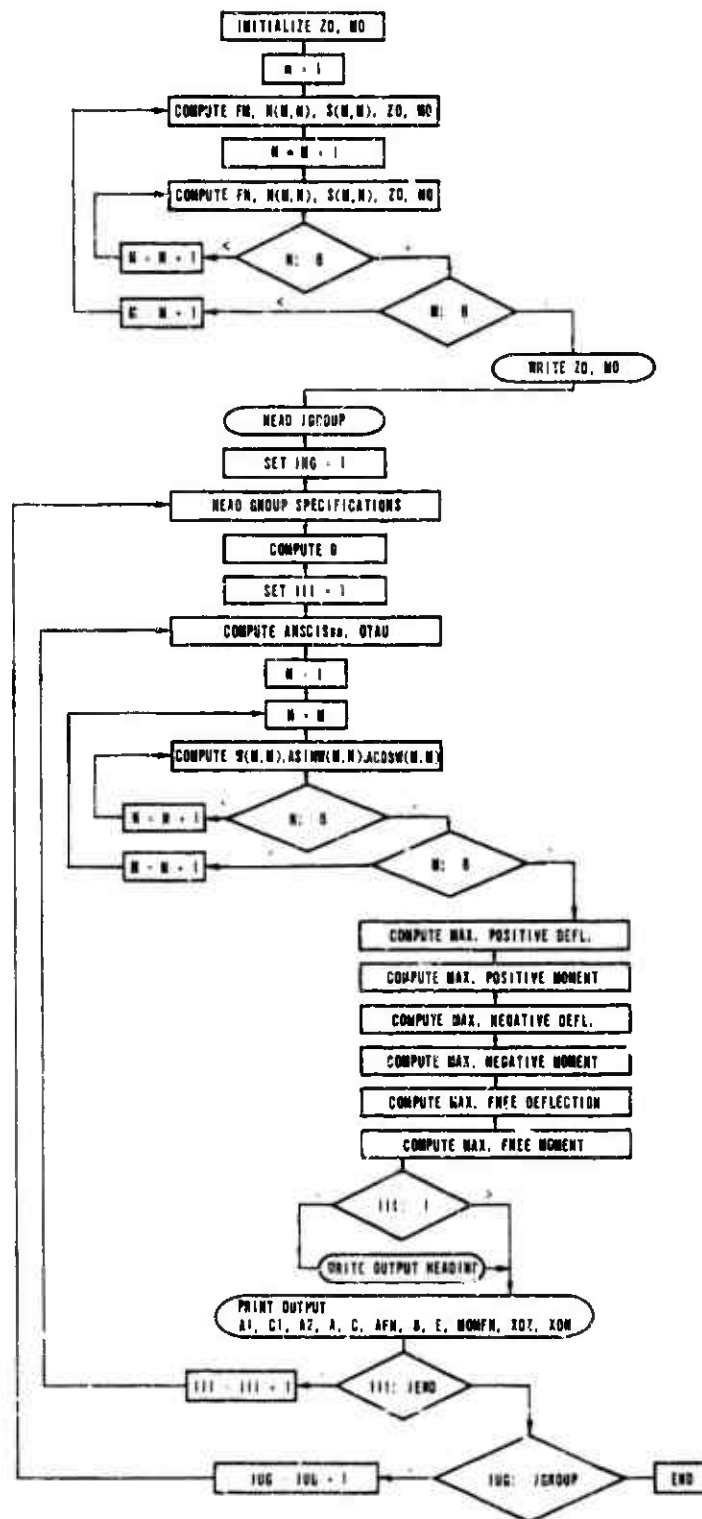
Flow charts for the program are shown in Figs. A.1 - A.3. Most of the variables have been defined in the previous discussion. Comment cards in the program listing further help to clarify the computation system used. The program is written in Fortran IV and has been used with both a Burroughs B5500 and a CDC3200. The input parameters required for the program are explained in the program. A sample set of data cards are

- (1) 2
- (2) 40 21 0.02 0.02 0.005
- (3) 20 21 1.00 0.05 0.005

The first card indicates that there will be two groups of data. The second requires a calculation for 40 values of the abscissa, $\omega t/2\pi$, starting with 0.02 and proceeding to 0.80 in increments of 0.02. The third card produces a calculation for 20 values of abscissa, from 1.00 to 1.95 in steps of 0.05.

The program prints out the input parameters for reference and lists the results in 15 columns. The first column is the abscissa, $\omega t/2\pi$. The next group of six columns are results for the fundamental mode only and consist of A_1 , C_1 , A_2 , A_1 , C_1 , and A_2 . The next six columns are results for all modes up to 11, 11. The printout is in the order A, C, AFR, B, E, MOMFR. The final two columns, headed $X(Z)$ and $X(M)$ indicate the value of ωt at which the negative maximum occurs for deflection and moment, respectively.

Until the abscissa exceeds 0.50, the maximum negative response during forcing is zero. The program does not correctly provide for this



79-6045-25

FIG. A.1 FLOW CHART FOR MULTIPLATE PROGRAM TO COMPUTE MULTIMODAL DYNAMIC AMPLIFICATION FACTORS

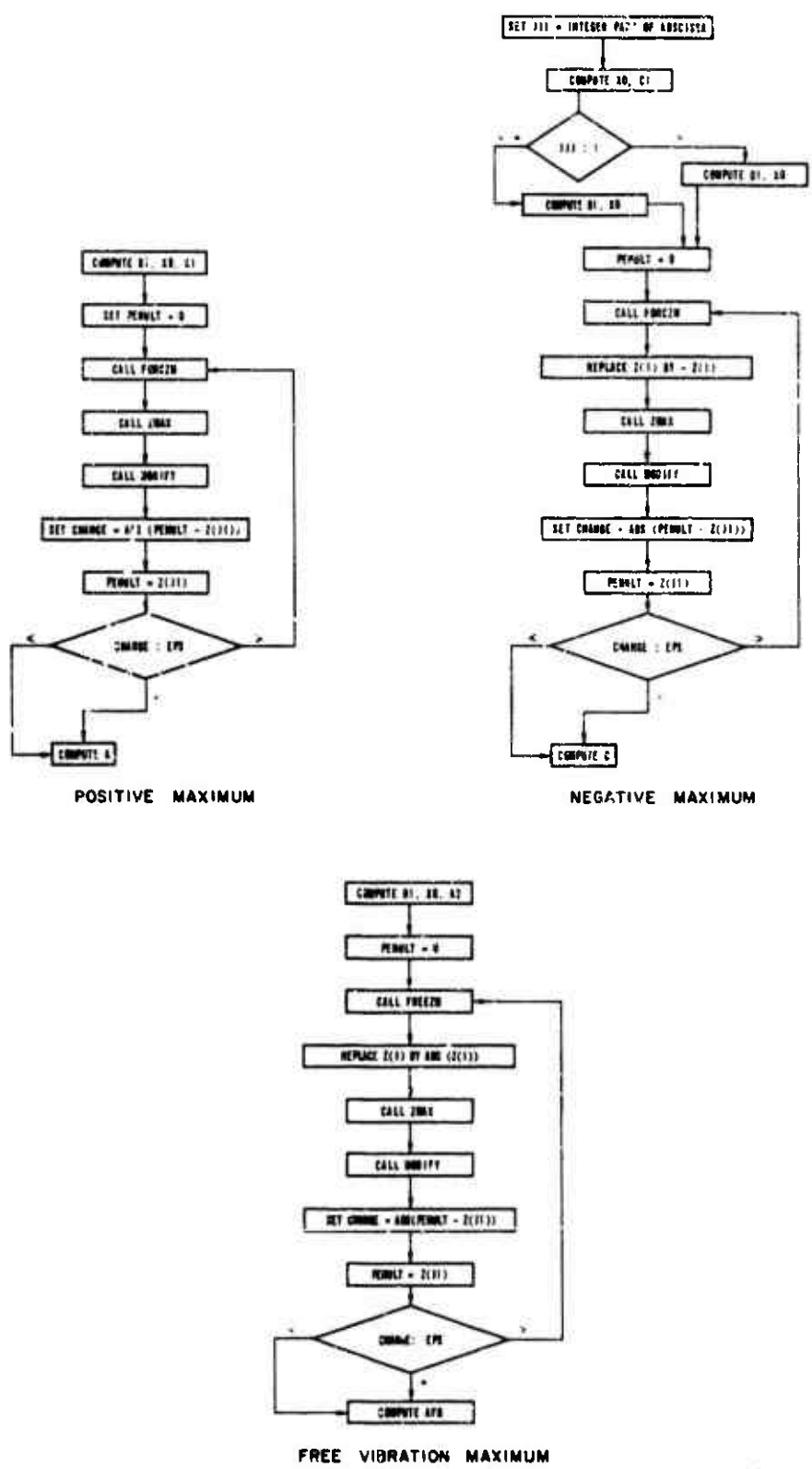
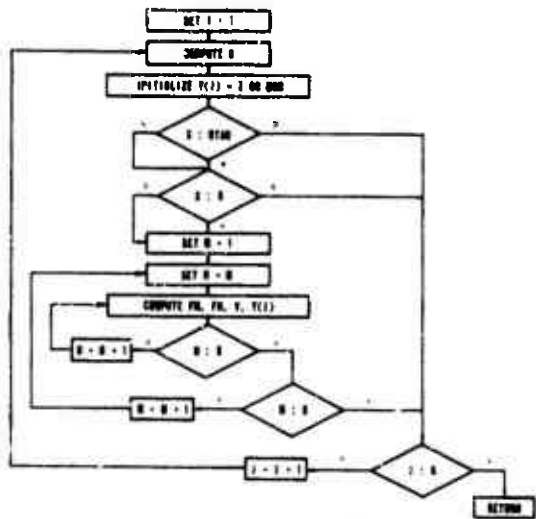
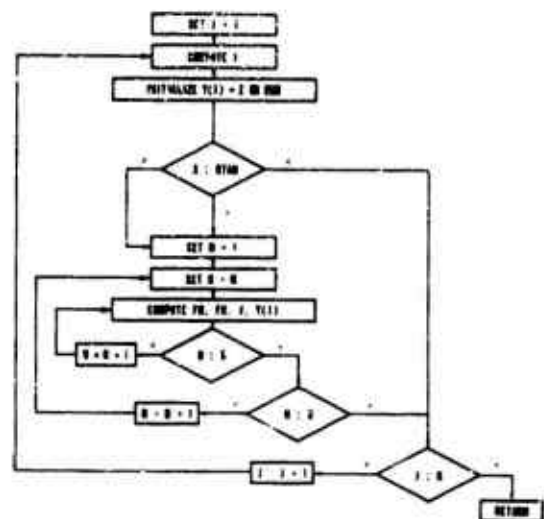


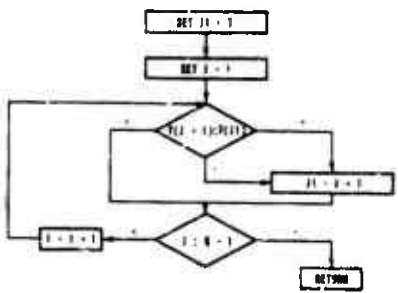
FIG. A.2 FLOW CHARTS FOR PORTIONS OF THE MAIN MULTIPLETE PROGRAM FOR COMPUTATION OF DEFLECTIONS (portions for calculating moments are similar)



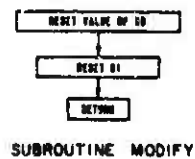
SUBROUTINE FORCZM



SUBROUTINE FREEZM



SUBROUTINE ZMAX



SUBROUTINE MODIFY

TC-600C-37

FIG. A.3 SUBROUTINES USED IN MULTIPLATE PROGRAM

eventuality so that small positive or negative numbers are listed for C and E with $0 < \omega\tau/2\pi < 0.50$. Such values should be disregarded.

The compile time was about 80 seconds on either the CDC3200 or the B5500. The execution time per abscissa value was 9 to 10 seconds on the 3200 and 12 to 13 on the 5500.

The results of the program are depicted in Figs. 4, 5, and 6. The first is the maximum deflection or moment in the first mode. This figure shows the fundamental pattern of the response which is only slightly modified by the participation of higher modes. The first maximum to occur during forcing is called the positive maximum, corresponding to the positive pressure of the N-wave. The curve of positive maximum is monotonically increasing with abscissa values, approaching 20 at infinity. The negative maxima occur at the largest negative oscillation during the time of forcing. Negative maxima may occur under two conditions: at the peak of an oscillation where $dw/dt = 0$ and at the end of forcing when $t = \tau$. The decreasing portions of the curve pertain to the first condition, increasing portions to the second. The free maxima show the largest values and most clearly show the dependence of the maxima on the natural frequencies. For abscissa values of 1.43, 2.46, and 3.47, there is no motion after the time of forcing.

The multimode deflection is very similar to the first mode deflection. The positive maxima show a 2% or 3% increase over the response in the fundamental mode. Negative maxima are very similar to the first mode response throughout and coincide exactly during decreasing portions. The curves for free vibration maxima show a slightly broader hump and about a 4% increase for the first hump, less for later humps. The minimum points on the free vibration curve are not zero, showing that there is always some residual motion following forcing.

In Fig. 6 it is evident that the moment maxima receive a significant contribution from the higher modes. The curve of positive maximum is augmented up to 20%. In spite of this fairly large contribution, the response curve is smooth except for a slight undulation near the origin. The average increase in amplification factor is 0.26. The curve of negative maximum is about 5% higher than those from the first mode. The

curve is bumpy, showing the participation of higher modes, particularly the second symmetric (1,3). The free vibration maxima are modified most significantly by the higher modes. The contribution of the 1,3 mode is clearly evidenced by the triple humps at each main hump of the curve. The increase over the first mode curve varies from 0 to 0.56 with an average value of 0.28.

PROGRAM MULTIPLATE

```

C PROGRAM COMPUTES CENTRAL STRESS AND DEFLECTION OF A SQUARE PLATE UNDER ACTION
C OF AN N-WAVE. FIRST ELEVEN MODES (LINEAR THEORY) ARE USED.
COMMON W,D1,X0,J1,K,OTAU,ASINW,ACOSW
DIMENSION W(6,6),Z(40),R(6,6),S(6,6),MOM(40),ASINW(6,6),ACOSW(6,6)
REAL M0,MOM, MOMFR,INCREM
960 FORMAT(/8H GROUP ,I2,6X,32HABSCISSA = OMEGA TAU/2PI FROM , FORM 960
1 F6.3,4H TO ,F6.3,10X,2HK=,I3,6X,4HEPS=,F6.3//)
961 FORMAT (11X,29HFIRST MODE ONLY,19X,23HELEVEN FORM 961
1MODES)
962 FORMAT (9H ABSCISSA,2X,2HZ+,6X,2HZ-,4X,6HZ FREE,4X,2HM+,6X,2HM-, FORM 962
1 4X,6HM FREE,4X,2HZ+,6X,2HZ-,4X,6HZ FREE,4X,2HM+,6X,2HM-,4X, FORM 962
2 6HM FREE,4X,4HX(Z),3X,4HX(M))
963 FORMAT (1X,F6.3,12F8.4,2X,2F7.3)
980 FCRMAT(1X,13HSTATIC DEFL =,F8.4,9X,13HSTATIC MOMENT =,F8.4)
986 FORMAT (I3,I3,F6.3,F6.3,F6.3)
987 FORMAT (I3)
C BEGIN LOOP TO CALCULATE Z0 AND M0, STATIC DEFL AND MOMENT
Z0=0
M0=0
DO 120 M=1,6
FM=2*M-1
R(M,M)=0.25/FM**6
S(M,M)=0.25/FM**4
Z0=R(M,M)+Z0
M0=S(M,M)+M0
MM=M+1
DO 115 N=MM,6
FN=2*N-1
R(M,N)=(2.0/(FM*FN*(FM**2+FN**2)**2))*(-1.0)** (M-N)
S(M,N)=(1.0/(FM*FN*(FM**2+FN**2)))*(-1.0)** (M-N)
Z0=R(M,N)+Z0
M0=S(M,N)+M0
115 CONTINUE
120 CONTINUE
WRITE (6,980)Z0,M0 WRITE
C CALCULATIONS ARE MADE FOR GROUPS OF VALUES OF ABSCISSA, OMEGA TAU/2PI
C ON FIRST DATA CARD ENTER VALUE FOR THE NUMBER OF DATA GROUPS,JGROUP.
C ON SECOND AND SUCCEEDING DATA CARDS ENTER JEND, K, FIRST, INCREM,
C AND EPS. JEND IS THE NUMBER OF INCREMENTS OF SIZE INCPM IN EACH
C GROUP. K IS THE TOTAL NUMBER OF STEPS TAKEN ON BOTH SIDES OF THE
C FIRST GUESS,X0. K MUST BE ODD. FIRST IS THE FIRST VALUE OF
C ABSCISSA IN EACH GROUP. INCREM DEFINES THE INCREMENTAL CHANGE
C IN ABSCISSA WITHIN EACH GROUP. EPS IS THE ACCURACY REQUIREMENT
C USED IN DECIDING WHETHER TO ACCEPT THE CURRENT MAX OR TO RECYCLE
READ (5,987) JGROUP
DO 691 JUG=1,JGROUP
READ (5,986) JEND,K,FIRST,INCREM,EPS
FK=K
D=1.6/(FK-1.0)
DO 690 III=1,JEND
FIII=III
ABSCIS=FIRST+INCREM*(FIII-1.0)

```

```

    OTAU=ABSCIS*6.2832
    00 180 M=1,6
    00 170 N=M,6
    FM=2*M-1
    FN=2*N-I
    W(M,N)=OTAU*(FM**2+FN**2)/2.0
    ASINW(M,N)=SIN(W(M,N))
    ACOSW(M,N)=COS(W(M,N))
170  CONTINUE
180  CONTINUE
C BEGIN CALC FOR POSITIVE OAF FOR DEFL -- A AND A1
    DI=0
    X0=2.0*ATAN(OTAU/2.0)
    A1=1.0-COS(X0)-2.0*X0/OTAU+2.0*SIN(X0)/OTAU
C CALC 9 VALUES OF Z
    PENULT=0
250  CALL FORCZM (Z,R)                CALL SUB
    CALL ZMAX (Z)                    CALL SUB
    CALL MOOIF                         CALL SUB
    CHANGE=ABS(PENULT-Z(J1))
    PENULT=Z(J1)
    IF (CHANGE-EPS) 280,280,250
280  A=Z(J1)/Z0
C BEGIN CALC FOR POSITIVE OAF FOR MOMENT, B
    DI=0
    X0=2.0*ATAN(OTAU/2.0)
    PENULT=0
310  CALL FORCZM (MOM,S)              CALL SUB
    CALL ZMAX (MOM)                  CALL SUB
    CALL MOOIFY                       CALL SUB
    CHANGE=ABS(PENULT-MOM(J1))
    PENULT=MOM(J1)
    IF (CHANGE-EPS) 340,340,310
340  B = MOM(J1)/M0
C CALCULATE OAF NEG FOR Z
    JJJ = ABSCIS
    OJJJ=JJJ
    X0 = 6.2832 * OJJJ
    C1 = 1.0 - COS(X0) - 2.0 * X0/OTAU + 2.0 * SIN(X0)/OTAU
    IF (JJJ-I) 402,402,404
402  OI=0.5*OTAU/(FK-I.0)
    X0=0.75*OTAU
    GO TO 410
404  OI=(OTAU-6.2832*OJJJ)/(FK-3.0)
    IF (OI-D) 406,406,408
406  OI=0
408  X0=OTAU/2.0+3.1416*OJJJ-OI
410  PENULT=0
420  CALL FORCZM (Z,R)                CALL SUB
    DO 430 I=1,K
    Z(I)=-Z(I)
430  CONTINUE
    CALL ZMAX (Z)                    CALL SUB
    CALL MODIFY                       CALL SUB
    CHANGE=ABS(PENULT-Z(J1))

```

```

PENULT=Z(J1)
IF (CHANGE-EP5) 455,455,420
455 C=Z(J1)/Z0
X0Z=X0
C CALCULATE DAF NEG FOR MOMENT
IF (JJJ-1) 462,462,464
462 O1=0.5*OTAU/(FK-1.0)
X0=0.75*OTAU
GO TO 470
464 O1=(OTAU-6.2B32*0JJJ)/(FK-3.0)
IF (O1-0) 466,466,46B
466 O1=0
46B X0=OTAU/2.0+3.1416*DJJJ-O1
470 PENULT=0
480 CALL FORCZM (MOM,5) CALL SUB
OO 490 I=1,K
MOM(I)=-MCM(I)
490 CONTINUE
CALL ZMAX (MOM) CALL SUB
CALL MODIFY CALL SUB
CHANGE=ABS(PENULT-MOM(J1))
PENULT=MOM(J1)
IF (CHANGE-EP5) 510,510,480
510 E = MOM(J1)/M0
XOM=X0
C CALC MAX OEFL DURING FREE VIBRATION
D1=0
X0= OTAU/2.0 + 3.1416*(DJJJ+1.0)
A20= -1.0 -COS(OTAU) +2.0*SIN(OTAU)/OTAU
A2V= SIN(OTAU)- 2.0/OTAU +2.0* COS(OTAU)/OTAU
A2 = A20 *COS(X0-OTAU) + A2V *SIN(X0 -OTAU)
PENULT=0
606 CALL FREEZM (Z,R) CALL SUB
OO 610 I=1,K
Z(I)=ABS(Z(I))
610 CONTINUE
CALL ZMAX (Z) CALL SUB
CALL MODIFY CALL SUB
CHANGE=ABS(PENULT-Z(J1))
PENULT=Z(J1)
IF (CHANGE-EP5) 620,620,606
620 AFR= Z(J1)/Z0
C CALC MAX MOMENT OURING FREE VIBRATION
D1= 0
X0= OTAU/2.0 + 3.1416*(OJJJ+1.0)
PENULT=0
635 CALL FREEZM (MOM,S) CALL SUB
OO 640 I=1,K
MOM(I)=ABS(MOM(I))
640 CONTINUE
CALL ZMAX (MOM) CALL SUB
CALL MODIFY CALL SUB
CHANGE=ABS(PENULT-MOM(J1))
PENULT=MOM(J1)
IF (CHANGE-EP5) 650,650,635

```

```

650 MOMFR= MOM(J1)/M0
    IF (111-1) 660,660,661
660 DATEND=JEND
    FLAST=FIRST+INCREM*(OATEND-1.0)
    WRITE (6,960) JUG,FIRST,PLAST,K,EPS
    WRITE (6,961)
    WRITE (6,962)
661 WRITE (6,963) ABSCIS,A1,C1,A2,A1,C1,A2,A,C,AFR,B,E,MOMFR,XOZ,XOM
690 CONTINUE
691 CONTINUE
    ENO

```

```

SUBROUTINE FREEZM (Y,G) SUB
COMMON W,O1,X0,J1,K,OTAU,ASINW,ACOSW
DIMENSION W(6,6),Y(40),G(6,6),ASINW(6,6),ACOSW(6,6)
OO 712 J=1,K
DIFF=J-(K+1)/2
X=X0 +DIFF * O1
Y(J) = 0
IF (X-OTAU) 712,704,704
704 OO 711 M=1,6
    DO 710 N=M,6
        FM=2*M-1
        FN=2*N-1
        V=X*(FM**2+FN**2)/2.0
        Y(J)= G(M,N)*((2.0*ASINW(M,N)/W(M,N)-1.0-ACOSW(M,N))*COS(V-W(M,N))
1+(ASINW(M,N)-2.0/W(M,N)+2.0*ACOSW(M,N)/W(M,N))*SIN(V-W(M,N)))+Y(J)
710 CONTINUE
711 CONTINUE
712 CONTINUE
    RETURN
    ENO

```

```

SUBROUTINE FORCZM (Y,G) SUB
COMMON W,O1,X0,J1,K,OTAU
DIMENSION W(6,6),Y(40),G(6,6)
OO 820 J=1,K
DIFF=J-(K+1)/2
X=X0 + DIFF * O1
Y(J) = 0
IF (X-OTAU) 802,802,820
802 IF (X) 820,804,804
804 DO 819 M=1,6
    OO 818 N=M,6
        FM=2*M-1
        FN=2*N-1
        V=X*(FM**2+FN**2)/2.0
        Y(J)=G(1,N)*(1.0-COS(V)-2.0*V/W(M,N)+2.0*SIN(V)/W(M,N))+Y(J)
818 CONTINUE
819 CONTINUE
820 CONTINUE
    RETURN
    ENO

```

```

SUBROUTINE ZMAX (Y) SUB

```

```

COMMON W,D1,X0,J1,K,OTAU
DIMENSION W(6,6),Y(40),G(6,6)
J1=I
KKI=K-1
00 870 J=I,KKI
IF (Y(J+I)-Y(JI)) 870,865,865
865  JI =J+I
870  CONTINUE
C MAXIMUM Y IS AT Y(J1)
RETURN
END

```

```

SUBROUTINE MODIFY
COMMON W,D1,X0,J1,K,OTAU
DIMENSION W(6,6)
DIFF =J1-(K+1)/2
X0=X0+DIFF*D1
FK=K
O1=2.0*O1/(FK+1.0)
RETURN
END

```

```

3
10 21 1.00 0.02 0.005
10 21 2.00 0.02 0.005
10 21 3.00 0.02 0.005

```

APPENDIX B

RESPONSE TO INTERNAL PRESSURE

The response of an enclosing structure to the combination of boom loading and internal pressure will be considered in two ways. First, it will be assumed that the internal pressure is a function of the deflection of the element considered. This corresponds to the case in which the moving element is the main contributor to the deflection which is causing the internal pressure rise. For the second calculation, it is assumed that the internal pressure is known and is not modified by motion of the element. This situation occurs if the motion of the element is making only a small contribution to the internal pressure.

For the first case the relevant equation of motion is

$$D \left(\frac{\partial^4 w}{\partial x^4} + 2 \frac{\partial^4 w}{\partial x^2 \partial y^2} + \frac{\partial^4 w}{\partial y^4} \right) + \frac{\gamma}{g} \frac{\partial^2 w}{\partial t^2} = q(t, x, y) - Gw \quad (B.1)$$

where

- D is the plate stiffness
- w is the deflection
- x, y are rectangular coordinates in the plate
- γ is the weight/unit area
- g is the acceleration of gravity
- t is time
- q is the boom loading
- G is a coefficient relating deflection and internal pressure generated by this deflection. Possible units are pounds/cubic inch.

Following the derivation in Chapter 5 of Norris, et al.²¹, let

$$w = \sum \sum D_{mn}(t) \psi_{mn}(x, y) \quad (B.2)$$

end

$$q(t, x, y) = f(t) q(x, y) q_1$$

where

- $D_{mn}(t)$ is the dynamic amplification factor for each mode, mn
- ψ_{mn} is the participation factor for each mode
- $\varphi_{mn}(x,y)$ is the shape factor for each mode
- $f(t)$ is the time variation of applied pressure
- $q(x,y)$ is the spatial variation of pressure
- q_1 is the peak amplitude of pressure.

A uniform pressure distribution over the plate is assumed, so that $q(x,y) = 1.0$. Then, for the modal deflection

$$\varphi_{mn}(x,y) = \sin(m\pi x/a) \sin(n\pi y/a) \quad (B.3)$$

the participation factor is

$$\begin{aligned} \psi_{mn} &= \frac{16q_1 a^4}{\pi^6 D_{mn} (m^2 + n^2)^2} \quad \text{for } m \text{ and } n \text{ odd} \\ &= 0 \quad \text{for } m \text{ and/or } n \text{ even.} \end{aligned} \quad (B.4)$$

The participation factor is identical for static and dynamic loading.

In Norris, et al.²¹, it is shown that

$$q_1 a(x,y) = \sum_{m=1}^{\infty} \sum_{n=1}^{\infty} \psi_{mn} \omega_{mn}^2 \frac{Y}{g} \varphi_{mn}(x,y) \quad (B.5)$$

and that

$$D \left(\frac{\partial^4}{\partial x^4} + \frac{\partial^4}{\partial x^2 \partial y^2} + \frac{\partial^4}{\partial y^4} \right) \varphi_{mn} = \omega_{mn}^2 \frac{Y}{g} \varphi_{mn} \quad (B.6)$$

Now Eq. B.2 is substituted into Eq. B.1 taking into account Eqs. B.5 and B.6. The following result is obtained:

$$\sum_{m=1}^{\infty} \sum_{n=1}^{\infty} \frac{Y}{g} \psi_{mn} \varphi_{mn} \left[\frac{d^2 D_{mn}}{dt^2} + \omega_{mn}^2 D_{mn} + \frac{G}{Y} D_{mn} - \omega_{mn}^2 f(t) \right] = 0 \quad (B.7)$$

In order to satisfy this equation, each of the terms of the doubly infinite series must be zero. The solution for any term is

$$D_{mn} = \frac{\omega_{mn}^2}{\sqrt{\omega_{mn}^2 + \frac{Gg}{\gamma}}} \int_0^t f(t') \sin [\sqrt{\omega_{mn}^2 + \frac{Gg}{\gamma}} (t-t')] dt' \quad (B.8)$$

Compare Eq. B.8 with the solution for external loading only, which is

$$D_{mn} = \omega_{mn} \int_{t_0}^t f(t') \sin [\omega_{mn} (t-t')] dt' \quad (B.9)$$

The effect of internal pressure is to increase the frequency by the ratio

$$R_D(m,n) = \frac{\sqrt{\omega_{mn}^2 + \frac{Gg}{\gamma}}}{\omega_{mn}} \quad (B.10)$$

and to decrease the dynamic amplification factor by the same ratio. For the further discussion only the first mode, ω_{11} , will be considered. For this case Fig. 4 can be used to determine D_{11} provided the frequency and D_{11} are modified by the ratio in Eq. B.10.

For the second case the internal pressure is assumed to be sinusoidal, given by the equation

$$\begin{aligned} q &= q_2 \sin 2\pi t/\tau \quad \text{during forcing} \\ &= 0 \quad \text{after forcing} \end{aligned}$$

where

τ is the duration of forcing, and coincides with the boom duration
 q_2 is peak applied pressure.

For a combination of boom and internal pressure, the loading is

$$\begin{aligned} q &= q_1(1-2t/\tau) - q_2 \sin 2\pi t/\tau \quad (t \leq \tau) \\ &= 0 \quad (t > \tau) \end{aligned} \quad (B.11)$$

A solution was obtained for the first mode only using the methods of Appendix A. The deflection during forcing is

$$\begin{aligned} \frac{Z}{Z_1} = & q_1 [1 - \cos(\omega t) - 2t/\tau + \frac{2}{\omega\tau} \sin(\omega t)] \\ & - q_2 \frac{1}{1 - 4\pi^2/\omega^2\tau^2} [+ \sin(2\pi t/\tau) - 2\pi/\omega\tau \sin(\omega t)] \end{aligned} \quad (\text{B.12})$$

where

Z_1 is the static deflection under $q_1 = 1.0$

With internal pressure alone ($q_1 = 0$) the maxima occur for

$$\cos(2\pi t/\tau) = \cos(\omega t)$$

The relevant maxima occur at the times

$$t = \frac{2n\pi}{\omega + \frac{2\pi}{\tau}} \quad (\text{B.13})$$

The time of positive maximum is given by $n = 1$. The time of negative maximum is given by the largest even value of n such that $t \leq \tau$.

During free vibration the deflection is

$$\begin{aligned} \frac{Z}{Z_1} = & q_1 \left\{ [-1.0 - \cos(\omega\tau) + \frac{2}{\omega\tau} \sin(\omega\tau)] \cos[\omega(t-\tau)] + [\sin(\omega\tau) \right. \\ & \left. - \frac{2}{\omega\tau} + \frac{2}{\omega\tau} \cos(\omega\tau)] \sin[\omega(t-\tau)] \right\} - q_2 \left[\frac{\omega\tau/2\pi}{1 - 4\pi^2/\omega^2\tau^2} \right] \left\{ \sin(\omega\tau) \cos[\omega(t-\tau)] \right. \\ & \left. + [-1.0 + \cos(\omega\tau)] \sin[\omega(t-\tau)] \right\} \end{aligned} \quad (\text{B.14})$$

For $q_1 = 0$, the condition for a maximum is that

$$\cos[\omega(t-\tau)] = \cos(\omega\tau)$$

That is, for

$$\frac{\omega t}{2\pi} = \frac{n}{2} + \frac{1}{2} \frac{\omega\tau}{2\pi} \quad (\text{B.15})$$

Two programs were written to carry out the required computations. The one called Boom-and-Internal makes calculations of maxima when both q_1 and q_2 are not zero. No flow chart is provided for it as the program is a simplification of the Multiplate program in Appendix A. The input parameters are the same as for Multiplate with the addition of Q_1 and Q_2 which are the coefficients of the boom and internal pressure terms. The maxima of Eqs. B.12 and B.14 were determined by trial using the same system as in Multiplate.

When $q_1 = Q_1 = 0$, the terms of the maxima can be determined analytically, so a special program called Sinusoid1 was written to calculate this case. There are no data cards needed for this program as the input is part of the program instructions.

Both programs were written in Fortran IV and run on a Burroughs B5500 computer. Compilation times were about 50 seconds. Sinusoid1 executed at a rate of 0.12 seconds per abscissa value, Boom-and-Internal took 0.15 seconds for each.

The results of the Sinusoid1 program are in Fig. 7. This shows some of the same features as the response to booms but the first peaks are higher and later peaks are lower.

The results of Boom-and-Internal for $Q_2 = 0.25$ and 0.50 are shown in Figs. 8 and 9. Evidently the main effect of internal pressure is to decrease the first hump in the response curve. Otherwise the curves are essentially the same as those in Fig. 4 for boom loading only.

PROGRAM BOOM AND INTERNAL

```

C PROGRAM COMPUTES MOTION OF A 1 DOF SYSTEM TO A BOOM LOADING AND AN
C INTERNAL PRESSURE IN THE FORM OF A SINE WAVE
COMMON D1,X0,J1,K,OTAU,Z,ABSCIS,Q1,Q2,EPS
DIMENSION Z(40)
901 FORMAT (9H ABSCISSA,4X,4HPOS,4X,4HNEG,3X,5HDFREE,4X,4HTPOS,4X,
1 4HTNEG,3X,5HTFREE)
950 FORMAT(S2H DAF FOR 1DOF SYSTEM UNDER SINUSOID AND BOOM LOADING)
955 FORMAT (/10X,2HK=,12,4X,4HEPS=,F6.3,4X,3HQ1=,F6.3,4X,3HQ2=,F6.3/)
963 FORMAT (1X,F6.2,6F8.3)
986 FORMAT (I3,I3,5F6.3)
987 FORMAT (I3)
WRITE (6,950)
READ (5,987) JGROUP
DO 691 JG=1,JGROUP
READ (5,986) JEND,K,FIRST,DELTA,EPS,Q1,Q2
WRITE (6,955) K,EPS,Q1,Q2
WRITE (6,901)
FK=K
D=1.6/(FK-1.0)
DO 690 I=1,JEND
F11I=I
ABSCIS = FIRST+DELTA *(F11I-1.0)
OTAU = ABSCIS*6.2832
C*****CALCULATE ZPOS
D1=D
X0=2.0*ATAN(OTAU/2.0)
PENULT = 0
250 CALL FORCEZ
CALL ZMAX
CHANGE = ABS(PENULT-Z(J1))
PENULT = Z(J1)
IF (CHANGE-EPS) 280,280,250
280 ZPOS=Z(J1)
XPOS = X0/OTAU
C*****CALCULATE ZNEG
JJJ = ABSCIS
DJJJ=JJJ
X0 = 6.2832*DJJJ
IF (JJJ-1) 402,402,404
402 D1=0.5*OTAU/(FK-1.0)
X0=0.75*OTAU
GO TO 418
404 D1=(OTAU-6.2832*DJJJ)/(FK-3.0)
IF (D1-D) 406,406,408
406 D1=D
408 X0=OTAU/2.0+3.1416*DJJJ-D1
418 PENULT = 0
420 CALL FORCEZ
DO 430 I=1,K
Z(I) = -Z(I)
430 CONTINUE
CALL ZMAX

```

```

        CHANGE = ABS(PENULT-Z(J1))
        PENULT=Z(J1)
        IF (CHANGE-EPS) 455,455,420
455     ZNEG = Z(J1)
        XNEG = X0/OTAU
C*****CALCULATE ZFREE
        Q1=0
        X0 = OTAU/2.0+3.1416*(DJJJ+1.0)
        PENULT = 0
606     CALL FREEZ
        DO 610 I=1,K
        Z(I) = ABS(Z(I))
610     CONTINUE
        CALL ZMAX
        CHANGE = ABS(PENULT-Z(J1))
        PENULT=Z(J1)
        IF (CHANGE-EPS) 620,620,606
620     ZFREE = Z(J1)
        XFREE = X0/OTAU
        WRITE (6,963) ABSCIS,ZPOS,ZNEG,ZFREE,XPOS,XNEG,XFREE
690     CONTINUE
691     CONTINUE
        END
C
C*****SUBROUTINE FORCEZ
        SUBROUTINE FORCEZ
        COMMON D1,X0,J1,K,OTAU,Z,ABSCIS,Q1,Q2,EPS
        DIMENSION Z(40)
        DO 820 J=1,K
        DIFF = J-(K+1)/2
        X = X0 + DIFF * D1
        Z(J) = 0
        IF(X-OTAU) 802,802,820
802     IF(X) 820,803,803
803     AA=ABS(ABSCIS-1.0)
        Z1 = 1.0-COS(X)-2.0*X/OTAU+2.0/OTAU*SIN(X)
        IF (AA-EPS) 810,810,804
804     Z2= -ABSCIS**2/(1.0-ABSCIS**2)*(-SIN(X)/ABSCIS) + SIN(X)/ABSCIS)
        GO TO 815
810     Z2= -0.5*(SIN(X)-X*COS(X))
815     Z(J) = Q1*Z1 + Q2*Z2
820     CONTINUE
        RETURN
        END
C*****SUBROUTINE FREEZ
        SUBROUTINE FREEZ
        COMMON D1,X0,J1,K,OTAU,Z,ABSCIS,Q1,Q2,EPS
        DIMENSION Z(40)
        DO 712 J=1,K
        DIFF = J-(K+1)/2
        X = X0 + DIFF*D1
        Z(J) = 0
        IF(X-OTAU) 712,704,704
704     AA=ABS(ABSCIS-1.0)
        Z1 = (-1.0-COS(OTAU)+2.0*SIN(OTAU)/OTAU)*COS(X -OTAU)

```

```

1 +(SIN(OTAU)-2.0/OTAU+2.0*COS(OTAU)/OTAU)*SIN(X -OTAU)
IF (AA-EPS) 710,710,706
706 Z2=- (ABSCIS/(1.0-ABSCIS**2))*(SIN(OTAU)*COS(X -OTAU)+(-1.0+
1 COS(OTAU))*SIN(X -OTAU))
GO TO 711
710 Z2= 3.1416*COS(X-OTAU)
711 Z(J) = Q1*Z1 + Q2*Z2
712 CONTINUE
RETURN
END
C*****SUBROUTINE ZMAX
SUBROUTINE ZMAX
COMMON D1,X0,J1,K,OTAU,Z,ABSCIS,Q1,Q2,EPS
DIMENSION Z(40)
J1=1
KK1=K-1
DO 870 J=1,KK1
IF (Z(J+1)-Z(J)) 870,865,865
865 J1 = J+1
870 CONTINUE
DIFF = J1-(K+1)/2
X0 = X0 + DIFF * D1
FK = K
D1 = 2.0*D1/(FK+1.0)
RETURN
END
?DATA                                C078SEAMAN/TAPES
4
25 21 0.5 0.02 0.005 1.0 0.0
20 21 1.6 0.02 0.005 1.0 0.0
15 21 2.7 0.02 0.005 1.0 0.0
15 21 3.7 0.02 0.005 1.0 0.0
?END OF DECK

```

PROGRAM SINUSOID

```

C SINUSOID CALCULATES THE PEAK POSITIVE, NEGATIVE, AND FREE RESPONSE
C OF A 1 DOF SYSTEM TO A LOADING IN THE FORM OF A SINE WAVE EXTENDING
C FROM ZERO TO 2 PI , WITH NO LOADING THEREAFTER
900  FORMAT (1X,F6.2,2X,6F8.3)
901  FORMAT (9H ABSCISSA,4X,4HDPOS,4X,4HDNEG,3X,SHDFREE,4X,4HTPOS,4X,
      1 4HTNEG,3X,5HTFREE)
902  FORMAT (35H DAF FOR 1DOF SYSTEM UNDER SINUSOID)
      WRITE (6,902)
      WRITE (6,901)
      DO 100 I1=1,200
      IF (I1-50) 10,5,10
5     DPOS=1.5708
      DNEG=-3.1416
      DFREE=3.1416
      TPOS=0.5
      TNEG=1.0
      TFREE=1.0
      ABSCIS = 1.0
      GO TO 90
10    BII=I1
      ABSCIS=BII*0.02
      DPOS = ABSCIS/(1.0-ABSCIS)*SIN(6.2832*ABSCIS/(1.0+ABSCIS))
      TPOS = 1.0/(1.0+ABSCIS)
      M = 0.5 + 0.5*ABSCIS
      FN = 2*M
      DNEG = ABSCIS/(1.0-ABSCIS)*SIN(6.2832*FN*ABSCIS/(1.0+ABSCIS))
      DNEG2 = ABSCIS/(1.0-ABSCIS**2)*SIN(6.2832*ABSCIS)
      TNEG = FN/(1.0+ABSCIS)
      DIFF = -DNEG + DNEG2
      IF (DIFF) 15,20,20
15    DNEG=DNEG2
      TNEG=1.0
      N = ABSCIS + 1.0
20    DFREE = 2.0*ABSCIS/(1.0-ABSCIS**2)*SIN(3.1416*ABSCIS)*(-1.0)**N
      M = ABSCIS + 1.5
      FM = 2* M-1
      TFREE = 0.5 + FM/4.0/ABSCIS
90    WRITE (6,900) ABSCIS,DPOS,DNEG,DFREE,TPOS,TNEG,TFREE
100   CONTINUE
      END

```

APPENDIX C

NONLINEAR LOAD-DEFLECTION RELATIONS

The purpose of this appendix is to determine the form of the large-deflection relations between load and deflection, and between stress and deflection for square plates. These relations will be used in the next appendix as a basis for reducing available experimental data.

In the literature the large deflection of square plates has been determined only for some specific values of Poisson's ratio and certain boundary conditions; the available solutions do not precisely fit the present requirements. An approximate rather than rigorous solution seemed adequate, and it was also desirable to have the results in analytical rather than graphical form. A modification of the method recommended by Föppl (1924) was used for the calculations.

The method of Föppl is to seek a solution as the sum of two parts: one for membrane and one for bending behavior. Thus the applied loading can be represented as

$$Q = Q_b + Q_m \quad (C.1)$$

where

$$Q = \frac{qs^4}{Eh^4}, \text{ a nondimensional loading parameter and subscripts refer to bending and membrane.}$$

q = pressure

s = length of the side of the square plate

In Föppl's approach, the relations between the Q 's and the deflection are taken from the solutions of the small deflection bending and of the membrane problems. These solutions have the form

$$Q_b = A_0 \xi \quad (C.2)$$

$$Q_m = B_0 \xi^3$$

so that Eq. C.1 becomes

PRECEDING PAGE BLANK

$$Q = A_0\xi + B_0\xi^3 \quad (C.3)$$

where

ξ is the nondimensional deflection w_0/h

w_0 is the central deflection

A_0 and B_0 are functions of Poisson's ratio.

When this cubic equation is solved, the membrane and bending stresses can be determined from

$$S_b = C_0\xi \quad (C.4)$$

$$S_m = D_0\xi$$

where

$$S = \frac{\sigma a^2}{Eh^3}$$

σ = stress

C_0 and D_0 are functions of Poisson's ratio, ν .

The natural boundary conditions for this solution are the simple support for bending and the immovable edge for membrane action. However, in our case the edge is movable. Therefore, the sought solution was assumed to have the form of Eqs. C.3 and C.4 but with unknown coefficients B_1 and D_1 . Further, it was assumed that B and B_1 would vary in the same way as a function of ν so that

$$\frac{B_0(\nu_1)}{B_1(\nu_1)} = \frac{B_0(\nu_2)}{B_1(\nu_2)} \quad (C.5)$$

and similarly for D and D_1 .

The steps taken in the solution were the following:

1. Find the relations between deflections and pressures for the separate cases of membrane and bending, that is, find $A_0(\nu)$ and $B_0(\nu)$ in Eq. C.2.
2. Use the theoretical solution of Levy¹⁵ to determine the coefficients B_1 and D_1 (for the case $\nu = 0.316$).
3. Determine the coefficients B_1 and D_1 for the case $\nu = 0.23$ using Eq. C.5.

The values of A_0 and C_0 are readily determined from Chapter 5 of Timoshenko (1959). The results are given in Table C.1.

TABLE C.1
COEFFICIENTS FOR LARGE DEFLECTION OF SQUARE PLATES

ν	A_0	B_0	C_0	D_0	B_1	D_1
0.23	21.7	28.65	5.91	2.434	12.8	1.32
0.316	22.8	31.3	6.635	2.582	14.0	1.40

The coefficients B and D were determined from the analysis on p. 419 of Timoshenko (1959) for the membrane problem. The following expressions were taken for the displacements

$$\begin{aligned}
 w &= w_0 \cos \frac{\pi x}{a} \cos \frac{\pi y}{a} \\
 u &= c \sin \frac{2\pi x}{a} \cos \frac{\pi y}{a} \\
 v &= c \sin \frac{2\pi y}{a} \cos \frac{\pi x}{a}
 \end{aligned} \tag{C.6}$$

where u , v are displacements in the plane of the plate in the x and y directions, respectively, and the origin is at the center of the plate. The strain energy of the plate is then

$$V = \frac{Eh}{2(1-\nu^2)} \left\{ \frac{5\pi^4}{64a^2} w_0^4 - \frac{5-3\nu}{3a} \pi^2 c w_0^2 + \left[\frac{9-\nu}{4} \pi^2 + \frac{32}{9} \frac{(1+\nu)}{2} \right] c^2 \right\} \tag{C.7}$$

The principle of virtual displacements was used then as outlined in Timoshenko to find c and w_0 as functions of the applied pressure. The values of B and D in Table 1 are the calculated results.

The theoretical values of Levy¹⁵ were used to find B_1 and D_1 . His results were plotted as membrane and bending stresses versus applied pressure for the case $\nu = 0.316$. Two relations were used for the determination. The first was the requirement that the deflection in Eq. C.4

be unique, that is, that

$$\xi^2 = \frac{S_b^2}{C_0^2} = \frac{S_m}{D_1} \quad (C.8)$$

Levy's results were used for S_b and S_m and a value of $D_1 = 1.40$ was found (see Fig. C.1). Then Eqs. C.3 and C.4 were combined as

$$Q = \frac{A_0}{C_0} S_b + B_1 \left(\frac{S_m}{D_1}\right)^{3/2} \quad (C.9)$$

Using Levy's values for Q , S_b and S_m , a solution was obtained for B_1 . The determination of B_1 is shown in Fig. C.2 from which it is evident that Eq. C.9 is a good representation of the relation. Following this evaluation of B_1 and D_1 for $\nu = 0.316$, B_1 and D_1 for $\nu = 0.23$ were calculated using Eq. C.5.

The following equations are then available for solving large deflection problems in square plates with simply supported boundaries.

$$\begin{aligned} Q &= A_0 \xi + B_1 \xi^3 \\ S_b &= C_0 \xi \\ S_m &= D_1 \xi^2 \end{aligned} \quad (C.10)$$

In the next appendix experimental values are used to re-evaluate the coefficients A_0 through D_1 in these equations.

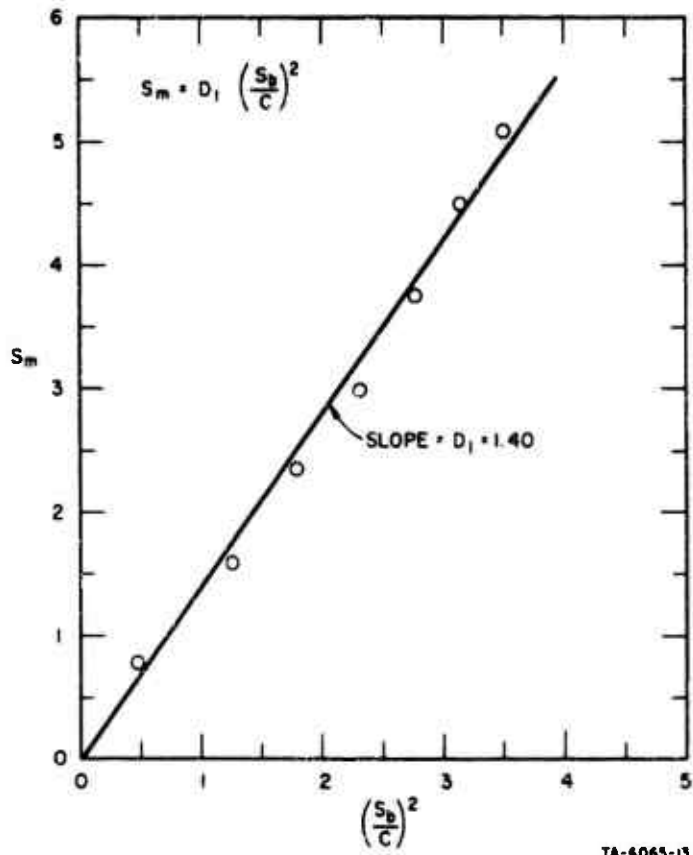
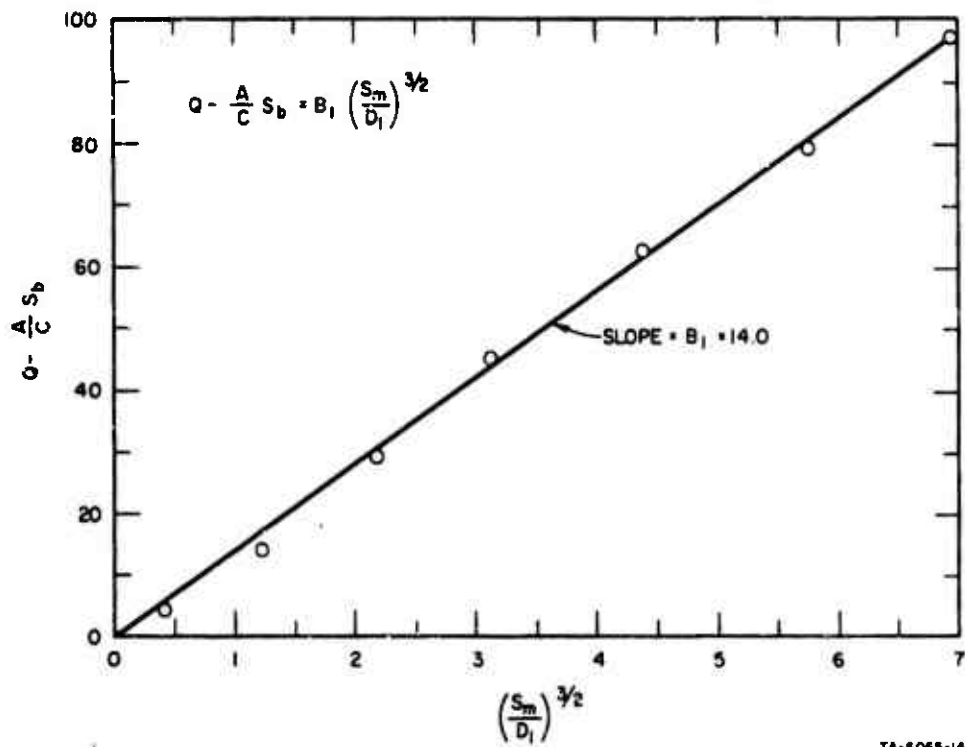


FIG. C.1 GRAPH FOR DETERMINATION OF D_1



TA-6065-14

FIG. C.2 GRAPH FOR DETERMINATION OF B_1

APPENDIX D

EXPERIMENTAL DATA ON WINDOW RESPONSE

Load-deflection and stress-deflection relations can be obtained from results of several experimental studies. This study is based on the results of Bowles and Sugarman (1952), Orr (1957), and Fraynik (1963). The data are fitted to equations in the form of those in Appendix C.

Load-Deflection Relations

A load-deflection equation like Eq. C.3 will be determined first.

$$Q = A_0 \xi + B_0 \xi^3$$

where

$$Q = \text{nondimensional load} = \frac{q}{E} \left(\frac{a}{h}\right)^4$$

$$\xi = \text{nondimensional deflection} = w_0/h$$

$$q = \text{applied pressure}$$

$$E = \text{Young's modulus}$$

$$a = \text{distance between supports of square panel}$$

$$h = \text{thickness}$$

$$w_0 = \text{center deflection}$$

The value of A_0 will be taken as 21.7, the theoretical value obtained from small-deflection plate theory for Poisson's ratio equal to 0.23. The data will be related to this equation to determine the value for B_0 , and to indicate how well the data follow the analytical equation. We will use the data on ultimate deflection (deflection just preceding fracture) from Orr (1957) and from Bowles and Sugarman (1952). The resulting equation should be especially applicable at the ultimate strength of panels, but will not necessarily describe the load-deflection relation at low pressures. The data used are in Tables D.1 and D.2. Orr's results represent individual panels whereas Bowles and Sugarman tested 30 or 40 panels of each size and reported mean values and standard deviations from the mean. The results are treated here as though they were from square panels although Orr's panels were rectangular,

TABLE D.1

ULTIMATE DEFLECTION AND BURSTING PRESSURES

(Data from Orr)

h Thickness (in.)	s ² ares (in. ²)	a/h	q Msx. Pres. (psf)	Q* Nondim. Pressure	w ₀ Max. Defl. (in.)	$\xi = \frac{w_0}{h}$
PLATE						
0.2373	6720	346	52.25	516	1.200	5.05
0.240	6720	342	51.87	491	1.189	4.95
0.303	6720	271	80.65	300	1.200	3.96
0.301	6720	273	56.17	214	1.000	3.32
0.2344	8360	389	39.26	631	1.300	5.54
0.2453	8360	373	36.02	84	1.200	4.89
0.3045	8360	300	54.09	305	1.200	3.94
0.305	8360	299	54.02	303	1.200	3.93
0.242	9840	410	32.52	638	1.400	5.78
0.239	9840	416	23.58	485	1.200	5.02
0.303	9840	327	44.56	355	1.311	4.33
0.304	9840	327	44.00	343	1.300	4.28
0.369	9840	269	56.13	204	1.200	3.25
0.372	9840	267	57.85	203	1.200	3.23
0.114	8640	816	16.72	5120	1.400	12.3
SOLEX						
0.248	8640	387	54.22	740	1.400	5.65
0.373	8640	257	73.20	197	1.200	3.22
0.383	8640	251	61.36	148	1.000	2.61
0.255	11530	421	38.56	847	1.502	5.88
0.248	11530	433	41.52	1015	1.600	6.45

* $Q = \frac{qa^4}{Eh^4}$, E was taken as 10^7 psi.

TABLE D.2

ULTIMATE DEFLECTION AND BURSTING PRESSURES
(Data from Bowles and Sugarman)

Sample Description (in.)	No. of Samples	h Thickness (in.)	a/h *	q Max. Pres. (paf)	Q** Nondim. Pressure	w ₀ Max. Defl. (in.)	$\xi = \frac{w_0}{h}$
1/8 plate	40	0.122	328	0.754	871	0.760	6.22
3/16 plate	30	0.197	203	1.412	240	0.726	3.69
1/4 plate	30	0.25	160	1.811	118.7	0.651	2.60
3/8 plate	30	0.373	107	3.625	48.0	0.610	1.63
24 oz sheet	30	0.110	363	0.692	1210	0.807	7.33
32 oz sheet	30	0.158	253	1.369	562	0.870	5.50
3/16 sheet	30	0.195	205	1.910	339	0.860	4.41

* a = 40 in. for all samples.

** $Q = \frac{qa^4}{Eh^3}$ and E was taken as 10^7 psi.

with aspect ratios between 0.6:1.0 and 1.0:1.0. The data points are plotted in Fig. D.1. The trend line is given by the equation

$$Q = 21.7\xi + 2.80\xi^3 \quad (D.1)$$

which appears to fit the data quite well. For comparison the theoretical results of Levy (1942) for Poisson's ratio of 0.316 are also shown.

A check can be made to determine how well Eq. D.1 predicts deflections at low loads, using the data of Bowles and Sugarman on four panels (listed in Table D.3). These four sets of load-deflection points are shown in Fig. D.2 with the theoretical curve of Eq. D.1. Eq. D.1 will be used in subsequent work, with the understanding that its accuracy is limited at small deflections. It may be noted that the data from the tests of the 1/8-inch plate are far from the other points. This tendency is noted in later graphs also. The discrepancy may be caused by using the mean thickness of 0.122 inch in calculating ξ , Q , and S or there may have been some experimental error.

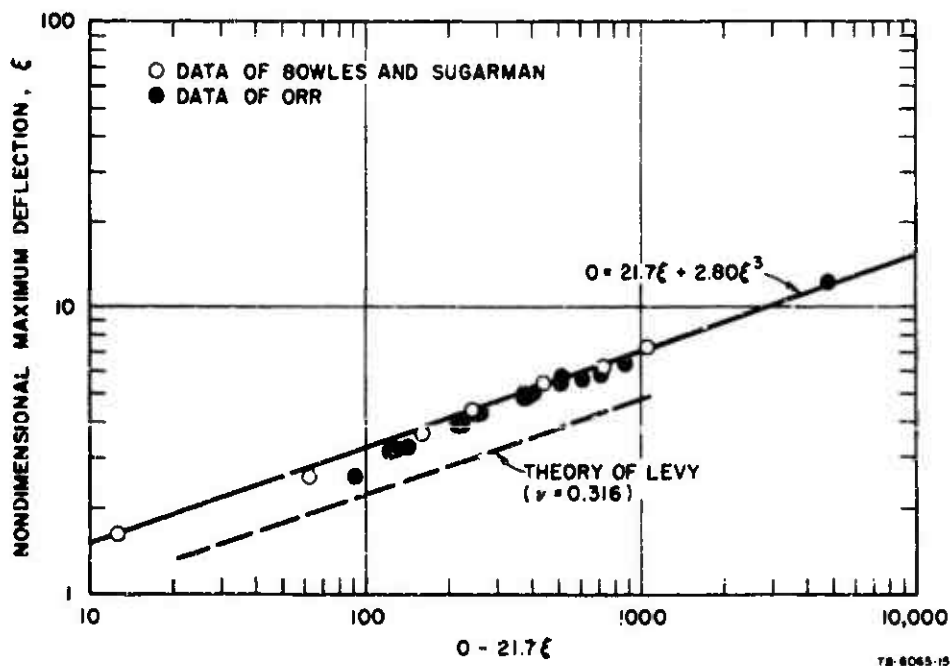


FIG. D.1 RELATION BETWEEN APPLIED PRESSURE AND DEFLECTION AT RUPTURE

TABLE D.3

STRESS DATA

(Data from Bowles and Sugarman)

h* Thickness (in.)	q Pressure (psi)	Q** Nondim. Pressure	$\xi = w_0/h$ Nondim. Deflection	σ_b Bending Stress (psi)	σ_m Membrane Stress (psi)	S _b ** Nondim. Bending Stress	S _m ** Nondim. Membrane Stress
0.122	0.05	57.8	1.61	595	215	6.40	2.315
	0.10	115.5	2.40	795	415	8.55	4.465
	0.15	173.2	2.98	900	580	9.68	6.24
	0.20	231.0	3.43	950	750	10.23	8.07
	0.25	269.0	3.78				
0.195	0.05	8.9	0.59	577	92	2.43	.39
	0.10	17.8	0.92	950	200	3.99	.84
	0.15	26.6	1.19	1222	297	5.14	1.25
	0.20	35.5	1.41	1430	400	6.01	1.68
	0.25	44.4	1.62	1595	525	6.71	2.21
	0.30	53.3	1.81	1725	645	7.25	2.71
	0.35	62.2	1.96	1827	752	7.68	3.16
0.25	0.1	6.55	0.42	670	40	1.715	0.10
	0.2	13.10	0.70	1240	160	3.17	0.41
	0.3	19.65	0.93	1705	295	4.37	0.75
	0.4	26.20	1.13	2075	435	5.31	1.11
	0.5	32.75	1.32	2367	563	6.06	1.44
	0.6	39.30	1.48	2615	685	6.69	1.75
	0.7	45.85	1.63	2825	815	7.23	2.09
	0.8	52.40	1.76	2990	950	7.65	2.43
0.373	0.2	2.65	0.25	595	45	0.684	0.052
	0.4	5.42	0.41	1170	100	1.345	0.115
	0.6	7.94	0.57	1730	180	1.99	0.207
	0.8	10.58	0.70	2270	270	2.61	0.311
	1.0	13.23	0.81	2740	380	3.15	0.437
	1.2	15.87	0.92	3170	520	3.64	0.598
	1.4	18.52	1.03				
	1.6	21.15	1.12				
	1.8	23.80	1.21				
	2.0	26.47	1.30				
2.2	29.10	1.38					

* The thickness of the specimen tested was not known, so the mean thickness for the group of specimens was used.

** Nondimensional pressures and stresses were calculated using $E = 10^7$ psi.

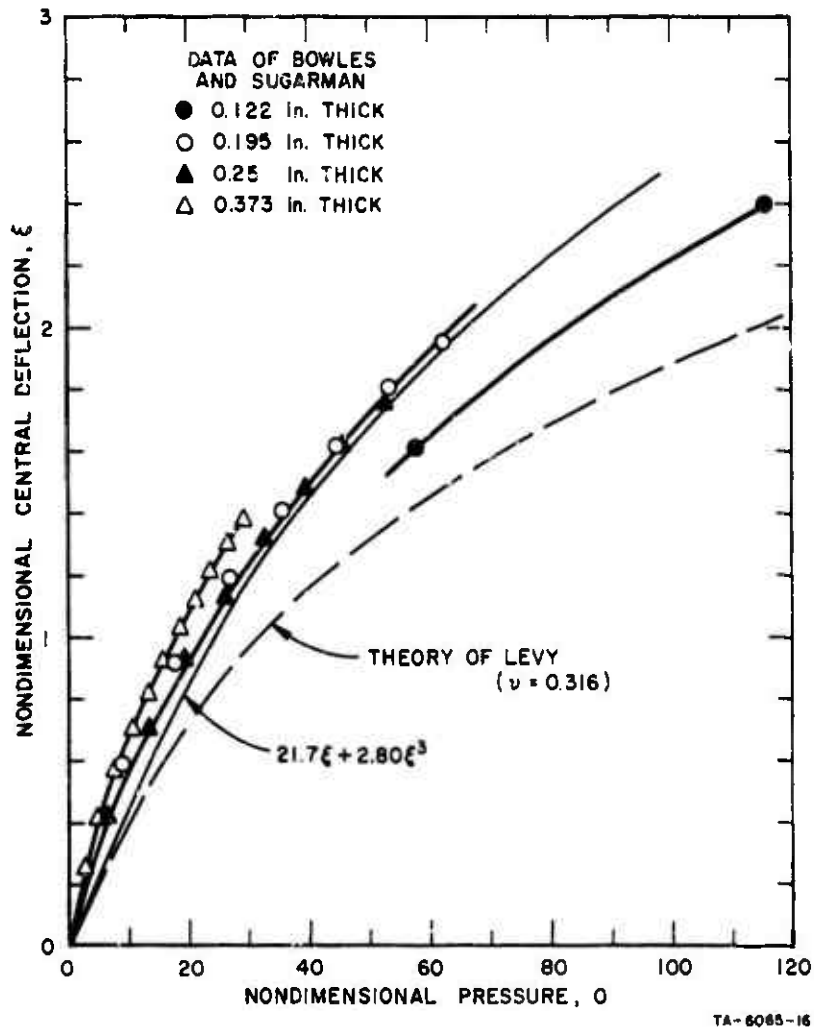


FIG. D.2 EXPERIMENTAL AND THEORETICAL LOAD-DEFLECTION CURVES

Ultimate Deflection and Ultimate Strength

The deflection which a panel can undergo before failing is closely related to the thickness of the panel. The deflection data of Tables D.1 and D.2 are plotted in Figs. D.3 and D.4 to show this relation. It is clear from the figures that there is a marked difference between the results of Orr (1957) and of Bowles and Sugarman (1952), and there is a noticeable difference between the plate and sheet glass results in the latter reference.

To predict ultimate strength of glass panes it is useful to plot nondimensional maximum pressure against the thickness ratio, e/h , as in Fig. D.5. Again there is a distinct difference between the results of Bowles and Sugarman (1952) and of Orr (1957). The pressures taken by the panes of the former are about 2.5 times those in the latter. This difference is only partly accounted for by the fact that Orr's panes were rectangular and tested at a slower loading rate.

To indicate the probable effect of testing rate on ultimate strength, we can examine the equation given by Frownfelter (1959)

$$\frac{\sigma_{\max}}{\sigma_0} = 1 + 0.5 \log_{10} \frac{d\sigma}{dt}$$

where

$d\sigma/dt$ is the rate of application of stress in psi/min
 σ_0 is a reference stress

With a reference stress of 2000 psi, this equation is plotted in Fig. D.6. In addition, the recommended strength values from Pittsburgh Plate Glass (1964) are shown and straight lines were drawn on the figure to indicate the trend of the points. Comparison of the testing rates of Bowles and Sugarman (1952) with those of Orr (1957) indicates that Orr's strength values should be about 75% of those from Bowles and Sugarman.

Stress-Deflection Ratios

Equations relating maximum stress and central deflection were determined using the data of Bowles and Sugarman (1952). The equations have

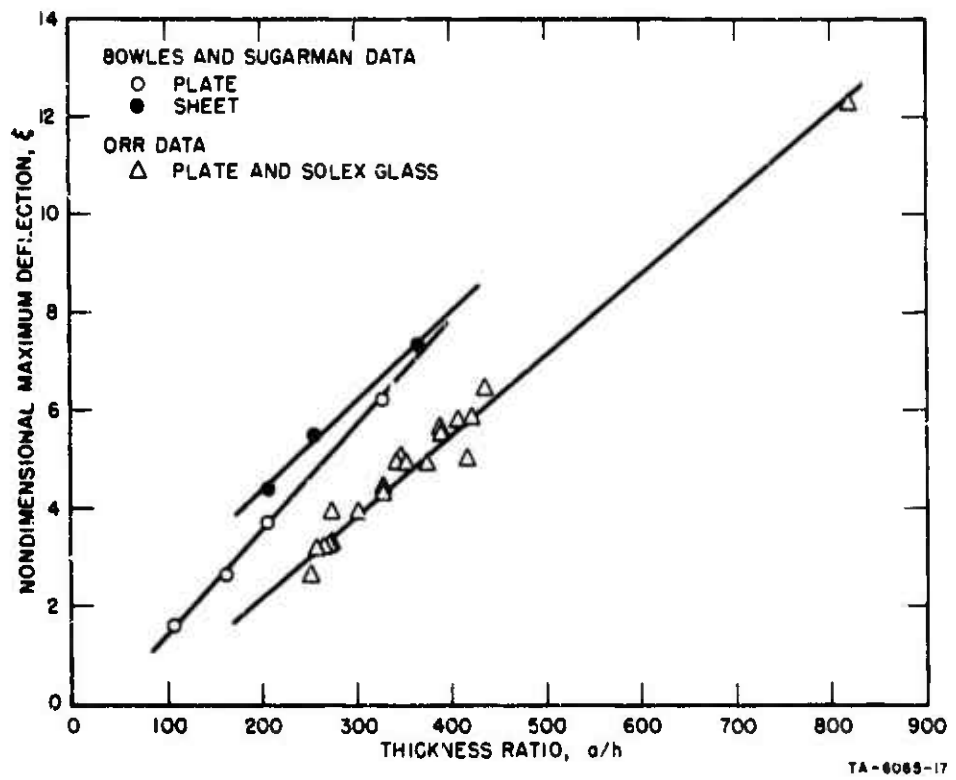


FIG. D.3 DEFLECTION AT RUPTURE AS A FUNCTION OF THICKNESS RATIO, a/h

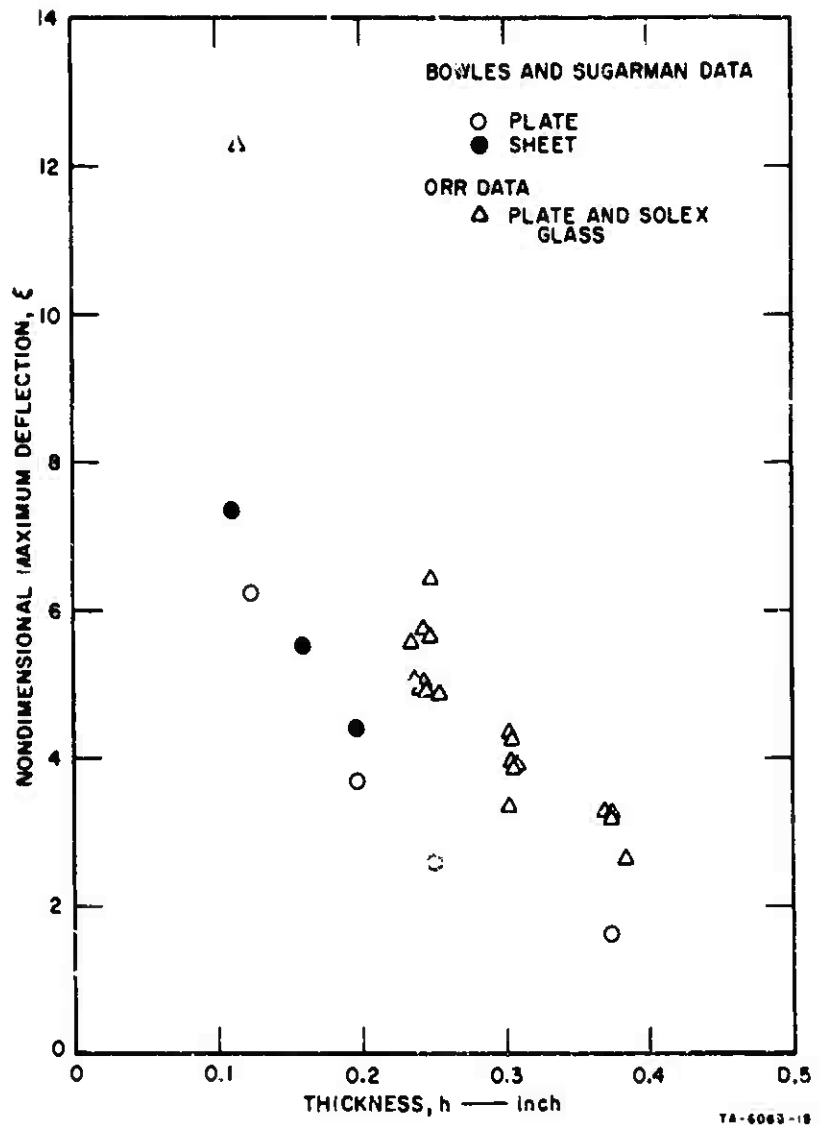


FIG. D.4 DEFLECTION AT RUPTURE AS A FUNCTION OF THICKNESS

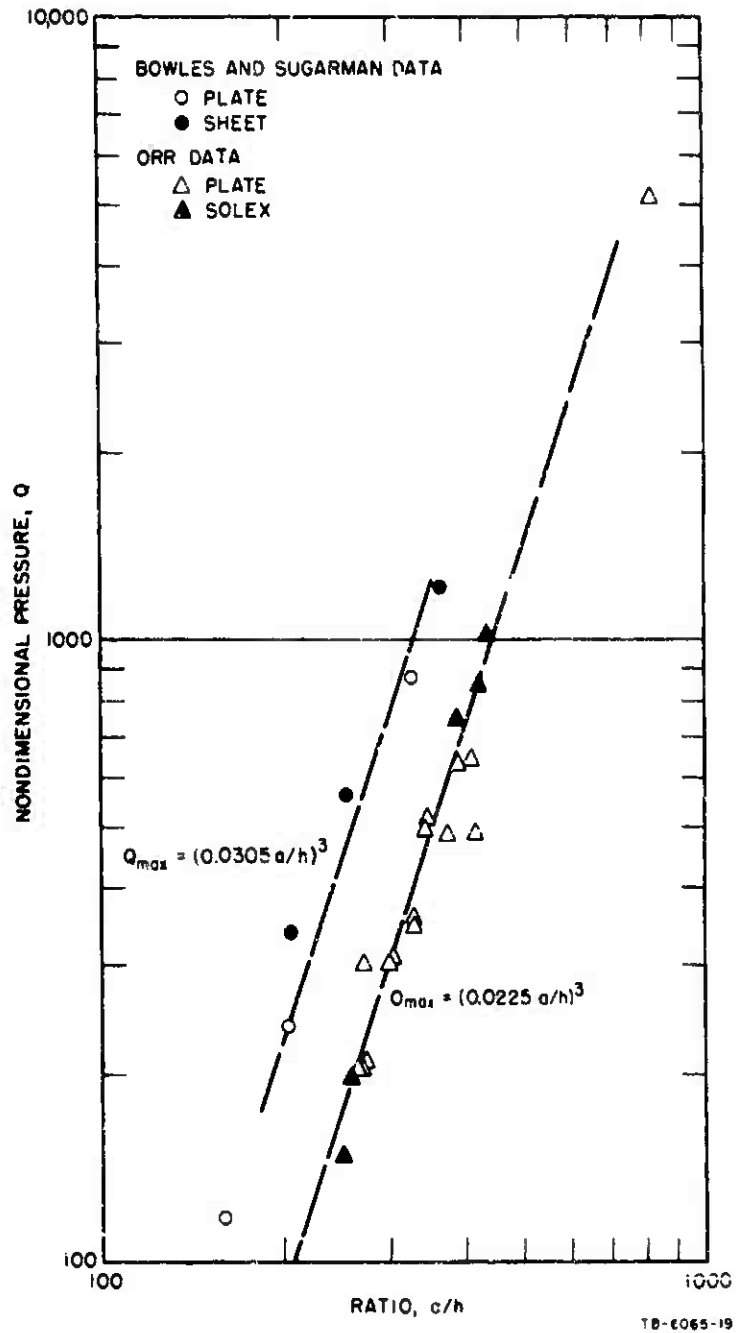
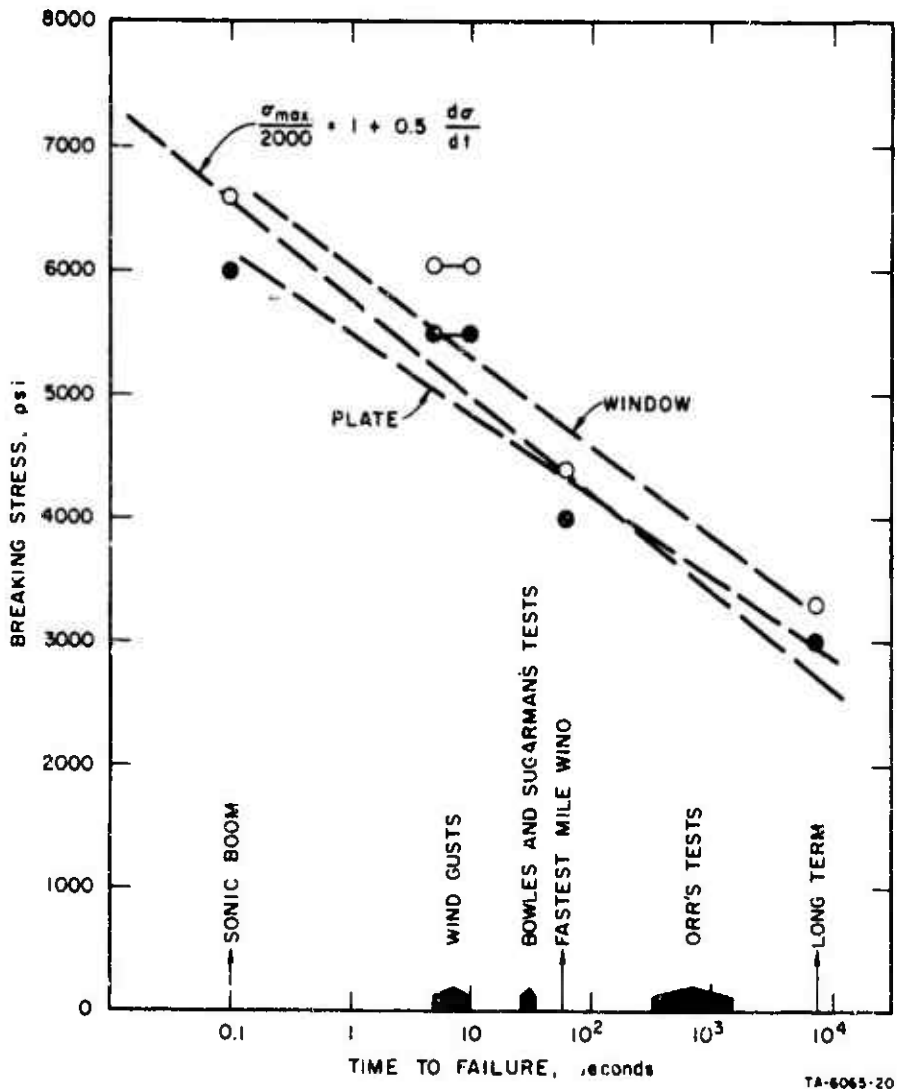


FIG. D.5 FAILURE PRESSURE ON PLATES AS A FUNCTION OF THE THICKNESS RATIO, a/h



TA-6065-20

FIG. D.6 EFFECT OF LOADING RATE ON ULTIMATE STRENGTH

the same form as those of Appendix C, that is

$$S_b = C_0 \xi$$

$$S_m = D_0 \xi^2$$

where

$$S = \frac{C\sigma^2}{Eh^3}$$

σ = stress

C_0, D_0 = constants

b, m = subscripts denoting bending or membrane.

The values used are listed in Table D.3 for the four panes instrumented with strain gages to indicate stress in the center of the pane. The data plotted in Figs. D.7 and D.8 give the following relations

$$S_b = 4.4 \xi \quad (D.2)$$

$$S_m = 0.82 \xi^2 \quad (D.3)$$

The bending stresses are about 65% of those given by Levy (1942) while the membrane stresses are 65% to 80% of Levy's values. It is improbable that these differences can be explained by the fact the Poisson's ratio for the glass was about 0.23, while Levy used $\nu = 0.316$. Because of the coefficient of 4.4 instead of 5.91 as from the linear analysis, stress-deflection results do not coincide with the linear theory even for small deflections.

Equations D.2 and D.3 are relations between the total stress in the center of the plate and the total deflection at that point. In the analytical work it will be necessary to have expressions relating stress and deflections in the first mode only. According to the linear theory of Appendix A the total static stress is 0.897 of the first mode stress; the total static deflection is 0.976 of the first mode deflection. We will assume that these factors from the linear theory are valid for bending but not for membrane stresses; that is, the total membrane stress is contributed by the first mode. Then

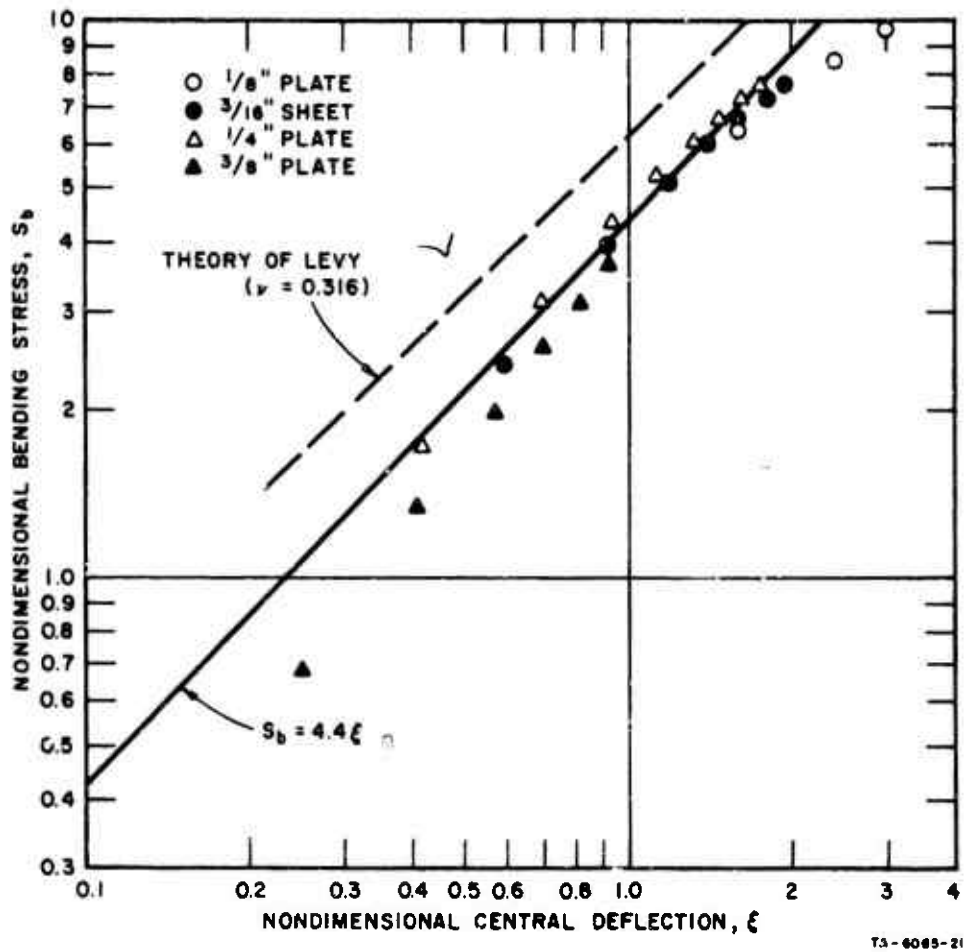


FIG. D.7 BENDING STRESS AS A FUNCTION OF CENTRAL DEFLECTION

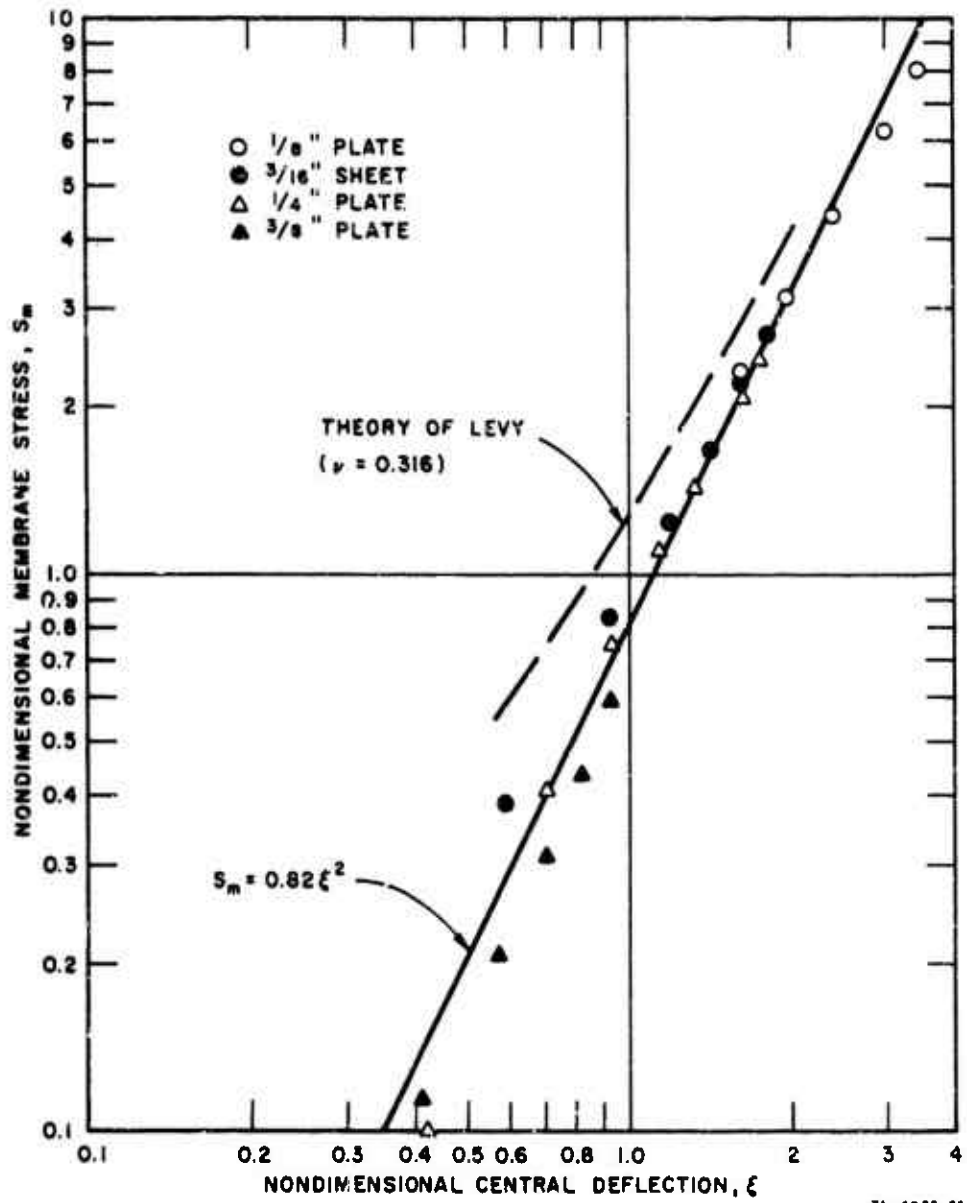


FIG. D.8 MEMBRANE STRESS AS A FUNCTION OF CENTRAL DEFLECTION

$$S_{b1} = \frac{4.4}{0.897} (0.978) \xi_1 = 4.8 \xi_1 \quad (D.4)$$

$$S_{m1} = 0.82 (0.976 \xi_1)^2 = 0.78 \xi_1^2 \quad (D.5)$$

where the subscript 1 refers to the first mode. In some cases we will want to relate first mode stresses to total deflections. The appropriate relations are

$$S_{b1} = \frac{4.4}{0.897} \xi = 4.9 \xi_1 \quad (D.6)$$

$$S_{m1} = 0.82 \xi^2 \quad (D.7)$$

or combining,

$$S_1 = 4.9 \xi (1 + 0.167 \xi) \quad (D.8)$$

Stress-Loading Relations

The bending and membrane stresses can be compared as direct functions of the loading. From the previous data reductions we have that

$$Q = 21.7 \xi + 2.80 \xi^3 \quad (D.1)$$

$$S_b = 4.4 \xi \quad (D.6)$$

$$S_m = 0.82 \xi^2 \quad (D.7)$$

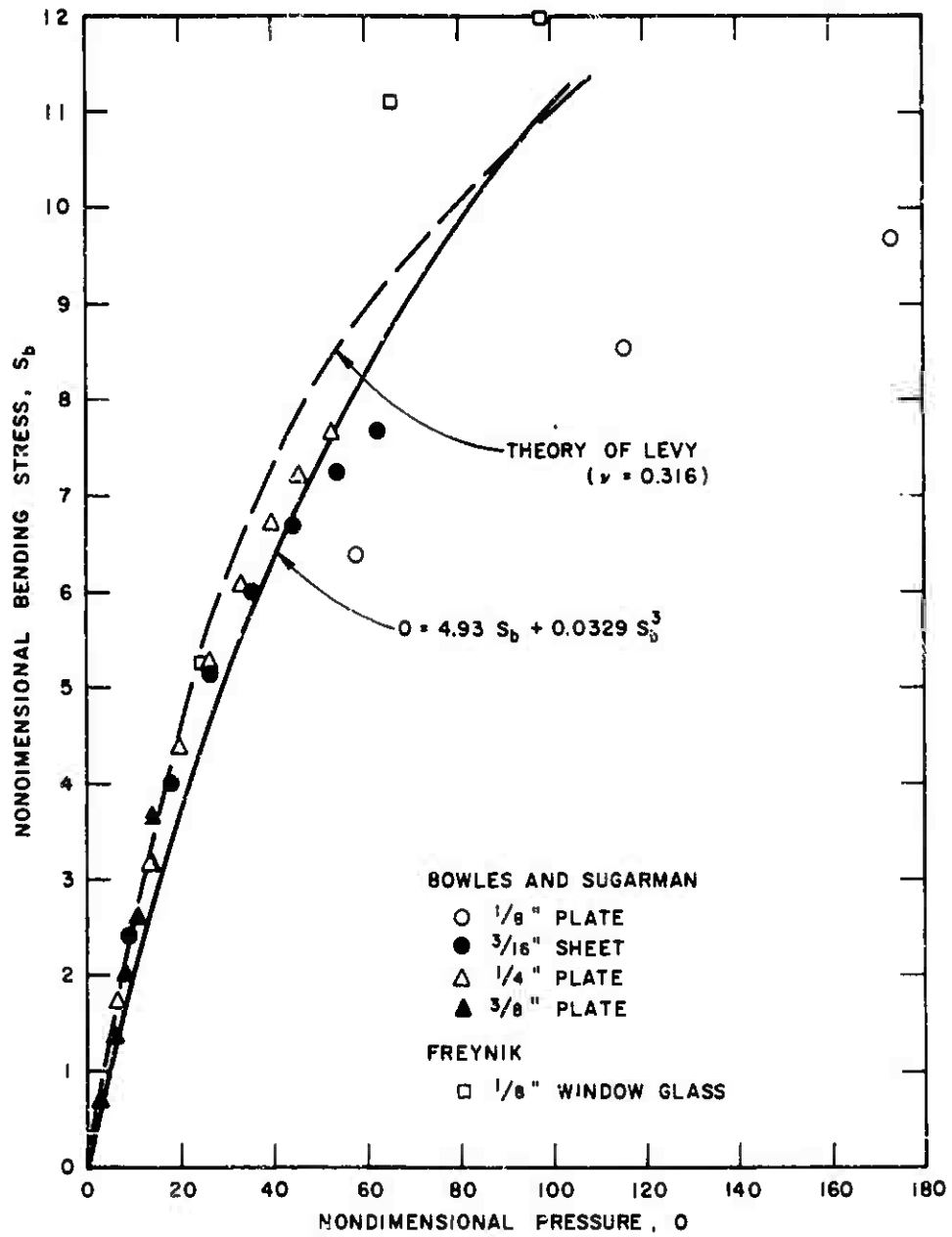
Substituting we obtain

$$Q = 4.63 S_b + 0.0329 S_b^3 \quad (D.9)$$

and

$$Q = 24.0 S_m^{1/2} + 3.77 S_m^{3/2} \quad (D.10)$$

The data of Bowles and Sugarman (1952) and Freynik (1963)¹ are compared with these equations in Figs. D.9 and D.10. The theoretical results of



TB-6065-23

FIG. D.9 RELATION BETWEEN CENTRAL BENDING STRESS AND APPLIED PRESSURE

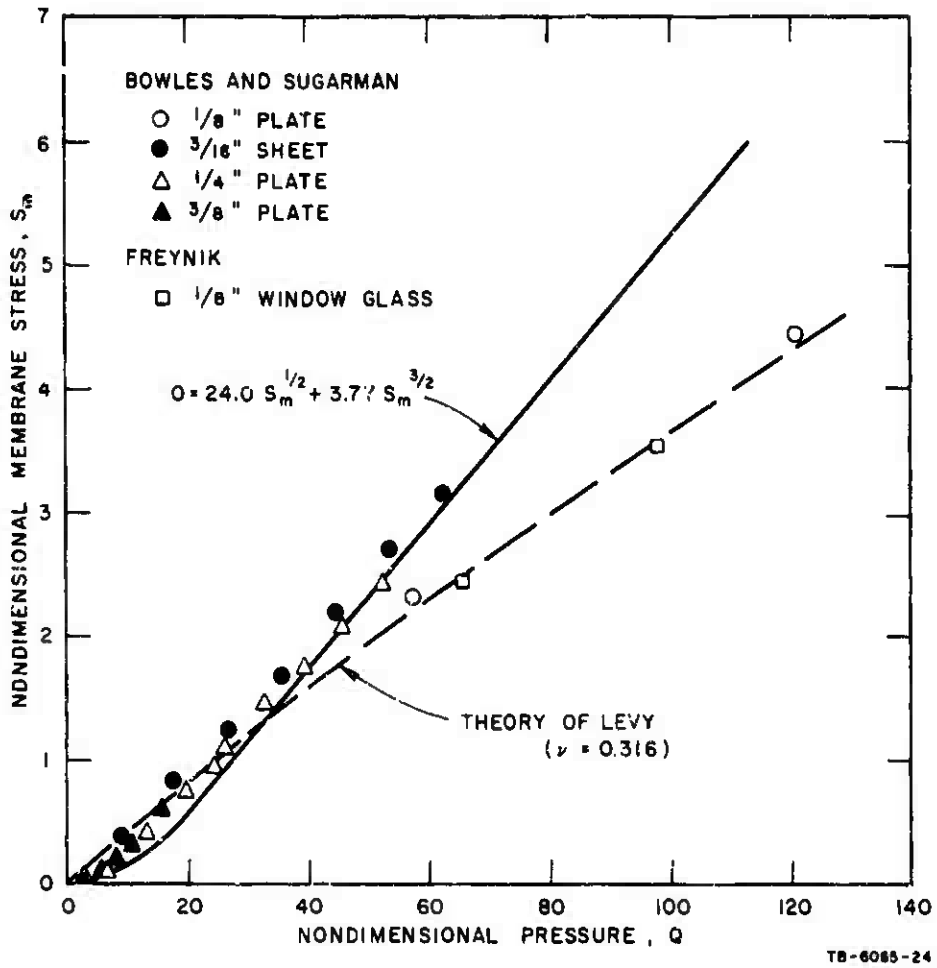


FIG. D.10 RELATION BETWEEN CENTRAL MEMBRANE STRESS AND APPLIED PRESSURE

Levy (1942) are also included. Equation D.9 agrees fairly well with Levy's results; the data of Bowles and Sugarman appear to fit Eq. D.9 somewhat better than the curve from Levy. The membrane stress results show a marked difference between the curves from Levy and Eq. D.10. The experimental data are divided between the two curves.

All of the stress-loading data above is for stresses from one-quarter to one-half the ultimate stress. Therefore, prediction of the stress condition at failure would require some extrapolation from the available data. Because the data do not correlate well with the theoretical or quasi-theoretical curves at high stress levels, it does not appear that stresses at failure can be predicted now. This situation is unfortunate because it means that ultimate strength data of glass specimens cannot be used directly to predict failure of glass panels.

Statistics of Failure

Strengths of glass specimens and window panels appear to vary widely from test to test; such variations are commonly observed with brittle materials. The experimental results have usually been reported in terms of the normal distribution although the data may fit some other distribution equally well.

Table D.4 lists the coefficients of variation (standard deviation divided by the mean) of the bursting pressure and the central deflection for the data of Bowles and Sugarman (1952). The variations appear to increase with the thickness of the specimens, as expected for a brittle material. It should be noted that these variations pertain to the pressure and deflection, not to the normalized quantities, Q and ξ . Therefore, the stated variations include the effects of randomness in the glass strength and in the glass dimensions.

Additional data on the statistics of the strength of glass are listed in Table D.5. The value given by Orr (1957) is for his estimates of the stress at failure in his glass panels. The other data are from strength tests on other types of glass samples. Note that these coefficients of variation pertain to stress at failure whereas the data of Table D.4 refer to applied pressure and ultimate deflection. Because we do not

have a sure relation between stress and applied pressure at failure, we cannot relate the coefficients of variation of these quantities. Hence, a knowledge of the statistical variation of breaking stress does not lead to a knowledge of the statistical variation of bursting pressure.

TABLE D.4

STATISTICAL DATA ON FAILURE
(Data from Bowles and Sugarman)

Sample Description	No. of Panels	Bursting Pressure Coeff. of Variation (%)	Central Deflection Coeff. of Variation (%)
1/8" plate	40	17.2	8.6
3/16" plate	30	17.9	9.2
1/4" plate	30	25.0	12.1
3/8" plate	30	23.7	13.9
24 oz sheet	30	14.0	7.55
32 oz sheet	30	15.9	7.17
3/16" sheet	30	26.8	10.95

TABLE D.5

STATISTICAL DATA ON BREAKING STRESS

Source	Coefficient of Variation (%)	Type of Glass
Frownfelter (1959)	22.0	- -
Orr (1957)	19.7	Plate and alex pane
McKinley (1964)	25.0*	Plate and window
Haaselman and Fulrath (1966)	12.7	Sodium Borosilicate

* Value recommended by McKinley for use in estimating safety factors.

APPENDIX E

DYNAMIC AMPLIFICATION FACTOR: NONLINEAR

When plates deflect beyond a small deflection range, their apparent stiffness increases because of membrane action. This change in stiffness increases the natural frequency and decreases the amplitude of motion. The purpose of this appendix is to determine the magnitude of these changes for the problem of window response to booms. The solution is developed first for the motion in the fundamental mode only, and then estimates are made for the effects of the higher modes.

First Mode Only

The equation of motion in the first mode has the following general form

$$\frac{d^2\xi}{dt^2} + \frac{k(\xi)}{m} \xi = \frac{Q_D f(t)}{m} \quad (\text{E.1})$$

where

- ξ is the nondimensional central deflection, w_0/h
- k is stiffness which is a function of deflection
- Q_D is the maximum amplitude of the nondimensional forcing function
- $f(t)$ is the temporal variation of that function.

From the solution of Eq. E.1, we want to develop curves of maximum deflection as a function of the period ratio, $\omega\tau/2\pi$, and of the loading. Hence, we must choose to plot deflection as a function of loading for specific values of $\omega\tau/2\pi$ or as a function of $\omega\tau/2\pi$ for specific loadings. The latter course seems appropriate because we can expect the deflection maxima to vary monotonically with load. The load values chosen are those producing specific values of static deflection. The next steps are to introduce the nonlinear relation for $k(\xi)$ and to replace Q_D by the static deflection it produces.

The load-deflection relation in Eq. C.10 will be used although it pertains to total deflection, not just first mode deflection. This is a

fairly small approximation because the difference between static total and first mode deflections is only 2.5%. The relation is

$$Q = A_0\xi + B_1\xi^3 = k(\xi)\xi \quad (\text{E.2})$$

so that the equation of motion is

$$\frac{d^2\xi}{dt^2} + \frac{A_0}{m} (\xi + \frac{B_1}{A_0} \xi^3) = \frac{Q_D f(t)}{m} = \frac{k(\xi_s)Q_D}{m k(\xi_s)} f(t) \quad (\text{E.3})$$

Note that $k(\xi_s)/m = (A_0\xi_s + B_1\xi_s^3)/m\xi_s$ is the square of the natural circular frequency, and $Q_D/k(\xi_s)$ is the static deflection ξ_s under the load Q_D . Now simplify the equation to the form

$$\frac{d^2\xi}{dt^2} + \alpha(\xi + \epsilon\xi^3) = \alpha(\xi_s + \epsilon\xi_s^3) f(t) \quad (\text{E.4})$$

where

$$\alpha = A_0/m$$

$$\epsilon = B_1/A_0$$

Equation E.4 was solved numerically using an Adams predictor-corrector method for integration. The computer program used had been previously developed for a three-degree-of-freedom system and reported by Bycroft (1965). The program was simplified slightly and changed to accept a sharply defined N-wave as the loading. The deflections and velocities were printed out after each step in the integration. Positive, negative, and free vibration maxima were taken from these listings by hand. The results are plotted in Figs. 12 - 15.

The program is listed at the end of this appendix. It is written in Algol for use on a Burroughs B5500. The compilation time is 40 seconds, and the execution time per abscissa value averages 14 seconds. The input data is entered on two types of cards. An example of input is given in the comment cards at the beginning of the program. The first card lists the number of abscissa values for which calculations are to be made. One card of the second type is required for each abscissa. On the second type of card the variables are

XI = ξ_s , the static deflection under the maximum pressure in the loading function
 ABSCISSA = $\omega t / 2\pi$
 FINAL = time at which calculation is terminated. It should be set at some value greater than 1.0 such that at least one free vibration maximum is reached.
 EPS = ϵ , the coefficient of the nonlinear term.

In the program the forcing function is the static deflection times a temporal function. If a response to a particular pressure level, Q_D , is required, the appropriate value of ξ_s can be found from the equation

$$Q_D = A_0(\xi_s + \epsilon \xi_s^3)$$

Alternatively, the 32nd card of the program could be changed from

$$ALFA \leftarrow (XI + EPS \times XI^3) \times OMEGA^2;$$

to

$$ALFA \leftarrow (Q_D/A) \times OMEGA^2;$$

where the values of Q_D and A would have to be supplied.

The program output lists the values of ABSCISSA and XI and then prints four columns of figures, headed TIME, DEFLECTION, VELOCITY, and DEFL/XI. The values printed under these headings are t/τ , ξ , $\tau d\xi/dt$, and ξ/ξ_s . The latter is the dynamic amplification factor.

Higher Modes

A rigorous analysis of the contribution of higher modes is not made for the large deflection case. However, some estimates are required of the importance of these higher modes. From Appendix A the contribution of these modes to the linear solution is known. What is needed now is a means for estimating changes in the amplitudes and frequencies of the higher modes. Such estimates will be made under the assumption that the motion in the higher modes can be merely added to that for the fundamental mode. With this assumption, the problem can be treated as that of a plate with stresses in its plane.

The deflection of a plate with stresses in its plane can be derived from section 93 of Timoshenko (1959). The result is

$$w = \frac{16q_0}{\pi^4 D} \sum_{\substack{m=1 \\ m, n \\ \text{odd}}}^{\infty} \sum_{\substack{n=1 \\ \text{odd}}}^{\infty} \frac{\sin(m\pi x/a) \sin(n\pi y/a)}{mn \left[\left(\frac{m^2+n^2}{a^2} \right)^2 + \frac{(m^2 N_x + n^2 N_y + 2mn N_{xy})}{\pi^2 a^2 D} \right]} \quad (\text{E.5})$$

where N_x , N_y , and N_{xy} are forces per unit width in the midplane of the plate. They are constants in Eq. E.5. In our dynamic case N_x , N_y , and N_{xy} all vary over the surface of the plate, oscillate at the fundamental frequency, and may be compressive or tensile. However, Eq. E.5 gives an indication of the nature of the effect of the membrane stresses on the deflections in the higher modes. In the central region of the plate, the membrane stresses are tensile and the shear is zero. Therefore the assumption is made that $N_x = N_y$ and $N_{xy} = 0$.

Then

$$w = \frac{16q_0}{\pi^4 D} \sum_{\substack{m=1 \\ m, n \\ \text{odd}}}^{\infty} \sum_{\substack{n=1 \\ \text{odd}}}^{\infty} \frac{\sin(m\pi x/a) \sin(n\pi y/a)}{mn(m^2+n^2)/a^2 \left[(m^2+n^2)/a^2 + N_x/\pi^2 D \right]} \quad (\text{E.6})$$

The moments are computed from

$$M_x = -D \left(\frac{\partial^2 w}{\partial x^2} + \nu \frac{\partial^2 w}{\partial y^2} \right), \text{ etc.} \quad (\text{E.7})$$

The moments are then

$$M_x = \frac{16q_0 a^2 (1+\nu)}{\pi^4} \sum_{\substack{m=1 \\ \text{odd only}}}^{\infty} \sum_{\substack{n=m \\ \text{odd only}}}^{\infty} \frac{H(m,n) \sin(m\pi x/a) \sin(n\pi y/a)}{mn \left[(m^2+n^2) + N_x a^2 / \pi^2 D \right]} \quad (\text{E.8})$$

where

$$\begin{aligned} H(m,n) &= 1/2 \text{ for } m = n \\ &= 1 \text{ for } m \neq n \end{aligned}$$

Evidently each term in the series for moment is reduced by the factor

$$\frac{1}{1 + N_x a^2 / [\pi^2 D (m^2+n^2)]}$$

from the value it would have if there were no membrane stresses. Using this factor a general expression can be developed to relate reduction of amplitude in the m,nth mode to reduction in the first mode. Let $R_E(m,n)$ be the ratio of amplitude for the nonlinear case to that for the linear case. Then

$$\frac{1}{1 + 2[1/R_E(1,1) - 1]/(m^2 + n^2)} \quad (E.9)$$

As an example let us assume that the amplitude in the fundamental mode was reduced by 30%. Then by how much are the higher modes reduced? The results for this example are in Table E.1.

TABLE E.1
AMPLITUDE REDUCTION FOR HIGHER MODES

Mode	Nonlinear/Linear Amplitude Ratio R_E	$N_x a^2 / \pi^2 D (m^2 + n^2)$
1,1	0.70 (assumed)	0.428
1,3 and 3,1	0.82	0.086
3,3	0.95	0.048
3,5 and 5,3	0.97	0.025

The values in the table indicate that the amplitudes of the higher modes are reduced by one-fifth (or less) as much as the first mode.

The natural frequencies are also altered by large deflections. The estimate of the frequency change is made on the same basis as the amplitude estimate above. That is, the modes are considered separately and the in-plane stresses caused by the fundamental mode are the source of the variations from the linear theory. The approach used is to calculate the strain energy and kinetic energy and equate them to find the natural frequencies.

Again taking the results of paragraph 93 of Timoshenko (1959),

the deflection is assumed to have the form

$$w = \sum_{m=1}^{\infty} \sum_{\substack{n=1 \\ \text{odd only}}}^{\infty} \varphi_{m,n} \sin(m\pi x/a) \sin(n\pi y/a) \quad (\text{E.10})$$

Then the strain energy is

$$V = \frac{\pi^4 D}{8a^2} \sum_{m=1}^{\infty} \sum_{n=1}^{\infty} \varphi_{m,n}^2 [(m^2+n^2)^2 + (m^2 N_x + n^2 N_y + 2mn N_{xy}) \frac{a^2}{\pi^2 D}] \quad (\text{E.11})$$

The kinetic energy is

$$T = \frac{\gamma h s^2}{8g} \sum_{m=1}^{\infty} \sum_{n=1}^{\infty} \left(\frac{d\varphi}{dt} (m,n) \right)^2 \quad (\text{E.12})$$

where

γ is the unit weight of the plate

h is the plate thickness.

By equating the maximum values for each mode of T and V and assuming that the motion is sinusoidal, we can obtain the following equation for frequency:

$$\omega_{m,n} = \frac{\pi^2}{a^2} \sqrt{gD/\gamma L} [(m^2+n^2)^2 + (m^2 N_x + n^2 N_y + 2mn N_{xy}) a^2 / \pi^2 D]^{1/2}$$

Again, let $N_x = N_y$, $N_{xy} = 0$. Then

$$\omega_{m,n} = \frac{\pi^2}{a^2} \sqrt{gD/\gamma L} (m^2+n^2) [1 + a^2 N_x / \pi^2 D (m^2+n^2)]^{1/2} \quad (\text{F.13})$$

The factor in Eq. E.13 raised to the one-half power contains the effect of the in-plane stresses. As might be expected, this is the same factor which entered the expression for the change in amplitude as a function of in-plane stresses. If the change in frequency is known for the fundamental mode, then Eq. E.13 permits a computation of the change for all modes. That is, if $B(m,n)$ is the ratio of frequencies in the nonlinear and linear cases, then

$$B_E(m,n) = \sqrt{1 + 2[B_E^2(1,1) - 1]/(m^2+n^2)} \quad (E.14)$$

Some sample results with Eq. E.14 are provided in Table F.2. Note that the same values of membrane stress, N_x , are used in Tables E.1 and E.2. There is evidently very little change in the frequency of the higher modes.

TABLE E.2
FREQUENCY INCREASE FOR HIGHER MODES

Mode	Frequency Ratio	$N_x a^2 / \pi^2 D (m^2 + n^2)$
1,1	1.20 (assumed)	0.428
1,3 and 3,1	1.04	0.086
3,3	1.025	0.048
3,5 and 5,3	1.01	0.025

The two analyses above have shown that the contribution of the higher modes to deflections and stresses are very little affected by the nonlinearities. Therefore it is suggested that, for purposes of estimation, the linear contributions of the higher modes be assumed to be valid for large deflections also.

PROGRAM NONLINEAR WINDOW

```

BEGIN COMMENT      LYNN SEAMAN EXT 3587
PROGRAM OF KRIEBEL WAS MODIFIED BY SEAMAN (JAN 67) TO CALCULATE THE
RESPONSE OF A 1 DOF WINDOW TO AN N-WAVE PRESSURE PULSE. PROGRAM USES
RUNGEKUTTA METHOD AS A STARTER AND CONTINUES WITH ADAMS PREDICTOR-
CORRECTOR METHOD.
  DATA IS ENTERED ON TWO GROUPS OF CARDS: ONE FOR ITER, ONE FOR XI,
  ABSCISSA, FINAL AND EPS. ITER IS THE NUMBER OF CASES TO BE HANDLED AND
  EQUALS THE NUMBER OF DATA CARDS TO FOLLOW. XI IS THE STATIC DEFLECTION,
  ABSCISSA = OMEGATAU/2PI, FINAL IS THE LAST TIME FOR WHICH A CALCULATION
  IS MADE, AND EPS IS THE COEFFICIENT OF THE NONLINEAR (CUBIC) TERM;
  COMMENT SAMPLE DATA CARDS
1,
3.0, 1.8, 1.5, 0.129,                                END SAMPLE;
REAL      INTIME,HZERO,INITIAL,FINAL,PRINT,RELB,ABS,DELTA,
          ABSCISSA,XI,OMEGA,EPS,DELTA,ALFA,DXI;
INTEGER   II,JJ,SIZE,NFIN,ITER,IC;
REAL ARRAY YINITIAL,YFINAL(1:2);
FILE      CR (1,15);
FILE      LP 4(1,15);
FORMAT OUT CLOCK (X36,"CALCULATION TIME OF PROGRAM =",F9.2,X3,
          "SECONDS",X36);

INTIME  + TIME (1);
SIZE+2; NFIN+1; DELTAT+1.0; INITIAL+0.0; RELB+0.001; ABS+0.001;
READ      (CR,/,ITER);
FOR IC=1 STEP 1 UNTIL ITER
DO BEGIN
OMEGA+0; ALFA+0; DELTA+0; EPS+0;
FOR II=1 STEP 1 UNTIL 2 DO YINITIAL(II) + 0;
READ (CR,/,XI,ABSCISSA,FINAL,EPS);
HZERO + 1.0/(60.0*ABSCISSA); PRINT + HZERO;
OMEGA + ABSCISSA*6.2832;
ALFA + (XI+EPS*XI*3)*OMEGA*2;
BEGIN
REAL      TESTIME1,TESTIME2,TP;
REAL ARRAY INF(0:NFIN);
REAL PROCEDURE FINPUT (T,FIN);
VALUE     T;
REAL     T;
REAL ARRAY FIN(0);
BEGIN COMMENT SECOND ORDER INTERPOLATION OF INPUT ACCELERATION.
          USE OF FORWARD DIFFERENCES;
REAL      IR,R,R1,R2;
INTEGER   II,II1,II2;
IF T<TESTIME1 THEN BEGIN
IR      + T/DELTAT;
II      + ENTIER (IR);
R      + IR-II;
IF ABS(R)>=0.06 THEN
FINPUT  + FIN(II)
          ELSE
          BEGIN
IF T<TESTIME2 THEN BEGIN
II1  + II+1;

```

```

II2  * III+I1
R1   * I-R1
R2   * 2-R1
FINPUT * 0.5*R1*(R2*FINC[II]-R*FINC[II2])+R*R2*FINC[III]
      ENO
      ELSE
IF T<TESTIME1 THEN BEGIN
III  * II+I1
R1   * I-R1
R2   * 2-R1
FINPUT * R1*FINC[II] + R*FINC[III]
      END
      ENO
      ENO
      ELSE
FINPUT * 0;
ENO OF FINPUT;
PROCEURE  FUNCT (TEMP,YTEMP,OERIV);
REAL      TEMP;
REAL ARRAY YTEMP,OERIV[1];
BEGIN COMMENT COMPUTATION OF OERIVATIVES;
REAL      Q12,Q13;
INTEGER   I;
Q12  * YTEMP[1]*YTEMP[1];
Q13  * YTEMP[1]*Q12;
OERIV[1] * YTEMP[2];
OERIV[2] * -(DELTA *YTEMP[2] + OMEGA*2 *(YTEMP[1] + EPS *Q13)) + ALFA
          * FINPUT(TEMP,INFC*J);
ENO OF FUNCT;
REAL ARRAY FORAOAMSC[0:3,I:30], YINCFORAOAMSC[1:30]; COMMENT GOES
BEFORE AOAMS;
PROCEURE  AOAMS(SIZE, HZERO, INITIAL, FINAL, PRINT, RELB, ABSB,          AOAMSOOI
              YINITIAL, YFINAL, FUNCT) ;
VALUE SIZE, HZERO, INITIAL, FINAL, PRINT, RELB, ABSB ;
INTEGER SIZE ; REAL HZERO, INITIAL, FINAL, PRINT, RELB, ABSB ;
REAL ARRAY YINITIAL, YFINAL[1] ;
PROCEURE  FUNCT ;
BEGIN COMMENT AOAMS VERSION OF APRIL 1, 1954 ;
OWN INTEGER I, J, N ;
OWN REAL X, H, RELTEST, ABSTEST, FACTOR ;
REAL H24, LB, BOUND, T, TEMPX, TEMPH ; BOOLEAN TEST ;
REAL ARRAY Y, F[0:4,1:SIZE], E, YPL[1:SIZE] ;
LABEL START1, START2, START3, MARCH, LASTSTEP, RETURN ;
DEFINE LOOPI = FOR I * 1 STEP 1 UNTIL N DO # ;
FORMAT OUT  MSSG (X4,"THE STEP SIZE IS NOW",E18.11);
          SINGY
(X30,"**EQUATIONS CANNOT BE SOLVED WITHIN THE GIVEN ERROR BOUNOS**",X30)
          TITLE
(X10,"SOLUTION OF NONLINEAR WINDOW MOTION"///X10,"ABSCISSA =",F8.4,
X5,"XI =",F8.4//X8,"TIME",X5,"OEFLECTION",X3,"VELOCITY",X3,"OEFL/XI"//1,
          FRMT (X5,F8.4,X4,F8.4,X4,F8.4,X3,F8.4));
LIST      LISTI (ABSCISSA,XI);
PROCEURE  RUNGEKUTTA(YOLO, FOLO, YNEW, FUNCT) ;
REAL ARRAY YOLO, FOLO, YNEW[1] ; PROCEURE  FUNCT ;
BEGIN

```

```

DEFINE K=KFORAOAMSH, YINC=YINCFORAOAMSH
REAL INC, H6 ; INTEGER L ;
L * 0 ; H6 * H/6.0 ;
LOOPI K[0,I] * FO[0,I] ;
FOR INC * H/2.0, INC, H 00
  BEGIN LOOPI YINC[I] * YOLDE[I]+INC*K[L,I] ;
    L * L +1 ; FUNCT(X+INC, YINC, K[L,*])
  ENO ;
  LOOPI YNEW[I] * YOLO[I]+H6*(K[0,I] *2.0*(K[1,I]+K[2,I]) +K[3,I])
  X * X +H
  ENO RUNGEKUTTA ;
  BOOLEAN PROCEDURE ERRTST(YP, YC, E) ;
  REAL ARRAY YP, YC, E[1] ;
  BEGIN REAL YCI, EI ; LABEL RETURN ;
  ERRTST * FALSE ;
  LOOPI BEGIN ECI * EI + ABS(YP[I]-(YCI+YC[I])) ;
    IF EI < ABS(YCI)*RELTEST THEN ECI * EI/ABS(YCI)
    ELSE IF EI < ABSTEST THEN ECI * EI*FACTOR
    ELSE BEGIN ERRTST * TRUE ; GO TO RETURN ENO ;
  END ;
  RETURN: ENO ERRTST ;
COMMENT INITIALIZE ;
WRITE (LP,PAGE) ;
WRITE (LP,TITLE,LIST1) ;
N * SIZE ; LOOPI Y[0,I] * YINITIAL[I] ;
X * INITIAL ; FUNCT(X, Y[0,*], F[0,*]) ;
OXI*YINITIAL[I]/XI ;
WRITE (LP,FRMT,INITIAL,LOOPI YINITIAL[I],OXI) ;
BOUNO * INITIAL+PRINT ;
IF (TEST * ABSB * 0) THEN
  BEGIN RELTEST * 14.2*RELB ; ABSTEST * 14.2*ABSB ;
  FACTOR * RELB/ABSB ; LB * RELTEST/200.0 ;
  H * PRINT ; FOR H*0.5*H WHILE H >HZERO 00 ;
  ENO
  ELSE BEGIN H*HZERO ; IF H>PRINT THEN PRINT*H ; GO TO START3 ENO ;
COMMENT RUNGE-KUTTA STARTING METHODO ;
START1: H * 2.0*H ;
  IF X+H2FINAL THEN BEGIN J * 0 ; GO TO LASTSTEP ENO ;
  RUNGEKUTTA(Y[0,*], F[0,*], YP, FUNCT) ; X * X-H ;
START2: H * 0.5*H ;
START3: IF X+H=X THEN
  BEGIN OXI * Y[0,I]/XI ;
  WRITE (LP,SINGY) ; WRITE (LP,FRMT,X,LOOPI Y[0,I],OXI) ;
  GO TO RETURN
  ENO ;
  RUNGEKUTTA(Y[0,*], F[0,*], Y[1,*], FUNCT) ; FUNCT(X, Y[1,*], F[1,*]) ;
  RUNGEKUTTA(Y[1,*], F[1,*], Y[2,*], FUNCT) ;
  IF TEST THEN IF ERRTST(YP, Y[2,*], E) THEN
    BEGIN LOOPI YP[I] * Y[1,I] ;
    X * X-H ; GO TO START2 ;
  ENO ;
  FUNCT(X, Y[2,*], F[2,*]) ;
  WRITE (LP,MSSG ,H) ;
  IF X+H2FINAL THEN BEGIN J * 2 ; GO TO LASTSTEP ENO ;
  RUNGEKUTTA(Y[2,*], F[2,*], Y[3,*], FUNCT) ; H24 * H/24.0 ;

```

```

COMMENT CHECK STARTING VALUES FOR PRINTING ;
T = X-3.0*X H ;
FOR J = 1,2,3 DO
  BEGIN T = T+H ;
    IF T=BOUND THEN
      BEGIN BOUND=BOUND+PRINT ; DXI = Y[J,I]/XI ;
        WRITE (LP,FRMT,T,LOOPI Y[J,I],OXI) END
      ELSE IF T>BOUND-H24 THEN
        BEGIN TEMPX = X ; TEMPH = H ;
          X = T-H ; H = BOUND-X ;
          RUNGEKUTTA(Y[J-1,*], F[J-1,*], YP, FUNCT) ;
          DXI = Y[J,I]/XI ;
          WRITE (LP,FRMT,X,LOOPI Y[J,I],OXI) ;
          X = TEMPX ; H = TEMPH ; BOUND = BOUND+PRINT
        END ;
      END ;
COMMENT ADAMS MARCHING METHOD ;
MARCH: FUNCT(X, Y[3,*], F[3,*]) ;
IF X+H2FINAL THEN BEGIN J = 3 ; GO TO LASTSTEP ENO ;
LOOPI Y[1,I] = Y[3,I] +H24*(55.0*F[3,I] -59.0*F[2,I]
+37.0*F[1,I] -9.0*F[0,I]) ;
X = X + H ; FUNCT(X, YP, F[4,*]) ;
LOOPI Y[4,I] = Y[3,I] +H24*(9.0*F[4,I] +19.0*F[3,I]
-5.0*F[2,I] +F[1,I]) ;
IF TEST THEN IF ERRTST(YP, Y[4,*], E) THEN
  BEGIN LOOPI BEGIN Y[0,I] = Y[3,I] ; F[0,I] = F[3,I] END ;
  X = X -H ; H = 0.5*X ; GO TO STARTI ;
END ;
IF X=BOUND THEN
  BEGIN BOUND=BOUND+PRINT ; DXI = Y[4,I]/XI ;
  WRITE (LP,FRMT,X,LOOPI Y[4,I],OXI) END
ELSE IF X>BOUND-H24 THEN
  BEGIN TEMPX = X ; TEMPH = H ;
  X = X-H ; H = BOUND-X ;
  RUNGEKUTTA(Y[3,*], F[3,*], YP, FUNCT) ; DXI = Y[4,I]/XI ;
  WRITE (LP,FRMT,X,LOOPI Y[4,I],OXI) ;
  X = TEMPX ; H = TEMPH ; BOUND = BOUND+PRINT
  ENO ;
LOOPI BEGIN Y[3,I] = Y[4,I] ; F[0,I] = F[1,I] ;
  F[1,I] = F[2,I] ; F[2,I] = F[3,I] ; F[3,I] = F[4,I] ;
  ENO ;
COMMENT CAN INTERVAL H BE DOUBLED ;
IF H+H>PRINT OR NOT TEST THEN GO TO MARCH ;
LOOPI BEGIN IF E[I] > LB THEN GO TO MARCH ENO ;
  LOOPI BEGIN Y[0,I] = Y[3,I] ; F[0,I] = F[3,I] END ;
  H = 2.0*X H ; GO TO STARTI ;
LASTSTEP: H = FINAL-X ; RUNGEKUTTA(Y[J,*], F[J,*], YFINAL, FUNCT) ;
DXI = YFINAL[I]/XI ;
WRITE (LP,FRMT,X,LOOPI YFINAL[I],OXI) ;
RETURN: END ADAMS ;
TESTIME1 = NFIN*DELTAT ;
TESTIME2 = TESTIME1-DELTAT ;
INF[0] = 1.0 ; INF[I] = -1.0 ;
ADAMS (SIZE,HZERO,INITIAL,FINAL,PRINT,RELB,ABSB,YINITIAL,YFINAL,FUNCT) ;
ENO ;

```

```
WRITE (LP,DBL); WRITE (LP,DBL); WRITE (LP,CLOCK,(TIME (1)-INTIME)/60);  
END;  
CLOSE (CR,RELEASE);  
END.  
?DATA          CR  
1,  
3.0, 1.8, 1.5, 0.129,  
?END OF DECK
```

BIBLIOGRAPHY

- American Society for Testing Materials, Vol. 13, 1965, p. 142.
- Bowlea, R., and B. Sugarman, "The Strength and Deflection Characteristics of Large Rectangular Glass Panels Under Uniform Pressure," *Glass Technology*, Vol. 3, No. 5, October 1962, p. 156-170.
- Chu, Hu-Nan and George Herrman, "Influence of Large Amplitudes on Free Flexural Vibrations of Rectangular Elastic Plates," *Jour. of Appl. Mech.*, 1956, Vol. 23, No. 4, p. 532.
- Freyrik, Henry S., Jr., "The Nonlinear Response of Windows to Random Noise," NASA Technical Note, NASA TN D-2025, Dec. 1963.
- Frownfelter, C. R., "Structural Testing of Large Glass Installations," p. 19 of a symposium on Testing of Window Assemblies, ASTM Spec. Tech. Publ. No. 251, February 1958.
- Hasselman, D. P. H., and Fulrath, R. M., "Proposed Fracture Theory of a Dispersion-Strengthened Glass Matrix," *Jour. Am. Ceramic Soc.*, Vol. 49, February 1966, p. 68-72.
- Levy, Samuel, "Bending of Rectangular Plates with Large Deflections," NACA Report No. 737, 1942.
- Maglieri, D. J., V. Huckel, and T. L. Parrott, "Ground Measurements of Shock-Wave Pressures for Fighter Airplane Flying at Very Low Altitudes and Comments on Associated Response Phenomena," NASA Tech. Memo. No. X-611, December 1961.
- McKinley, R. W., "Response of Glass in Windows to Sonic Booms," *Materials Research and Standards*, Vol. 4, No. 11, November 1964, p. 594-600.
- Orr, Leighton, "Engineering Properties of Glass, Windows and Glass in the Exterior of Buildings," Pub. 478 of Bldg. Res. Inst. of NAS-NRC, 1957, p. 51.
- Pittsburgh Plate Glass Company, "Glass Product Recommendations: Structural, Technical," Service Report No. 101 of Pittsburgh Plate Glass Company, Pittsburgh, Pa., March 1964.
- Shand, E. B., "Glass Engineering Handbook," McGraw-Hill Book Co., New York, 1958, p. 47-49.
- Timoshenko, S., "Theory of Plates and Shells," Second Ed., McGraw-Hill Book Co., Inc., N. Y., 1959, Chap. 13, Large Deflection of Plates.
- Uniform Building Code, Vol. 1, 1964 Edition, International Conference of Building Officials, Pasadena, California, Chap. 54.